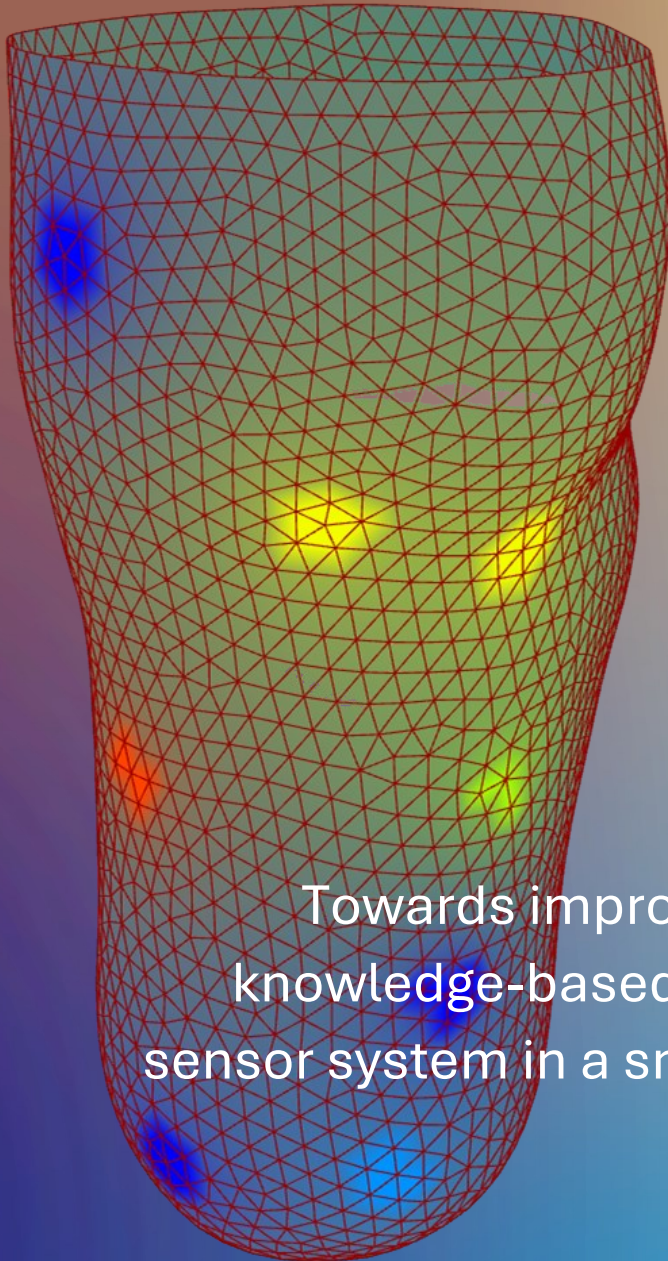


MSc. Integrated Product Design – Thesis
Faculty of Industrial Design Engineering
TU Delft



Towards improved user comfort with knowledge-based design: integration of sensor system in a smart prosthetic socket

Master Thesis Report

Santiago Andújar Arias

Student no. 5860105

Supervisory team:

Dr. Wolf Song (Chair)

Dr. Mohammad Mirzaali (Mentor)

Ir. Vahid Moosabeiki (Mentor)

Abstract

Prosthetic socket design and fit are key for a successful amputee rehabilitation and comfort, directly influencing patient satisfaction and quality of life. However, there is a lack of quantitative data on stump pressure distribution and how it changes over time, which could greatly contribute to the efforts of designers, prosthetists and doctors to improve patient comfort.

This study explores the use of Force Sensitive Resistors (FSRs) to measure and visualize stump pressure distribution, specifically for transtibial prosthetic sockets. The research involves testing an experimental prototype equipped with FSRs on a cyclic loading machine, followed by a comparison of the results with a simulation.

The findings indicate that the highest loads are registered by FSRs positioned at the bottom of the stump and below the knee. Some anomalies were observed, potentially due to specific geometric features of the prototype and the way the load was applied during testing.

Overall, the experimental data suggests that FSRs are effective for measuring stump pressure distribution. However, further testing with increasingly complex load cases is necessary to validate the sensors' reliability.

In conclusion, FSRs demonstrate significant potential for enabling knowledge-based designs focused on patient wellbeing. Through the course of this project, valuable design insights and requirements for integrating sensors into prosthetic sockets were identified. Moreover, this systematic sensor testing approach can be applied to explore and compare between other pressure sensors.

Acknowledgements

I came to TU Delft two years ago because I wanted to improve as a designer. After this time, I feel that I have not only improved skill-wise but also in how I take on challenges and projects. Through the course of the master's degree, I have finally found what I enjoy doing the most: prototyping with 3D printing and machining, electronics prototyping, design for manufacturing and making functional prototypes; in the end, devices that work.

I enjoy the point where design converges with engineering, and I also feel confident about approaching technical challenges in a proactive and hands on manner. I will regard this time at the IDE Faculty as a time that shaped me and allowed me to thrive in many ways.

I would like to especially say thank you to the people that made this such a great time:

To my parents, for their support. Without them this would not have even started.

To my mentors Wolf, Mohammad and Vahid for their support and advice during this project.

To my friends, who made this master's so memorable.

And thank you Esmee, for everything.

Table of contents

1.	Introduction	1
2.	Literature review	1
2.1.	<i>Lower limb prostheses</i>	1
2.2.	<i>Smart prosthetic solutions to improve comfort</i>	5
2.3.	<i>3D printed prostheses</i>	5
3.	Framework approach	8
4.	Materials and methods	8
4.1.	<i>Experiment setup</i>	8
4.1.1.	Prosthesis prototype	8
4.1.2.	Testing protocols	11
4.2.	<i>Simulation setup</i>	13
4.2.1.	Experimental test simulation	13
5.	Results	15
5.1.	<i>Experimental results</i>	15
5.1.1.	Sensor calibration test results	15
5.1.2.	Socket sensor test results	18
5.2.	<i>Experimental simulation results</i>	20
5.3.	<i>Comparison</i>	21
6.	Discussion	22
6.1.	<i>Reflection on the results</i>	22
6.2.	<i>Reflection on the methods</i>	22
6.3.	<i>Limitations of the study</i>	22
6.4.	<i>Design Implications</i>	23
6.4.1.	Applications	23
6.4.2.	Requirements	26
7.	Future recommendations	29
8.	Conclusion	30
9.	References	31
	Appendices	33

1. Introduction

Optimum comfort, socket design and fit are critical for a successful rehabilitation and therefore, patient satisfaction and quality of life. Despite advances in prosthetics, there is a lack of evidence-based knowledge on how the residual limb changes over time that affects diagnose, design and fit. This study aims to determine the stump pressure distribution in an experimental prototype through the use of Force Sensitive Resistors (FSRs) in a systematic way. The research contributes by providing design implications of the use of Force Sensitive Resistors to measure the pressure distribution in the stump, drawn from test results with an experimental prototype.

The paper is structured as follows: the Literature review section presents an overview of the topic, its context and the current advances gathered from relevant sources; the Materials and methods section is divided into Simulation setup and Experiment setup; the Results section presents findings from both setups, including a results comparison. The Discussion section reflects on the results and methods, addresses study limitations, and discusses design implications. Finally, the Conclusion section is presented.

2. Literature review

This section provides a general overview of below the knee prostheses, also called transtibial, user needs and comfort parameters, as well as a compilation of existing solutions.

2.1. Lower limb prostheses

Prostheses are devices that aim to restore the appearance and functionality of an amputated limb, therefore improving the independence and quality of life of the amputee. The design of a prosthetic socket, the part of the prosthesis that interfaces with the residual limb, is crucial for comfort and functionality and to the long-term satisfaction of the patient [1] [2].

Amputation are surgical procedures to remove of a limb or part of it, its causes can be broadly divided into traumatic and non-traumatic. Traumatic amputations result from accidents or injuries, such as those sustained in traffic accidents, industrial incidents, or military combat. Non-traumatic amputations are usually related to medical conditions such as peripheral artery disease (PAD), diabetes or tumours. Non-traumatic amputations is a major cause of amputations, for example, PAD accounts for around 55% of the total of lower limbs amputations in the US. This study predicts that that the number of amputees in the US will duplicate to 3.6 million by 2050, if the root cause is not addressed [3]. As the number of amputations is expected to grow due to diabetes, vascular diseases and trauma, the need for effective prostheses will become even more critical, proving better mobility, functionality and comfort. These are key to enhancing the quality of life of the amputee.

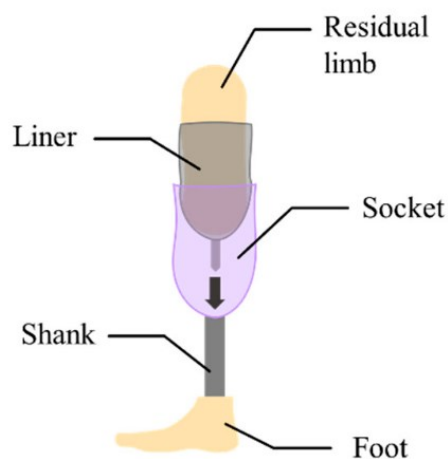


Figure 1. Parts of a below the knee prosthesis

Types of limb prostheses

Limb prostheses can be categorized into several types based on their function and complexity:

- Cosmetic Prostheses. These are designed primarily for appearance rather than functionality.
- Functional Prostheses. These are designed to restore some degree of function, which are divided into:

- Body-Powered Prostheses. Operated by the user's residual limb movements, typically through a harness and cable system.
- Externally Powered Prostheses. These include myoelectric prostheses that are controlled through the muscle's electrical signals.
- Hybrid Prostheses. Combine elements of both body-powered and externally powered systems.

Prostheses are also classified based on the level of amputation:

- Upper Limb Prostheses. These can be Transradial Prostheses (below the elbow), Transhumeral Prostheses (above the elbow) and Shoulder Disarticulation Prostheses (for amputations at the shoulder joint).
- Lower limb prostheses. These can be Transtibial Prostheses (below the knee), Transfemoral Prostheses (above the knee) and Hip Disarticulation Prostheses (for amputations at the hip joint).

Acceptance of prostheses

Successful acceptance of a prosthesis is influenced, among others, by the type of amputation, the type of prosthesis used, and personal factors such as pre-amputation lifestyle, physical condition, age and gender. Psychological factors, including expectations and mental health, are equally important. Studies have shown that individuals with a positive outlook and realistic expectations regarding their prosthesis tend to adapt better and report higher satisfaction levels. Psychological support and counselling can thus be crucial components of the rehabilitation process, helping individuals to cope with the changes and challenges brought by limb loss [4] [5] [6].

Benefits and limitations

Prostheses offer significant benefits, including improved mobility and independence. However, they also come with limitations. These can include discomfort, the need for regular maintenance, the high cost of advanced prostheses, constant rehabilitation and adaptation and the prescription of a prosthesis that matches the user expectations and goals.

Traditional and Digital Prosthesis making and fitting

The rehabilitation team is formed by a rehabilitation physician, a prosthetist and a physical therapist. The prosthetist is responsible of designing and fitting the prosthesis for the patient. Besides that, a physical therapist assists the patient in adapting to his or her prosthesis by relearning gait and improving the mobility.

Guidelines define recovery periods, which affect fitting: at the *immediate post-acute hospital stage* (4-8 week after surgery), after the patient's wounds have healed, the patient is ready for the first prosthetic fit; in the *intermediate recovery stage* (4-6 months after surgery), the patient gets its first formal prosthesis, which needs constant adjustments; at the *transition to a stable stage* (12-18 month after surgery), the shape and volume of the residual stump is stabilised and a definitive prosthesis is designed [7]. Nevertheless, close and constant monitoring from the prosthetist is necessary since the stump evolution is patient specific and the prosthesis fit will vary over time and throughout the day.

Overall, the fitting process of a prosthesis is critical for ensuring comfort and functionality, since early fitting provides benefits such as better gait rehabilitation, independent lifestyle, undergo more physical training, higher acceptance of amputation, better maturation of the limb and adaptation to the socket [8].

A distinction needs to be made between traditional prosthesis making and the additive manufacturing of prosthesis. Traditional prostheses are made with a plaster mould of the stump and requires a detailed evaluation of the residual limb, then the socket is made generally out of vacuum formed carbon fibre due to its strength and lightweight properties. Conventional prosthesis might require multiple fitting to get the right fit, it is expensive and takes some time to make since it is a complex process done by a highly experience prosthetist, who tailors a prosthesis with expertise and feel. On the other hand, 3D printing allows for accessible, time efficient, personalised and accurate designs to be made with just a 3D scan of the stump.



Figure 2. Traditional prosthesis check fitting [9].

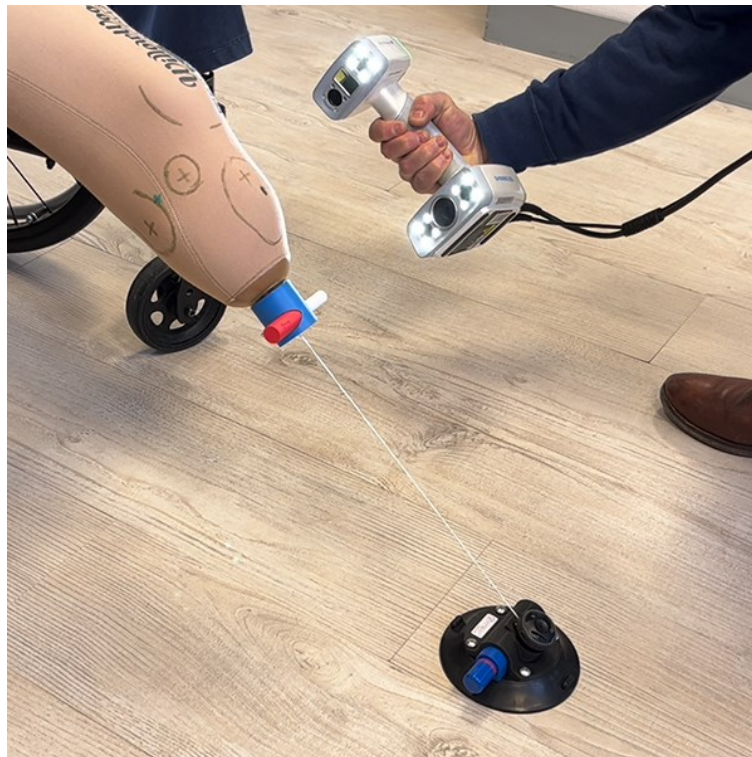


Figure 3. 3D scan of a below the knee stump (Source: www.vytruve.com/scanning-tools).

Key user needs

Optimal comfort, patient independence and prosthesis fit have been identified as critical user needs for amputees [1]. At the stump-socket interface, the part where the patient's residual limb interacts with the prosthetic socket, there are several parameters that produce discomfort in the form of pain, excessive sweat, bad smell and skin issues [2], [10]. In the long term, these factors might lead patients to stop using their prostheses, hampering their recovery and quality of life [11].



Figure 4. Word cloud of prosthesis user needs [1]

Comfort parameters

Three main factors have been pointed out to affect patient comfort. These are:

- Stress and pressure on socket-skin interface.
- Volume changes in the residual limb.
- High temperature inside the socket.

Issues such as irritation, ulcerations or increased perspiration and maceration are caused by high pressure applied to the skin for long periods. Tissue deformation and injury occur as a result of the shear stress between the limb and the socket. Discomfort can be reduced by identifying the pressure points and adding a feature that reduces them, such as a material or actuator [12].

Volumes changes in the stump are mainly due to the change of physical activities and complex fluid movements in the stump: pooling of blood in veins, arterial vasodilatation and changes in lymphatic fluid [13]. Generally, volume fluctuates mostly within the first weeks post-surgery, and even after the stump matures, changes over the day worsen prosthesis fit. Stump volume ranges from -11% to +7%, and an increase of 3 to 5% can already produce discomfort and a difficult donning [14].

The temperature inside the socket can increase rapidly producing excessive sweating and discomfort due to the heat which can lead to skin problems and bacterial invasion [15]. 58% of amputees experience discomfort with an increase of 2°C [16], and 10 minutes of light walking can produce discomfort from the heat and sweat [17]. It is difficult to determine a reference temperature value, as it depends on age, gender and type of activity carried out. The average skin temperature, around 31 degrees Celsius, can be used as a reference for thermal comfort [18].

All in all, these are interrelated issues that feedback into each other, so it can be that by addressing one of these factors, the patients will see his or her overall comfort improved.

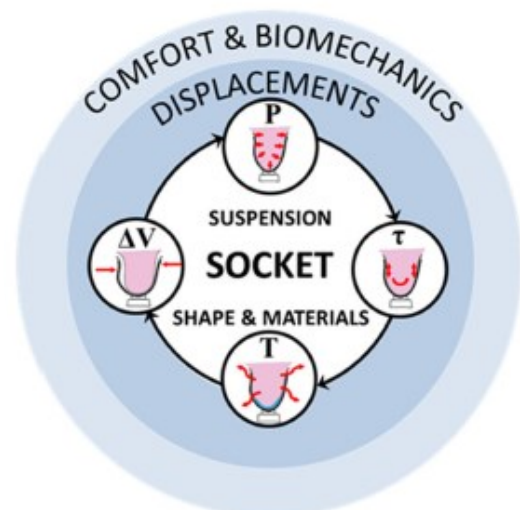


Figure 5. Parameters affecting prosthesis comfort [19].

2.2. Smart prosthetic solutions to improve comfort

The use of silicone pads and liners is one of several methods for controlling stump volume fluctuations. Aside from that, sockets can be fitted with straps, buckles, or dials to manually adjust the socket fit. These solutions are effective to some extent, but patients must rely on their sensations rather than quantitative data to determine whether those liners or pads need to be replaced or moved. Furthermore, their action range may be limited, and adding a liner will only add a few centimetres in thickness when the case is that more precision is required.

Smart prosthetics are artificial limbs that use quantitative data from sensors to control actuators that aim to improve temperature and pressure, and therefore improve the patient's comfort and usability. Furthermore, smart prosthetics can provide personalized adjustments and feedback on the go, which is critical for avoiding injuries and adjusting to changes in the residual limb over time. As a result, they represent a significant advancement in prosthetic technology, addressing users' complex needs more effectively.

Smart prosthetic sockets, in specific regarding below the knee prosthesis, use sensors to monitor data in real time and control actuators that regulate:

- Temperature inside the stump. Several studies propose a system consisting of a fan and heat sink to cool down the temperature [19], some more complex systems add heat pipes to increase cooling efficiency [20], another example adds a metal sheet to increase heat conduction [21].
- Pressure and volume. Regarding actuation, some studies propose the use of air-filled bladders to control the volume changes by means of an air pump, air pressure sensor and pneumatic valve [22] [23], other studies propose a bioimpedance sensing system that control liquid-filled bladders [24], and there are also examples of mechanically actuated panels that regulate the socket fit automatically [25].

Other studies propose smart prosthesis systems that gather quantitative data on the stump pressure to give feedback to researchers and prosthetists, such as a decision support system that outputs socket fitting suggestions to the prosthetists based on pressure sensor data [26], or an inductive sensor system that monitors body positions and activities [27].

2.3. 3D printed prostheses

3D printing technology provides many benefits regarding prostheses design, it can allow for personalised aesthetic designs made to the taste of the patient, but most importantly, it can enable functional designs that aim to improve the traditional prosthesis making process. Conventional prosthesis is a highly skilled task that is time inefficient since it might take multiple fittings to achieve the correct fit. Introducing digital manufacturing tools prosthesis enables personalised designs to be made quickly, affordable and broadens the access of good quality prostheses to the population. With this technology it is even possible for prosthetists to order proprietary designs and have them shipped overseas to any, since it just requires a 3D scan of the stump. Examples to highlight in this area are Limber Prosthetics, which produces a personalised fully FDM printed below the knee prosthesis [28]; Quorum Prosthetics produces an adjustable SLA printed socket that can compensate volume changes on the stump by turning a dial that regulates the compression of a lattice structured panel [29].

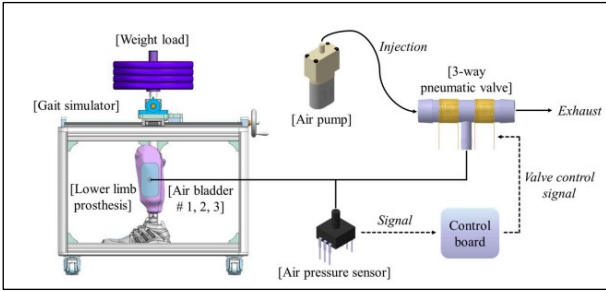


Figure 7. Schematic of automatic volume compensation socket [22].

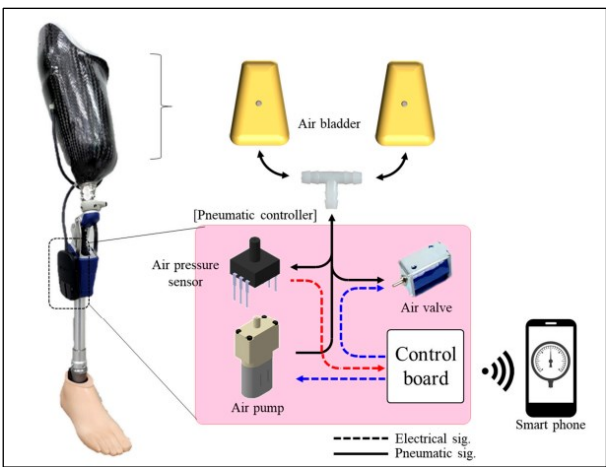


Figure 8. Pneumatic system for pressure regulation on transfemoral prosthesis [23].

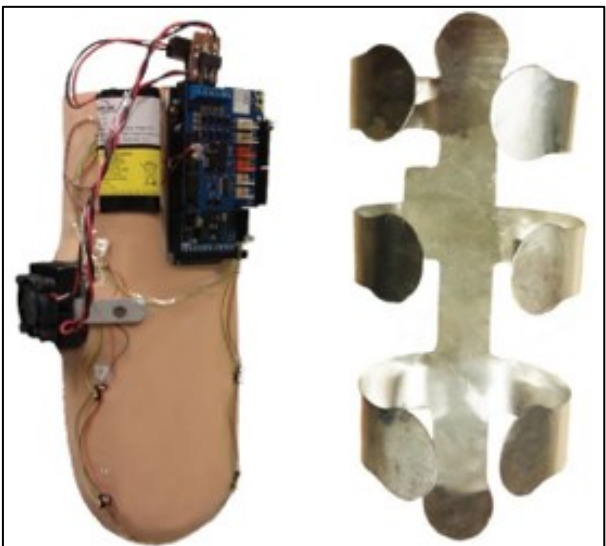


Figure 10. Socket thermoregulatory system [21].



Figure 6. Automatic control of prosthetic socket size [25].

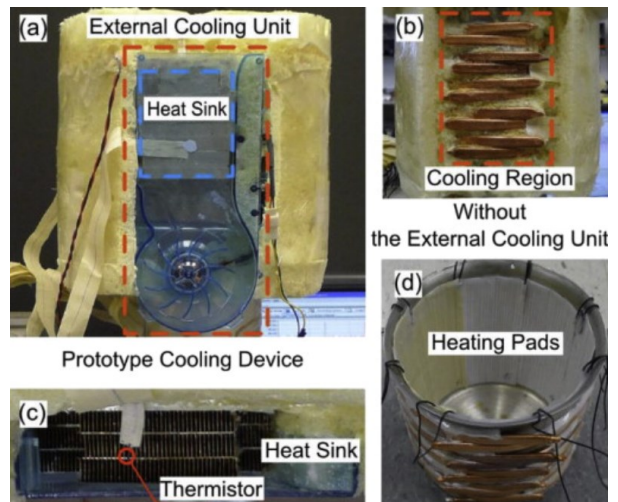


Figure 9. Cooling device prototype [20].



Figure 11. Aquilonix Prosthesis Cooling System by Leto Solutions [19].



Figure 12. Patient trying on a fully 3D printed prosthesis made by Limber Prosthetics (Source: Limber Prosthetics)

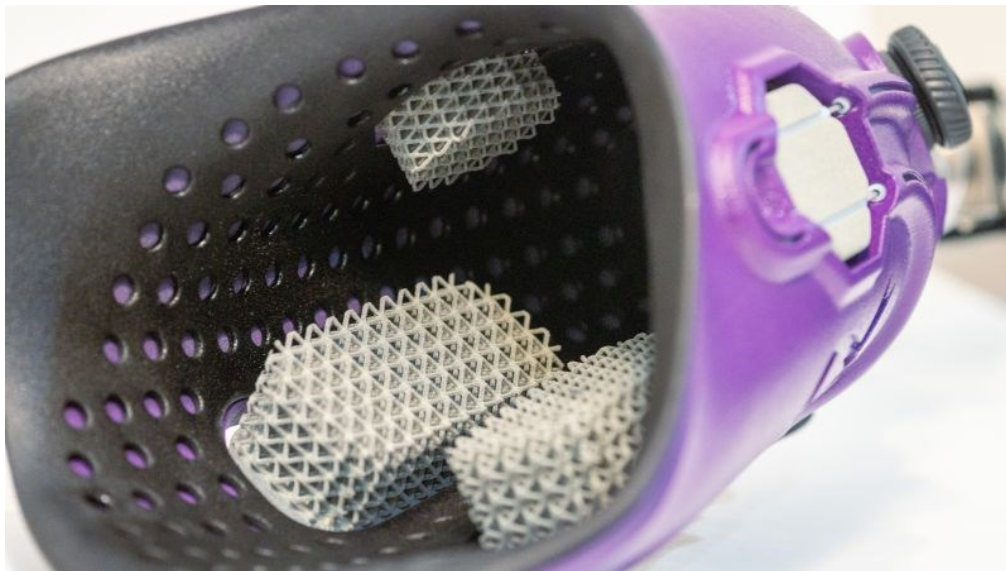


Figure 13. Inside of a Quorum Prosthetics socket, the lattice structure panels that regulate compression can be seen clearly (Source: Quorum Prosthetics)

3. Framework approach

The project approach aims to develop an experimental prototype to extract empirical data on the stump pressure distribution for a transtibial prosthetic socket and compare those results to a computational simulation that emulates that experiment. Finally, those results will be used to elaborate design implications to improve the comfort.



Figure 14. Breakdown of Framework approach steps and the respective items from each step.

4. Materials and methods

This section presents the experiment setup and computational simulation setup. The experiment setup is divided into the prototype components, the testing equipment as well as the sensor calibration, testing. The simulation setup describes the inputs in the computational model.

4.1. Experiment setup

The experiment setup is composed of:

- Prosthesis prototype. Further divided into:
 - Physical components
 - Sensor system and circuit
 - Software
- Testing equipment
 - Testing protocols.

4.1.1. Prosthesis prototype

Physical components (Appendix B, page 37)

The physical components of the prototype are:

- 3D printed socket. Made from PLA, its inner surface has 16 cavities to place each FSR.
- Prototype stump. Consisting of 3 parts: silicone part made of A12 casted silicone that emulates muscle[30], a cement core that emulates bone, and the aluminium fixture attaches the prototype to the cyclic loading machine (Figure 16). The silicone stump is fitted with a stocking to reduce the friction when introducing it in the socket. Within the stump there are 16 points where the Force Sensitive resistors are positioned with the goal of providing an overview of the pressure distribution (Figure 15). In a real leg, these points would correspond both to areas that have more muscle tissue and areas that are more bony, less sensitive and more sensitive respectively.

Sensor system and circuit

Composed of the following elements:

- Breadboard and perfboard.
- 16 FlexiForce A201 Force Sensitive Resistors, range of 445N (Appendix A).
- 32 PU rubber disc 12 mm of diameter and 2mm thick.
- Adafruit HUZZAH32 microcontroller [31].
- 100 k Ω resistor.
- 100 nF capacitor.
- HC4067 16-channel analog multiplexer [32].

The breadboard is used to quickly prototype electronic circuits, once the circuit was definitive it was translated into a perfboard. Force Sensitive Resistors are broadly used in application that require pressure and force sensing due to its ease of integration, varying sensing range and sturdiness. Following the manufacturer's

mechanical integration guidelines [33], PU discs are glued to both faces of each FSR sensor to ensure a good contact on the sensing area. The FSR sensors are adhered to the socket using double sided tape.

Regarding the microcontroller, this can be substituted in the future for a more compact version like the Seeeduino XIAO although it is important to take into account the ADC bit resolution of the microcontroller since the sensor reading range will be affected by that. This can be solved using the ADS1115 16-bit ADC module, that way the range will go from 0 to 65535 regardless of the microcontroller of choice; therefore, this module also will provide a much accurate and higher resolution in the reading.

The resistor is key since it determines the sensor sensitivity, although the range will stay the same. The resistor value is chosen from the recommended one for a voltage divider circuit in the electrical integration guideline of the manufacturer [34]. The capacitor reduces the spikes in voltage, therefore having a more stable and smoother sensor reading. The multiplexer combines multiple inputs into a single data stream, it allows to connect the 16 FSRs to the microcontroller using 5 GPIO pins instead of 16, which makes the setup simpler.

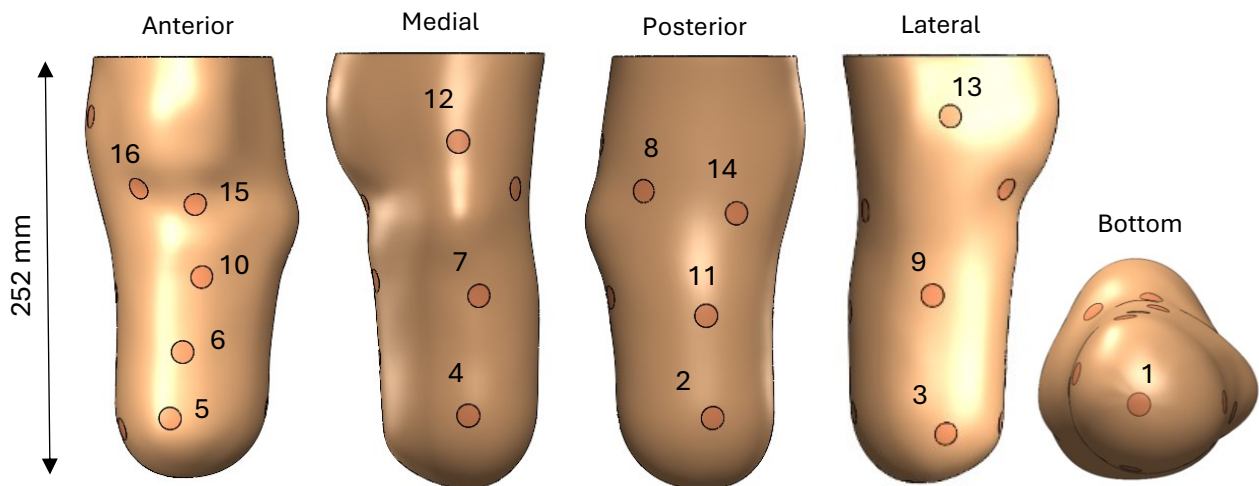


Figure 15. FSR sensors position on the stump



Figure 16. Realistic stump 3D model (left) and 3D printed socket (right)

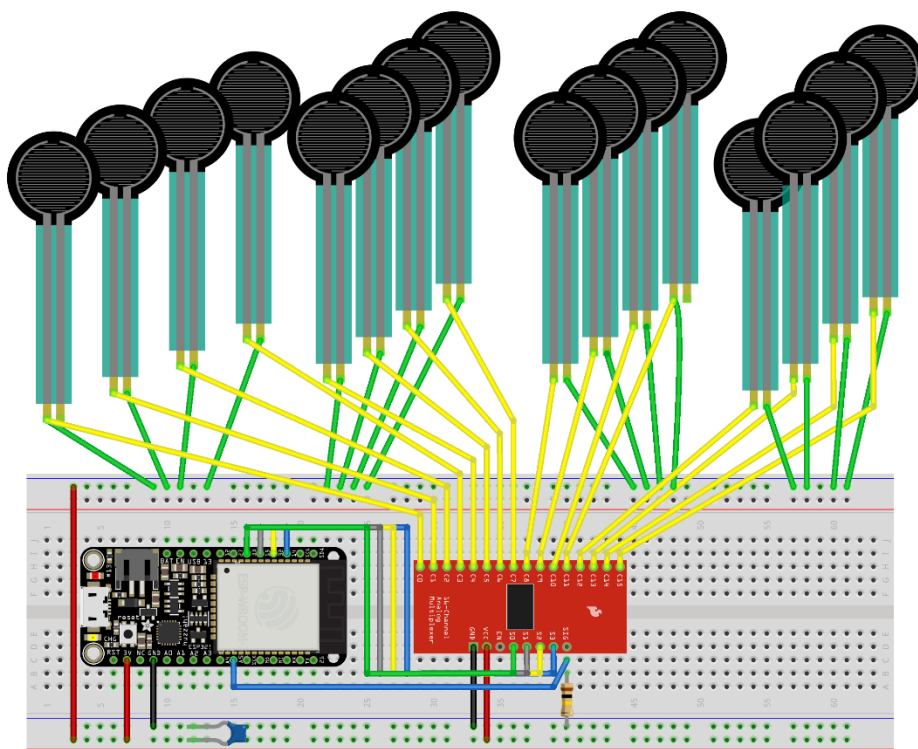
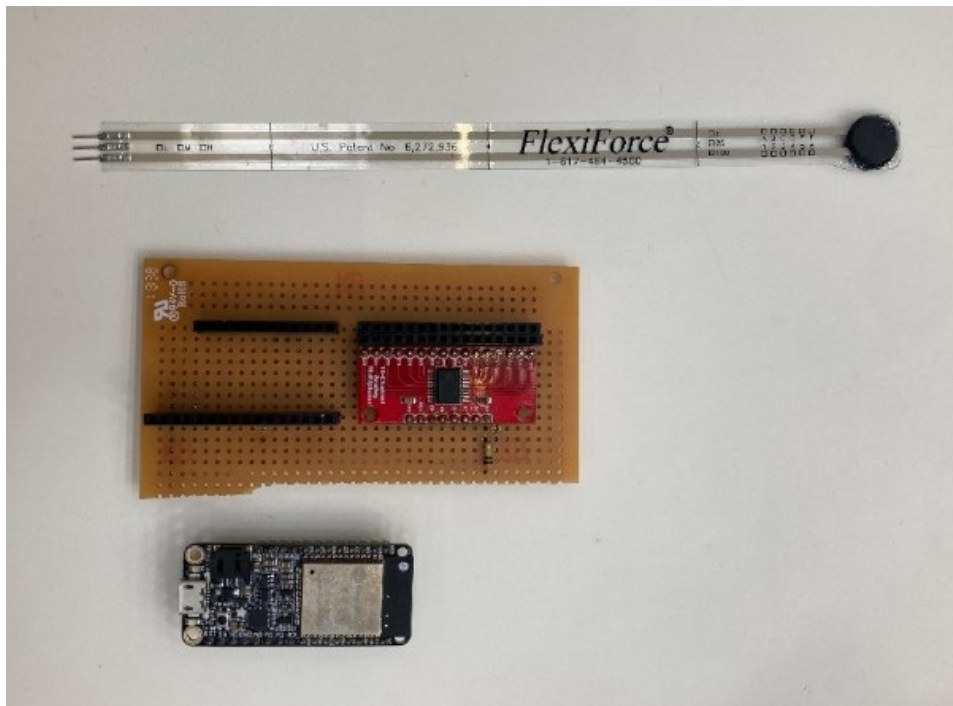


Figure 17. Last iteration of the electronics circuit mounted on a perfboard (top), and Fritzing schematic of the circuit (bottom).

Software

These are the programs used during the project to monitor the microcontroller, save the data and visualise it:

- Arduino IDE has been used to program the microcontroller. Two programs have been developed:
 - Sensor calibration code (Appendix C, page 3937). This code is used to calibrate the FSR sensors, the code reads the analog value of one FSR sensors which can be related to the known applied load from the machine.
 - Calibrated code (Appendix D, page 42). This code outputs sensor readings as a load based on the calibration test results, it reads the 16 FSR signals connected to one multiplexer, and outputs a string of 32 values. These are the raw sensor and calibrated value pairs for each of the 16 sensors.
- Python script to save sensor data as a .CSV file (Appendix E, page 45). The script connects the microcontroller COM port to read the string of sensor data and save a .CSV file to postprocess the data.
- Grasshopper file to visualise the sensor data. Python codes assign a jet colour map value to the given Force values on the respective point location and interpolates the colours over the mesh (Appendix F, Appendix G). The file has three inputs: the .CSV file with the FSR values, the stump mesh as an .STL file, and the 16 points of the FSR location as an .XYZ file. The outcome is attached in (Appendix R, page 86).

Testing equipment

The experimental prototype is tested on an Instron ElectroPuls E10000 cyclic loading machine.

4.1.2. Testing protocols

Sensor calibration test protocol

The goal of this test is to evaluate the repeatability of the acquired sensor data, as well as extracting the calibration curves for every sensor. This protocol is applied individually to each of the 16 sensors 3 times in total. The cyclic loading machine applies compression in the Z direction, the protocol is divided in the following stages:

1. Load step 1: from 0 to 50 N, hold 50 N for 20 seconds.
2. Load step 2: from 50 to 250 N, hold 250 N for 20 seconds.
3. Load step 3: from 250 to 500 N, hold 500 N for 20 seconds.
4. Load step 4: from 500 to 750 N, hold 750 N for 20 seconds.
5. Load step 5: from 750 to 1000 N, hold 1000 N for 20 seconds.

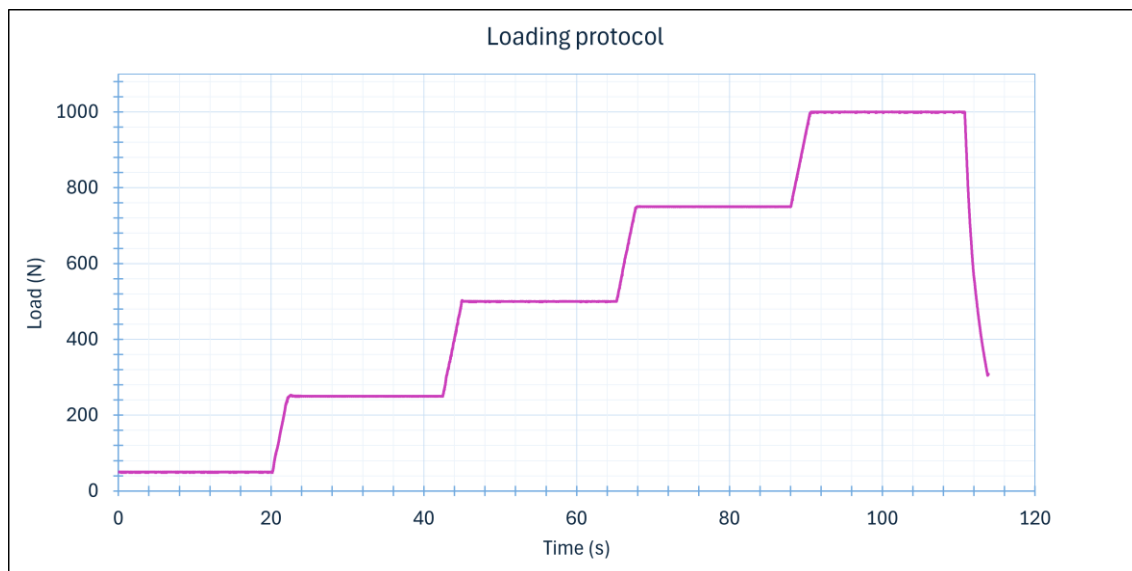


Figure 18. Loading protocol applied by the cyclic loading machine in the tests.

Socket step load test protocol

After the calibration was performed, the 16 FSRs were placed in the prosthesis prototype. The cyclic loading machine applies the previous loading protocol on the prototype fixed to the machine.

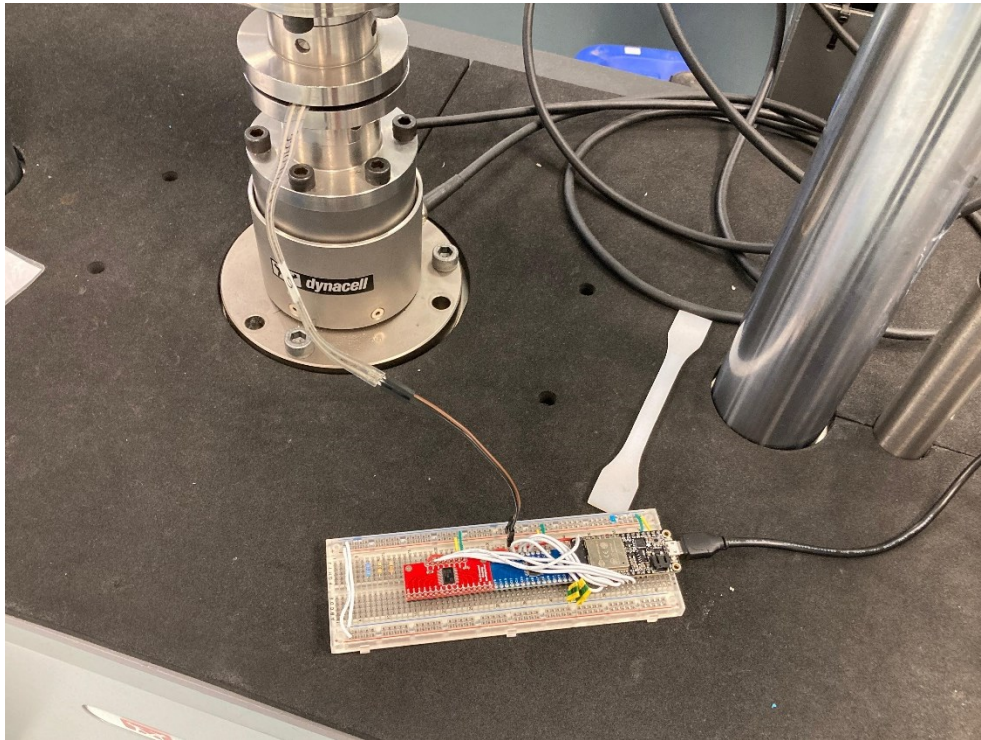


Figure 19. Sensor calibration setup

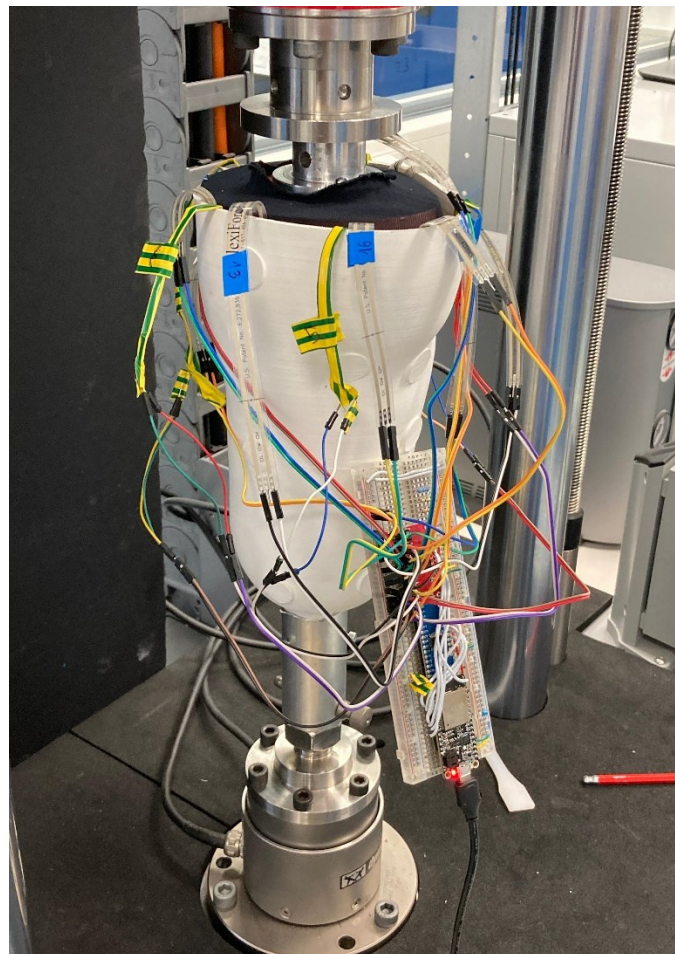


Figure 20. Socket sensor experiment setup.

4.2. Simulation setup

This section describes the simulation performed in this study with the goal of comparing the sensor data from the experiment with the aim of validating it.

4.2.1. Experimental test simulation

The simulation is setup to replicate the experiment conditions as close as possible, while modifying it slightly to simplify it. The imported 3d model of the stump is the same as the physical version, however the socket 3D model is modified to simplify the PU discs fixed to the FSRs, and the cement core and fixture are not included. The simulation inputs are described below:

Materials

- Silicone. Since the silicone manufacturer does not specify the mechanical properties of the material, this material inputs are adjusted so that the simulation has a comparable Load against Displacement curve to the one from the experiment (Appendix H):
 - Young’s Modulus: 2 units (2 MPa).
 - Poisson ratio: 0,45.
- PLA.
 - Young’s Modulus: 1650 units (1650 MPa).
 - Poisson ratio: 0,3.

Parts

- Stump. 3D deformable solid part, assigned the “Silicone” material.
- Socket. 3D deformable solid part, assigned the “PLA” material.

Steps

- Type: Static, general. Inserted after Initial Step:
 - Time period: 1.
 - Maximum number of increments: 10000.
 - Increment size: 0.001; 1E-11; 0.1.

Interaction

- Contact Interaction Property.
 - Tangential Behavior. Friction formulation: Penalty; Directionality: Isotropic; Friction Coefficient: 0,7.
 - Normal Behavior. Pressure-Overclosure: “Hard” contact; Constraint enforcement method: Default.
- Surface to Surface Contact.
 - Main surface: socket interior surfaces.
 - Secondary surface: stump exterior surfaces.

Constraints, Boundary Conditions and Loads

- Encastre Boundary Condition in the socket bottom cylinder.
- Reference Point in 0,0,330 (X, Y, Z).
- Coupling between Reference Point and Stump interior cavity.
- Displacement, applied on the Reference Point: -4.85mm in the Z direction.

Mesh

- Socket mesh size: 2.5 mm.
- Stump mesh size: 5 mm.

The extracted results will be taken from the respective FSR surfaces on the stump. The process is the following:

- Create XY Data. ODB field output. Variable: Contact Normal Force (Unique Nodal position). Pick the respective nodes manually.
- Plot > Operate XY Data > maxEnvelope operation to extract the maximum Contact Normal Force of the respective surfaces > Save plot > Plug-ins > Tools > Excel Utilities > Select respective XY Data.

Besides this, the Reaction Force and Displacement in the Z direction in the Reference Point are extracted to compare it with the cyclic loading machine data. The pressure values can be calculated from the Contact Normal Force knowing that the diameter of the FSR sensing area is 9.52 mm.

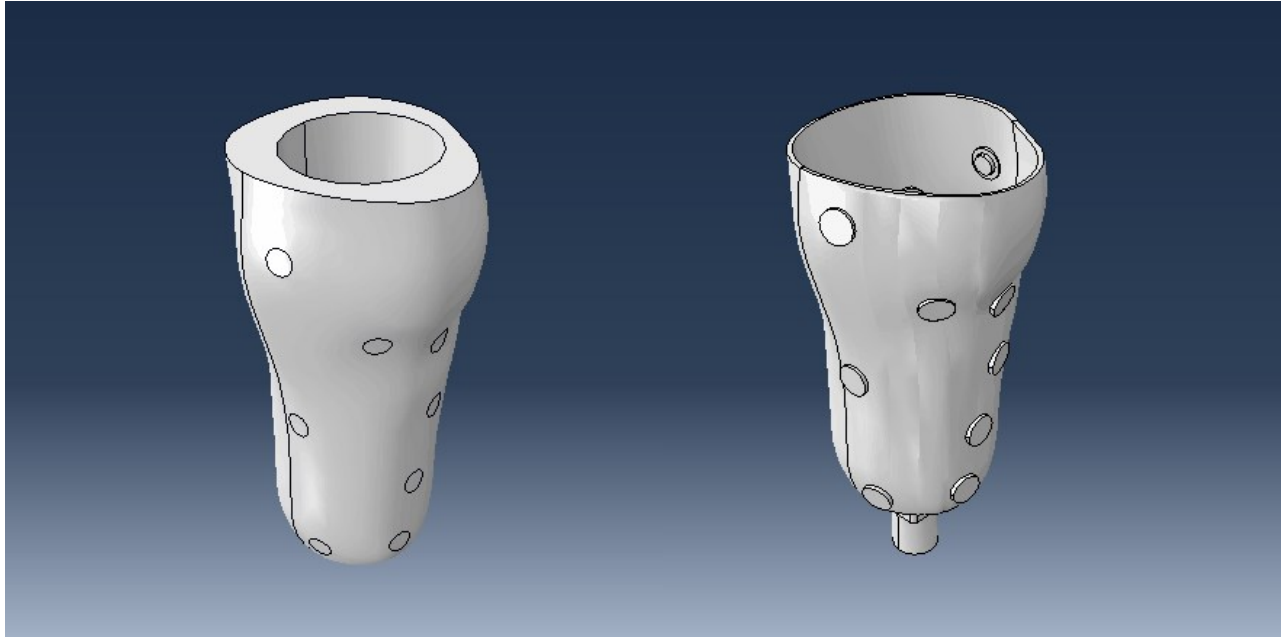


Figure 21. 3D models imported to the simulation. These are the same models used in the experimental prototype.

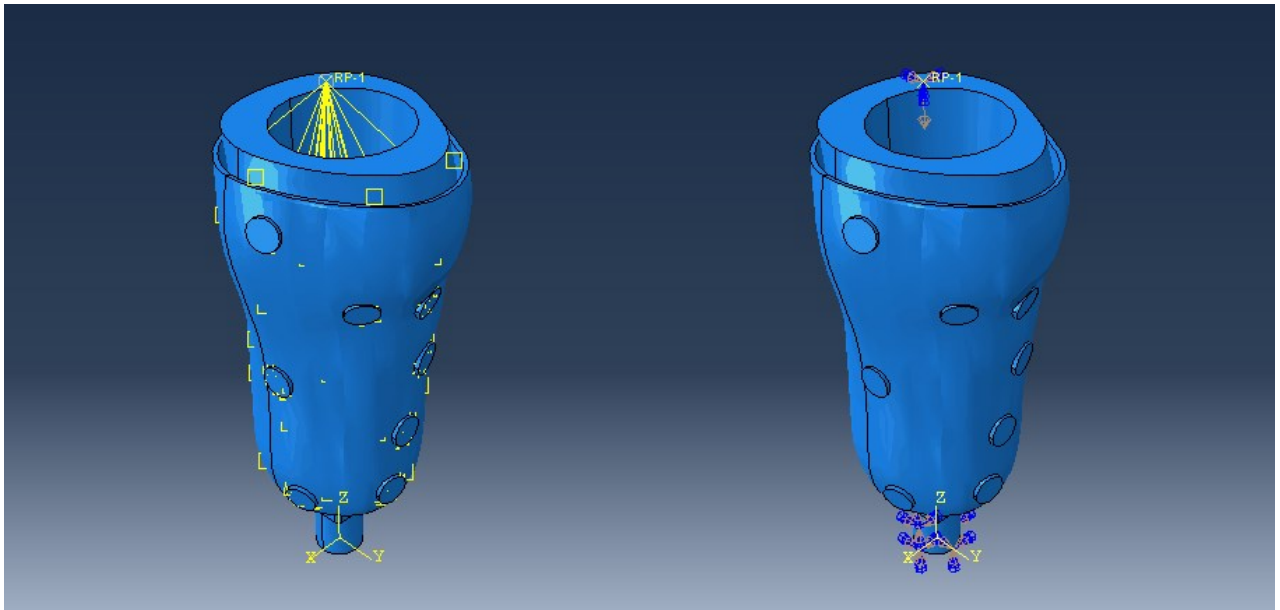


Figure 22. Boundary conditions, constraints and displacement input in the simulation.

5. Results

5.1. Experimental results

5.1.1. Sensor calibration test results

The first part of this test is focused on gathering a set of measurements with the goal of finding out how the sensor data for every sensor varies over time and across measurements, following the loading protocol previously described. This can prove how suitable the FSR sensors are for tracking the stump pressure distribution over time.

After the test the data needs to be postprocessed to assess the repeatability of the data and to extract the calibration curves for the FSR sensors. To do this, it is necessary to achieve a single representative value for each sensor in the 5 loading steps; that is, when the stump is applied 50, 250, 500, 750 and 1000N by the machine.

Each of the 16 sensors has 3 sets of measurements. Within the data corresponding to the respective loading steps 50 rows of data are averaged. This way, there are 3 average values for each loading step within a sensor. Afterwards, these 3 averaged values are averaged again to achieve a single representative value for the sensor in the respective Loading step. Table 1 shows the test results for FSR1 with its standard deviation, the rest of the FSR sensor calibration test results are attached in Appendix L.

Table 1. FSR1 measurements from sensor calibration test.

<i>Applied Load</i>	<i>AvgFSR1_1</i>	<i>AvgFSR1_2</i>	<i>AvgFSR1_3</i>	<i>AvgFSR1</i>	<i>SD</i>
N	Analog value	Analog value	Analog value	Analog value	Analog value
50	787.92	725.31	624.67	712.63	67.25
250	2700.47	2681.06	2665.94	2682.49	14.13
500	3123.04	3095.65	3085.00	3101.23	16.02
750	3196.41	3170.04	3153.90	3173.45	17.52
1000	3091.14	3094.24	3078.16	3087.84	6.97

Since the used microcontroller has a 12-bit ADC resolution, the analog value range of the measurement goes from 0 to 4095 ($2^{12} = 4096$).

Figure 23 shows the averaged analogue value of the FSRs grouped by the loading step. Within the different loading steps, the FSR outputs are different, this implies that the FSRs will require individual calibration. The standard deviation shows that within the sensors the distribution is relatively small. The sensor measurement dips considerably when the sensor is under 1000N. Besides that, the part-to-part difference is higher in the lower magnitude of the applied load, specifically under 50 N.

Figure 26 shows a line scatter plot of the 3 measurements for FSR1 and their average value, here we can see some small and occasional spikes in the measurement. The line scatter plots for all FSRs can be consulted in Appendix J.

It is important to remark that the values from Figure 23 do not tell anything about pressure distribution yet, for that they need to be calibrated. To calibrate the sensors, the analog value of the sensors (Y axis) has to be linked with the respective load (X axis) at which those values were recorded. Figure 27 shows the 16 calibration curves for the 16 sensors, the individual calibration curves for each FSR are attached in Appendix K.

To retrieve loads in between those recorded values, it is necessary to perform an interpolation. Since the B-spline interpolation is not possible to implement in Arduino, and the logarithmic or exponential interpolation curves did not fit the data correctly, it was decided to make a linear interpolation between the different points that define the sensor calibration curve.

Therefore, a sensor has 5 linear interpolation curves defined by 5 points, one derived from each loading step. This is implemented in Arduino in a similar way to a simple linear interpolation, which is generally described as:

$$y = y_1 + (x - x_1) \frac{(y_2 - y_1)}{(x_2 - x_1)}$$

The Arduino code (Appendix D, page 42) identifies in what linear interpolation the sensor analog value fits, and then calculates the Calibrated Load value. The code requires the input of a matrix with the Load values, and a matrix of 16 x 5 elements. calibration curve values. This implementation is easy and practical when the calibration values need to change or updated, for example if this process is repeated. In this stage it is important to introduce the values in the correct order, matching the order in the matrix where the values are declared with the order of the multiplexer channel reading.

In conclusion, this test provides the following insights and outcomes:

- The sensor data is repeatable.
- The sensors will require individual calibration.
- The sensor readings over 750 N are not reliable.
- The sensor calibration curves.

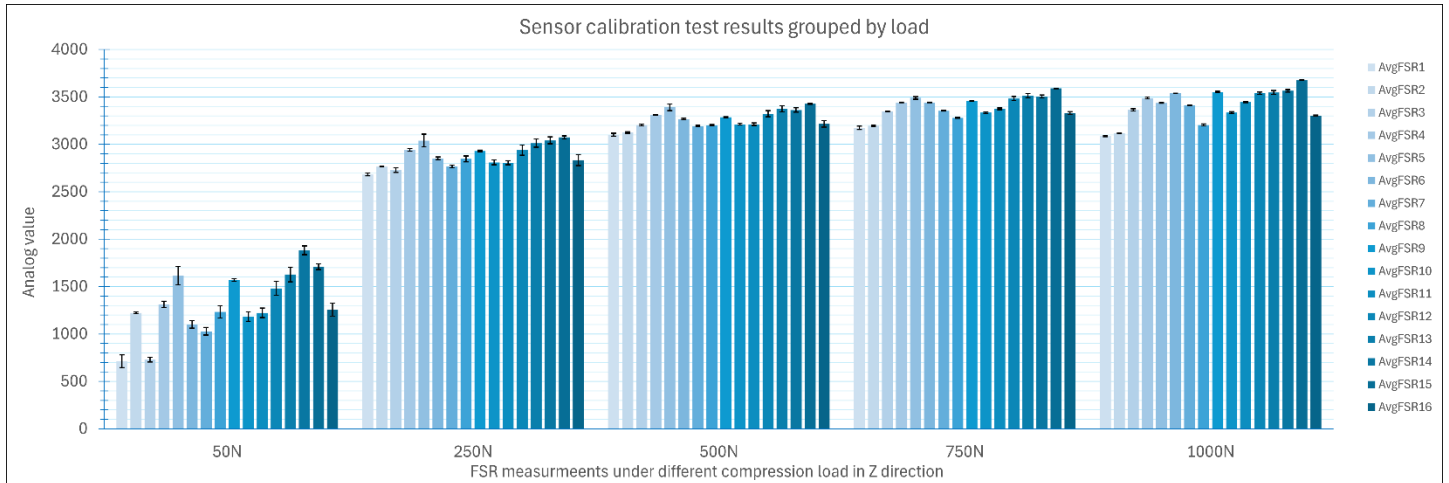


Figure 23. Sensor calibration test results grouped by load.

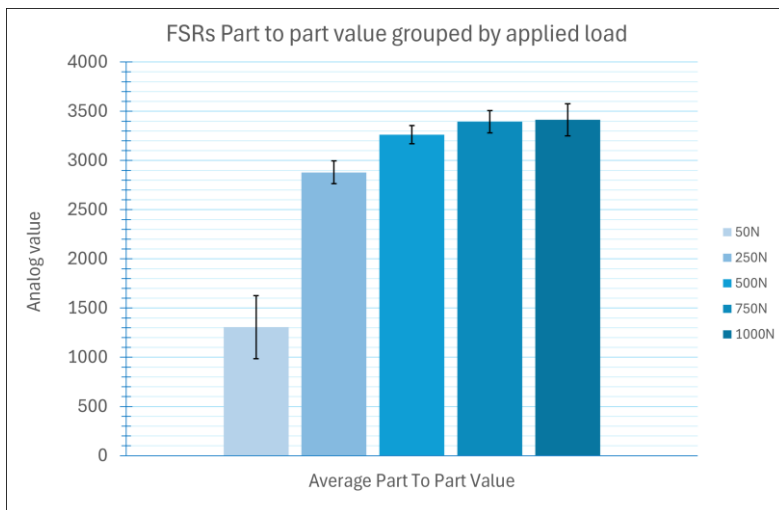


Table 2. Part to part value and error table corresponding to the graph on the left.

Applied Load	Avg Part to Part Value	SD	Mean SD
N	Analog value		
50	1305.36	319.36	144.74
250	2879.21	116.97	
500	3262.49	92.42	
750	3394.11	112.83	
1000	3413.06	163.10	

Figure 24. Part to part averaged value grouped by applied load graph. The standard deviation is particularly high under the lowest applied load.

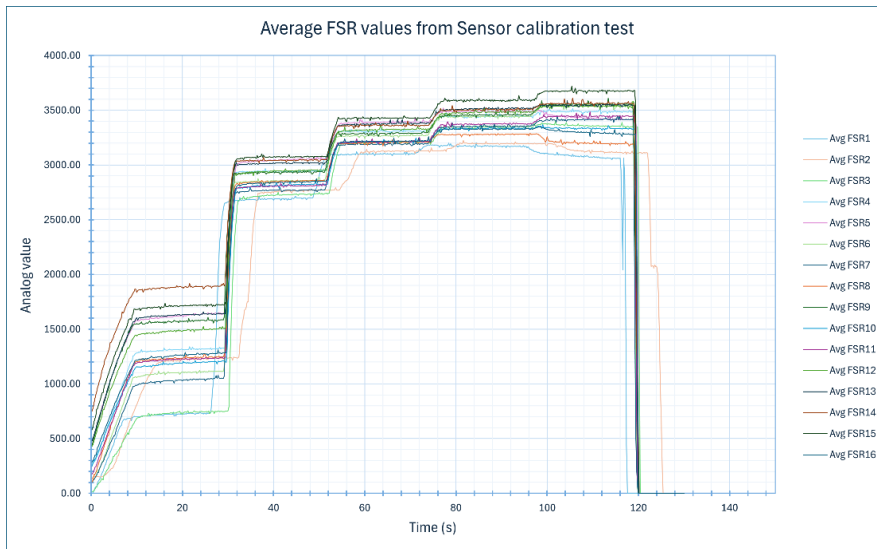


Figure 25. Average FSR values from the 3 measurements of Sensor calibration test.

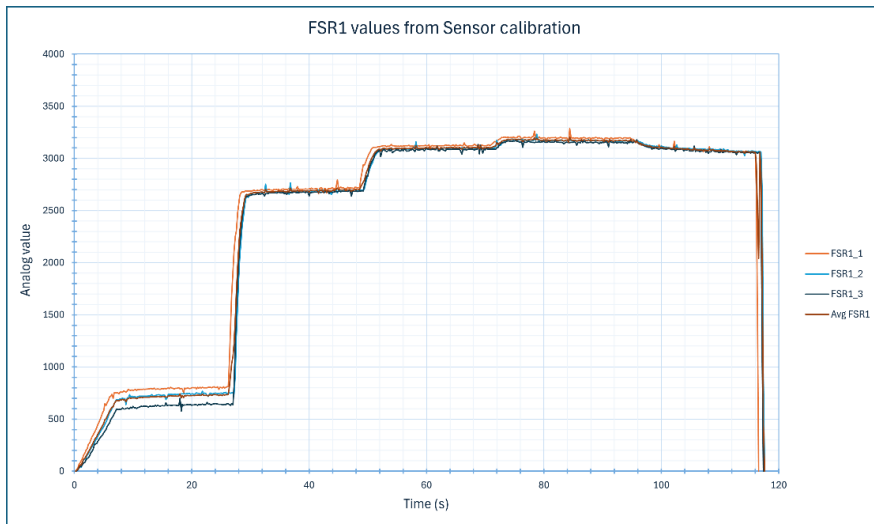


Figure 26. 3 measurements and their average for FSR1 Sensor calibration test.

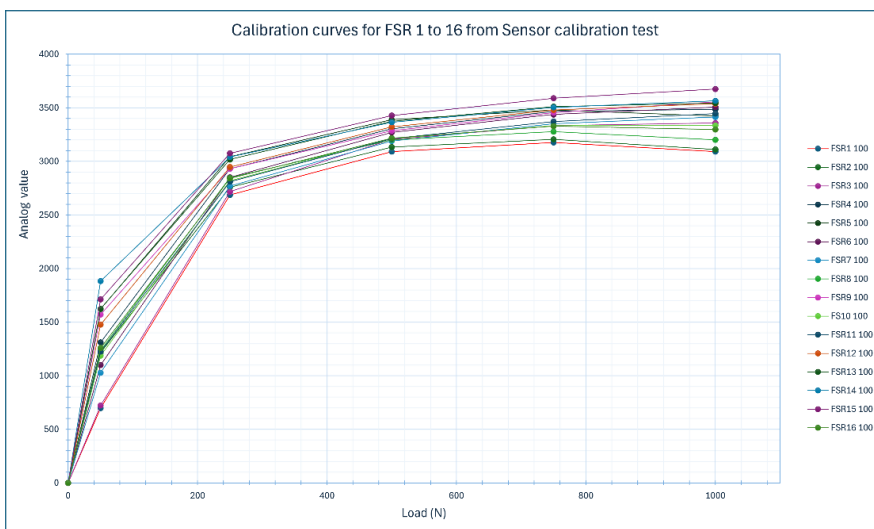


Figure 27. Calibration curves for FSR1 to 16.

5.1.2. Socket sensor test results

In this test, FSRs inside the socket output the calibrated load. The goal of this test is to find out the calibrated load in each FSR location, this will give an idea of the pressure distribution for the respective load case input in the machine.

Figure 28 and Table 3 show the averaged calibrated load results. More information is attached in the appendixes, Appendix M shows the raw and calibrated results in scatter plots, Appendix N shows the calibrated results for the three measurements and Appendix O shows the averaged calibrated values in a column chart.

Regarding the calibrated load, the sensors that output the highest loads are under the stump and under the knee, a sensor in lateral side of the stump, FSR9, outputs the highest load FSR9, about 48 or 50 N when the machine applies a compression of 750 N. FSR1, FSR15, FSR16 are also in the top of the graph, in a bracket between 38 and 42 N under 750 N. FSR3, 5 and 10 output around 35 N. FSR2 and 7 output around 28 and 26 N. On the lower end of the graph, FSR4 and around 7 N and FSR6 outputs around 6 N.

The sensors generally create a line in steps according to load case, the values are staggered. However, some sensors show different behaviours than the rest, describing rather flat lines across the test. FSR14 outputs a flat and high line of 32 N, FSR11 shows another flat line of about 18 N, FSR8 describes another flat line that starts on 17N and ends on 22N. On the lower end, FSR12 outputs a flat line around 4 N at its peak and FSR13 outputs 0 N across the tests.

Overall, these test results provide an overview of the stump pressure distribution. Across the tests, it is possible to identify that the sensors are responsive to the different loading steps and each sensor outputs a load value. Nevertheless, the sensors present spikes in measurements and drift, these are undesirable but unavoidable. Moreover, the measurements dip when the socket is applied a compression load of 1000 N, although the sensors are not close to the sensor range limit, but it is not a problem of the calibration since the raw analog values also show a dip in the same stage.

In this test, we have identified that the points under the highest stress are mainly below the knee and under the stump (FSR1, 9, 15 and 16), sensors with the lowest stress are FSR 6,12,13. All in all, the sensor measurements seem to be logical, but the data needs to be compared against the simulations to draw further conclusions from the results.

Applied Load	FSR1		FSR2		FSR3		FSR4		FSR5		FSR6		FSR7		FSR8	
	Avg Val	SD														
N	N	N	N	N	N	N	N	N	N	N	N	N	N	N	N	N
50N	24.61	1.48	6.95	1.11	3.59	0.41	2.45	0.42	11.27	1.00	0.00	0.00	14.69	1.02	17.22	0.36
250N	31.38	2.15	15.66	0.65	16.40	1.80	8.44	0.28	20.40	1.13	0.06	0.06	19.80	0.59	20.10	1.48
500N	37.14	2.17	19.64	3.53	27.54	0.95	14.05	0.47	29.41	0.75	5.52	1.23	24.42	1.60	21.41	1.27
750N	42.46	0.24	27.68	1.08	34.80	1.87	18.81	1.49	36.61	0.73	12.17	1.50	26.93	1.68	22.04	0.51
1000N	29.99	1.15	14.95	0.39	15.74	0.72	7.42	0.56	22.10	0.13	0.01	0.01	20.33	0.98	20.86	1.27

Applied Load	FSR9		FSR10		FSR11		FSR12		FSR13		FSR14		FSR15		FSR16	
	Avg Val	SD														
N	N	N	N	N	N	N	N	N	N	N	N	N	N	N	N	N
50	35.57	0.36	16.95	0.74	16.51	1.14	3.11	0.80	0.01	0.01	30.50	0.27	27.11	0.99	26.04	0.88
250	44.05	1.48	23.27	3.12	17.98	0.43	3.92	0.57	0.00	0.00	31.85	0.61	32.75	1.13	33.24	0.44
500	46.87	1.27	31.53	3.18	17.32	1.29	3.38	1.11	0.00	0.00	32.85	0.47	36.48	0.65	38.44	0.71
750	47.94	0.51	36.50	3.50	17.97	1.40	2.65	1.22	0.00	0.00	33.17	0.62	37.92	0.45	40.32	1.81
1000	41.08	1.27	24.60	1.69	15.10	0.70	2.56	1.03	0.00	0.00	32.10	0.45	32.01	0.58	33.96	0.63

Table 3. Socket sensor test results.

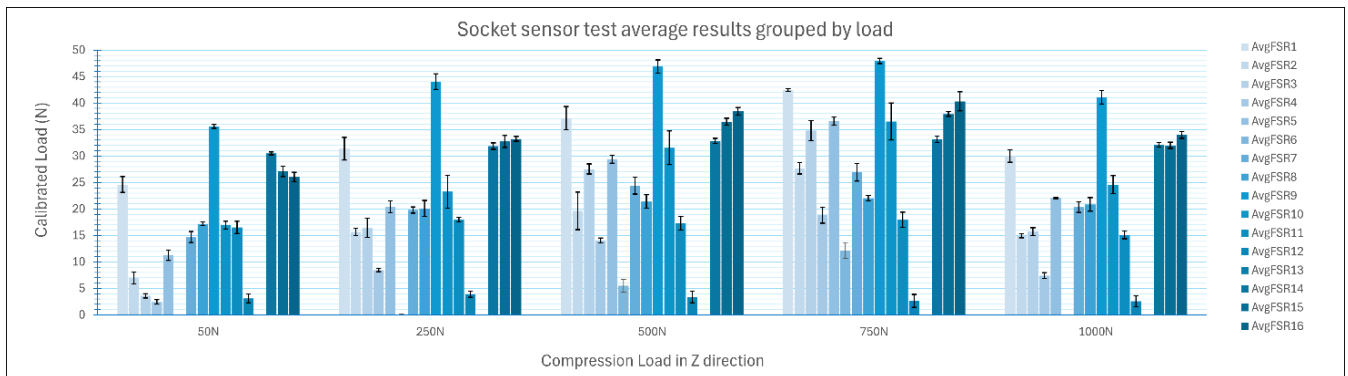


Figure 28. Socket sensor test results grouped by load.

5.2. Experimental simulation results

The model outputs the Normal Contact Force in Newtons with a displacement in the Z direction of 4.85 mm, which corresponding to a compression load of 496 Newtons. The simulation values are extracted from the corresponding FSR contact surfaces in the stump. The results are presented in the following sections below (Figure 30), in Appendix P there is a graph and a table that shows the simulation results over the simulation increments.

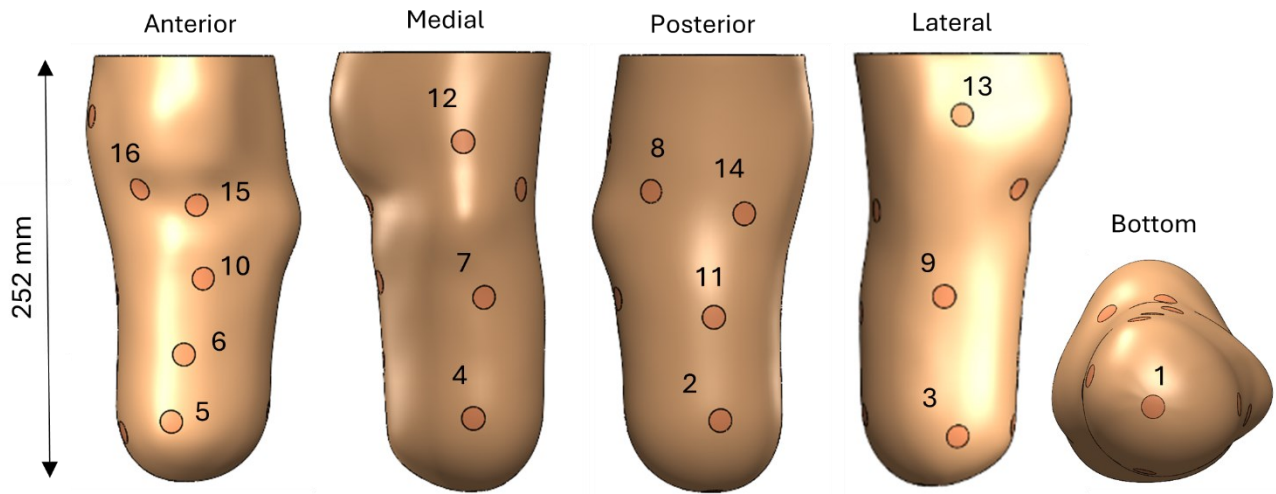


Figure 29. FSR sensor position on the stump.

The highest values occur in FSR1, on the bottom of the stump, which outputs around 10 N; and in FSR16, below the knee, with 6.55 N. Overall, the rest of the sensors output similar values between 1.75 and 3.81 N. FSRs 6, 12, and 13 output values close to 0 N. A reasoning for these results will be commented in the Discussion.

Table 4. Simulation results for FSRs under a compression of 496.33 N.

FSR	1	2	3	4	5	6	7	8	9	10	11	12	13	14	15	16
Contact Normal Force (N)	10.60	2.85	3.81	3.18	1.97	0.52	3.25	1.13	2.38	1.75	1.23	0.51	0.00	2.36	2.82	6.55
Applied Compression on Specimen (N)	496.33															

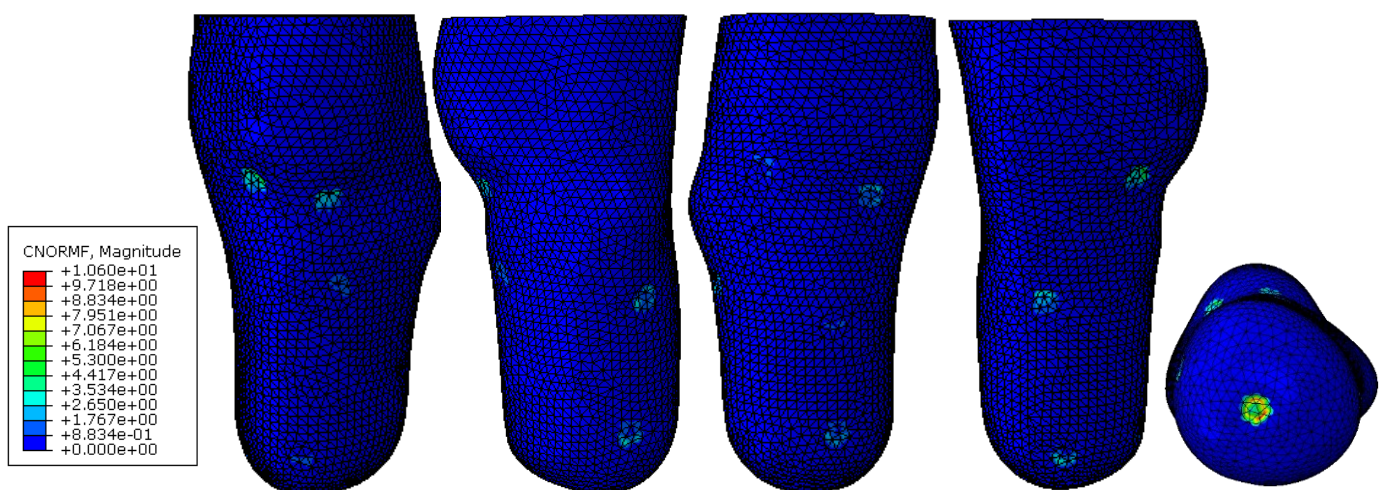


Figure 30. Simulation results views for an applied compression load of 496 N. From left to right: anterior, medial, posterior, lateral and bottom

5.3. Comparison

A selection of comparison is shown below, the complete chart with the comparisons for all the FSRs can be consulted in Appendix Q. Overall, the physiological conditions and the experimental data show a dissimilarity on the magnitude of force in the sensors, although there is a correspondence in the distribution of the highest and lowest pressure points across the experiment and simulation.

For example, FSR1 and 16 on the top end and FSR6, 12 and 13 on the bottom end. The highest values in the simulation are FSR1 and FSR16, their simulation value is around a third of the experiment one, but they show a similar slope. In the lower range, the results have a similar magnitude, where the values for FSR6, 12 and 13 are close to 0 N. There is an anomaly in the results, in the experiment FSR9 is the point with the highest force value while in the simulation it shows a much lower value, similar to the FSRs around it.

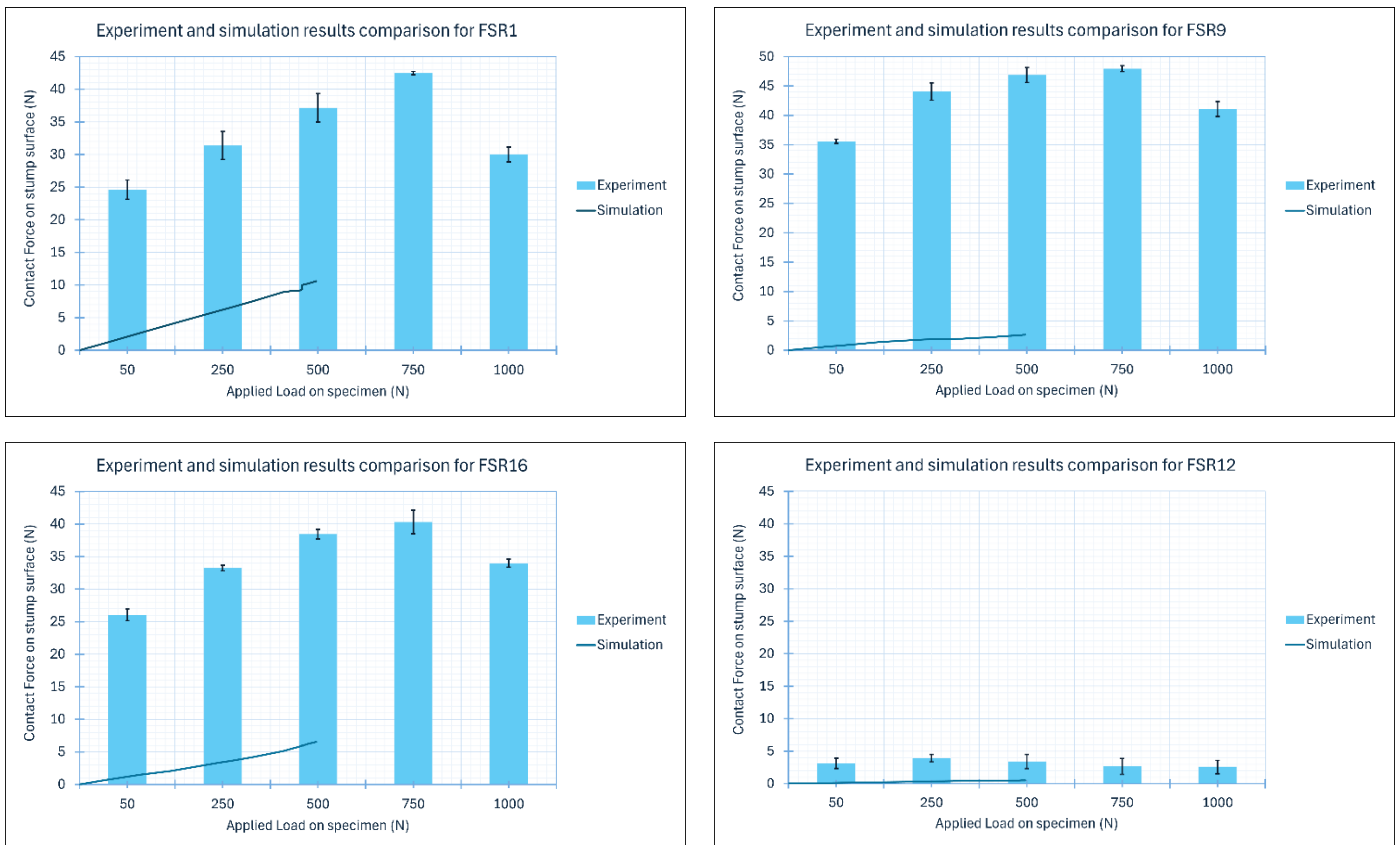


Figure 31. Comparison between the experiment and simulation results. From left to right, top to bottom: FSR1, FSR9, FSR16 and FSR12

Table 5. Comparison of the Experiment and Simulation Pressure and Force values when the specimen is under a compression load of 500N

Simulation and Experiment Force and Pressure output. Specimen under compression load of 500 N																	
Test	Unit	FSR															
		1	2	3	4	5	6	7	8	9	10	11	12	13	14	15	16
Sim	F (N)	10.60	2.85	3.81	3.18	1.97	0.52	3.25	1.13	2.38	1.75	1.23	0.51	0.00	2.36	2.82	6.55
	P (MPa)	0.09	0.03	0.03	0.03	0.02	0.00	0.03	0.01	0.02	0.02	0.01	0.00	0.00	0.02	0.02	0.06
Exp	F (N)	37.14	19.64	27.54	14.05	29.41	5.52	24.42	21.41	46.87	31.53	17.32	3.38	0.00	32.85	36.48	38.44
	P (MPa)	0.33	0.17	0.24	0.12	0.26	0.05	0.22	0.19	0.41	0.28	0.15	0.03	0.00	0.29	0.32	0.34

Area determined by the PU disc radius = 6.00 mm

6. Discussion

This section presents the interpretation of the data gathered on this study. The Discussion section is composed of the Reflection on the results, Reflection on the methods, Limitations of the study and Design implications.

6.1. Reflection on the results

About the Sensor Calibration tests, the error distribution seems to be the highest in the lower magnitude loads, specifically when the stump is subjected to a compression load of 50 N. This can be due to the contact pressure not being enough to produce a stable reading. In a similar line, Swanson et al. points out the same phenomenon for FlexiForce sensors with a range of 100 N, although the reasoning for this is not mentioned in the discussion [30]. Besides that, there is a higher error when the applied compression in the calibration test is 1000 N, and the value dips compared to the previous loading step of 750 N. The reason for this is that the sensor range upper limit has been exceeded, which is consistent with the specified range of 445 N of the acquired sensor.

About the Integrated Sensors in Socket tests, the sensors output dips when the applied load on the stump is 1000 N, although the load that the FSRs are under should be lower than that. A concrete explanation for this has not been formulated.

The comparison between the experiment and the simulation shows a similar distribution of pressure for the maximum and lowest values. And although the simulation values are noticeable lower than the experimental, they are in the same order of magnitude. Therefore, refining the simulation is required to further validate the experiment results.

On the experiment side, the difference in value can be due to poor reading of Force Sensitive Resistors when shear stress is the main force component, rather than normal. Moreover, it might be the case that in the experiment the stump is not making good contact with the FSR, or even that stump is pulling away from the sensor. For example, FSR 12 and 13 show results close to 0 N, and they are both angled inwards. Overall, the sensors are good at reading normal forces however, in the prototype the FSRs are under diverse angles and experience a combination of shear and normal stress. FSR9 might output such high value because it is closer to the axis where the load is applied from.

Altogether, the testing show the potential of FSR sensor to monitor the pressure distribution of the stump. The FSRs output useful values and demonstrate that the values under the most pressure are below the knee and at the bottom of the stump. Moreover, the simulation shows an incomplete picture that does not validate the experiment results, so further work is required in this area.

6.2. Reflection on the methods

The sensor calibration was performed with the FSR being sandwiched by the two metal plates of the cyclic loading machine, which does not match the individual load cases in the stump such as the contact angles. Moreover, it is still to be determined how often the FSRs need to be calibrated. It can be the case that it needs to be done every time before a test day, which is suitable for a laboratory setup although inconvenient for hypothetical socket that is worn daily by a patient.

Performing the test with 5 measurements instead of 3 will give a more precise standard deviation. At that time that was not done due to time constraints in the project as well as machine availability.

About the sensor range, the idea was to cover a range from 0 to a couple thousand of newtons to read both walking and jumping conditions and see how far the sensor range was. The acquired sensor range is 445 N and the sensor measurement value dips when it surpasses 500 N. A voltage divider circuit was used because of its simplicity but, the manufacturer mentions that with a non-inverting op amp circuit it can read up to 4448 N. There is the assumption that this would sacrifice sensitivity for range, but it would need to be explored through testing, such circuit was explored briefly but could not be tested due to time constraints (Appendix S).

The simulation results being off compared to the experiment can be due to the simulation not reflecting the experiment conditions. Mainly, because of the material model not being accurate despite approximating the Load vs Displacement to the test data, and because of the simplification of the geometry by joining together the FSR and disc surfaces to the stump or omitting the cement core. Besides that, it is worth mentioning that applying higher displacements that -4.85 mm in Z direction results in the simulation aborting, probably from non-convergence due to large deformations in the model.

6.3. Limitations of the study

The sensor calibration was conducted under a load case different from its intended application. Specifically, the load was applied by metal plates in a normal direction prior to integrating the FSRs into the socket, whereas the load conditions inside the socket are more complex and unique to each sensor. This could affect the results, as calibration should ideally be performed in a situation that is similar to the application.

Moreover, only one sensor type with a specific range was tested; additional tests with sensors of varying ranges integrated into the prototype socket are necessary to compare performance under identical load protocols.

The experiment was conducted in a laboratory using a cyclic loading machine that applied compression only in the Z direction. A sinusoidal cyclic loading test was briefly explored, but due to time constraint it could not be analysed in depth, consult Appendix T to see the graphs. Future steps should involve more realistic setups and load cases, such as applying cyclic load protocols, introducing physiological conditions, and eventually testing on treadmills or with patients. These approaches would simulate real-world conditions and provide a more comprehensive assessment of the suitability of FSRs. Ultimately, creating and testing a prosthetic socket integrated with FSRs in real patient scenarios will offer a definitive evaluation of their effectiveness, as laboratory experiments can oversimplify real gait and load applications.

Additionally, the material properties of the silicone stump in the prototype are unknown, complicating efforts to achieve a comparable result between simulations and experiments. Determining these properties through testing is essential if similar setups are to be used in future tests. Applying a load protocol with a constant load would also allow for a direct comparison of load against displacement on the stump. Finally, increasing the number of test repetitions from three to five would yield a more precise standard deviation, enhancing the reliability of the results.

6.4. Design Implications

This study provides quantitative data on the pressure distribution of the residual limb with an experimental prototype equipped with Force Sensitive Resistors, this data can be used to improve the patient's comfort while wearing the prosthesis through knowledge-based design. From the project, a series of design implications or insights have been gathered in the form of requirements and applications.

6.4.1. Applications

Integrating FSR sensors into prosthetics to provide an overview of the pressure distribution such as the one in Figure 32 can be used to improve user comfort through:

- Monitoring and tracking stump pressure evolution over time for diagnosis.
- Introducing knowledge-based designs and features that improve user comfort.
- Evaluating and validating prosthesis fit.

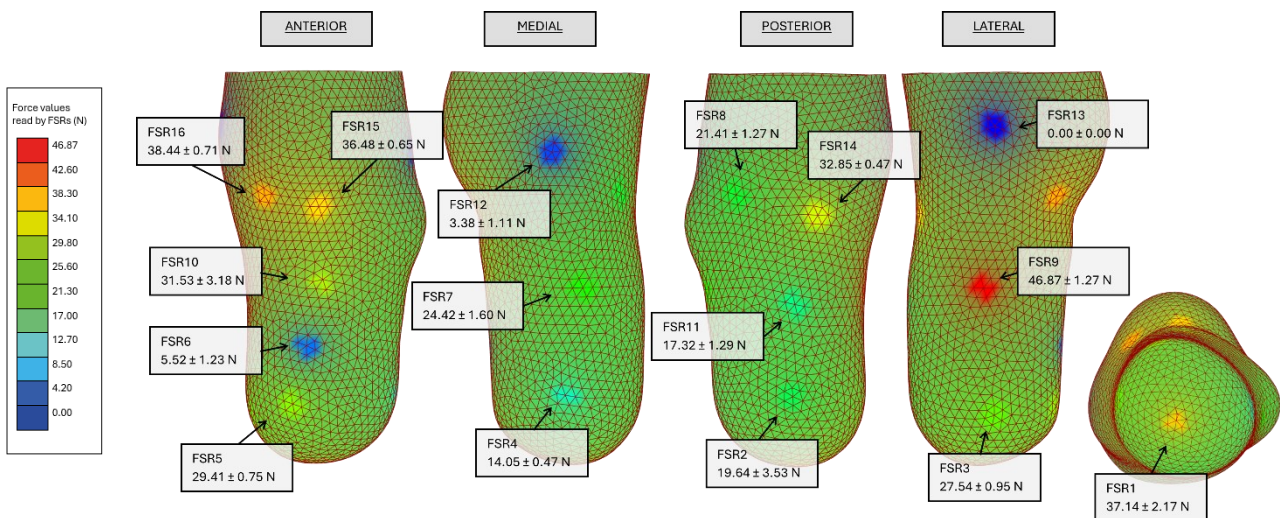


Figure 32. Stump pressure distribution visualisation generated in Grasshopper from experimental FSR data

These applications are developed further into design directions, which are presented as examples to illustrate the potential for this technology Figure 33. Introducing knowledge-based designs and features that improve comfort can take the form of 3D printed TPU structures for padding to reduce pressure points, incorporate shock absorption to 3D printed pylons and feet, provide quantitative data to develop and evaluate topology optimization designs. Moreover, sensor data can be used to control the socket fit through mechanical actuators depending on the pressure changes and activities. Besides, traditional socket design and parts such as liners or pads can be improved with provided quantitative sensor data. Additionally, validating the prosthesis fit and tracking the pressure over time can be done through a 3D printed prosthetic socket for a first fit test or for every-day use. Another possibility worth of mention is integrating the FSRs into liners.

The desirability, feasibility and viability of FSR in prosthetics is discussed below:

Desirability

A 3D printed prosthetic legs that senses the stump pressure distribution offers on the one hand a personalized, affordable, and quick delivery solution for amputees, and on the other hand it provides quantitative data that can be used to monitor the stump progress over time. This technology empowers amputees by providing greater accessibility, attention and care, therefore improving their quality of life. The combination of digital design tools, sensors and real-time data collection enables designers, prosthetists and doctors to valuate and act upon the ensuring that the prosthetic fits well and functions optimally.

Feasibility

The feasibility of 3D printed prosthetic legs is possible by advancements in 3D printing technology and materials, which highly accessible and relatively low budget. The process allows for precise, rapid prototyping and production, reducing the time and cost compared to traditional methods. Additionally, the availability of biocompatible materials ensures that the prosthetics are safe and comfortable for long-term use. FSRs into 3D printed prosthetic legs is a possibility because they can easily be integrated into the prosthesis, they are lightweight and affordable.

Viability

3D printed prosthetic legs are economically viable as they significantly reduce the cost and time of production and enable easier scalability. This option can cover the need of affordable and easily manufacturable prosthetics. The combination of reduced costs, increased accessibility, and the ability to iterate designs quickly makes this technology a sustainable business model with strong potential for future growth in the healthcare sector. While the including sensor adds a cost, the benefits they provide with the improvement of comfort make it and attractive and holistic solution.

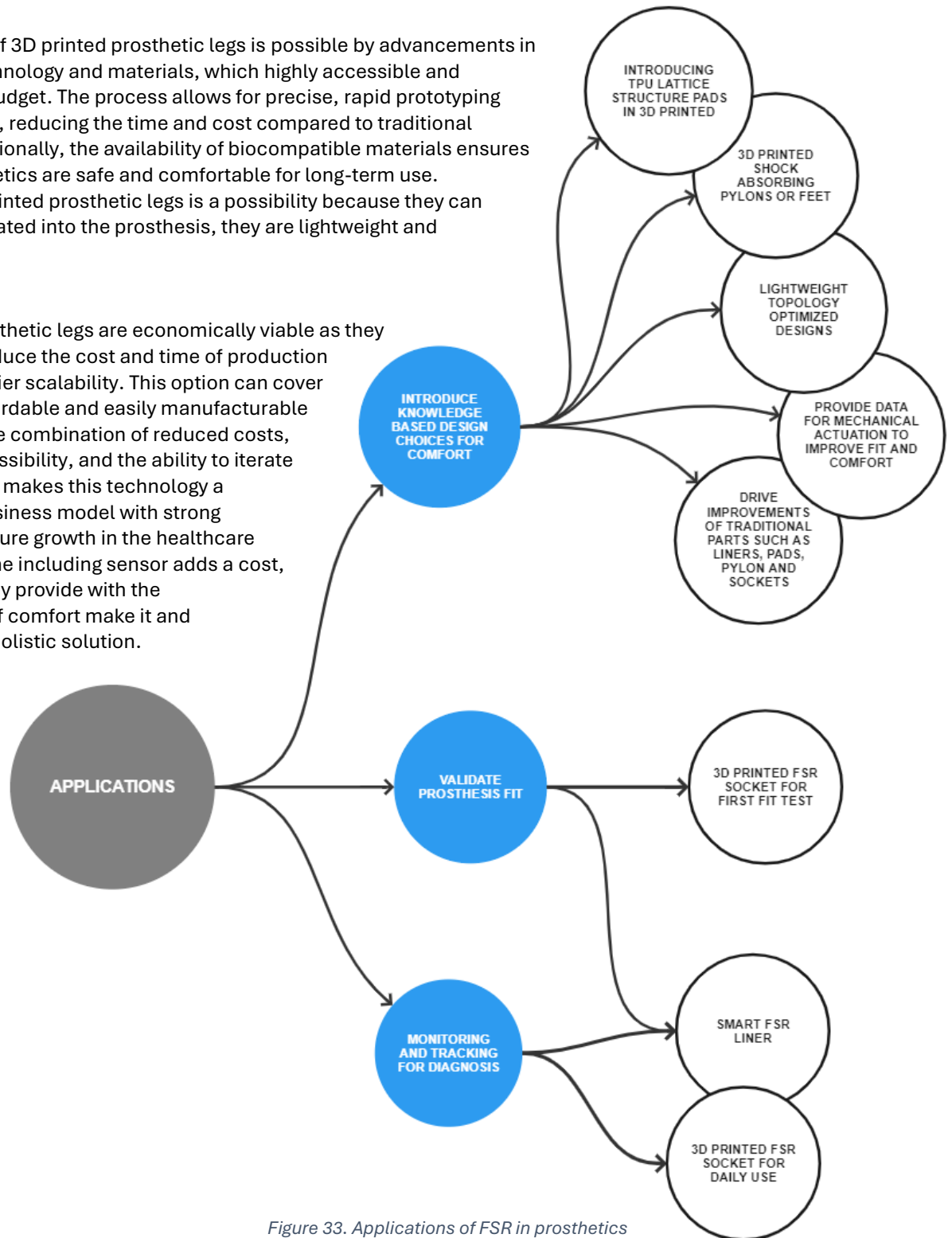


Figure 33. Applications of FSR in prosthetics and potential design directions

The design direction of a 3D printed sensor socket is presented in a conceptual sketch to illustrate its main characteristics and use (Figure 34). This concept presents the features of a future iteration on the experimental prototype elaborated during this project.

3D PRINTED SENSOR SOCKET

This design helps the prosthetist to validate the fit and design of the socket for better patient comfort. First, this socket can be used as a test for the fit, and once the design is set it will be a smart sensor socket that tracks and monitors the stump while it is being used regularly by the patient.

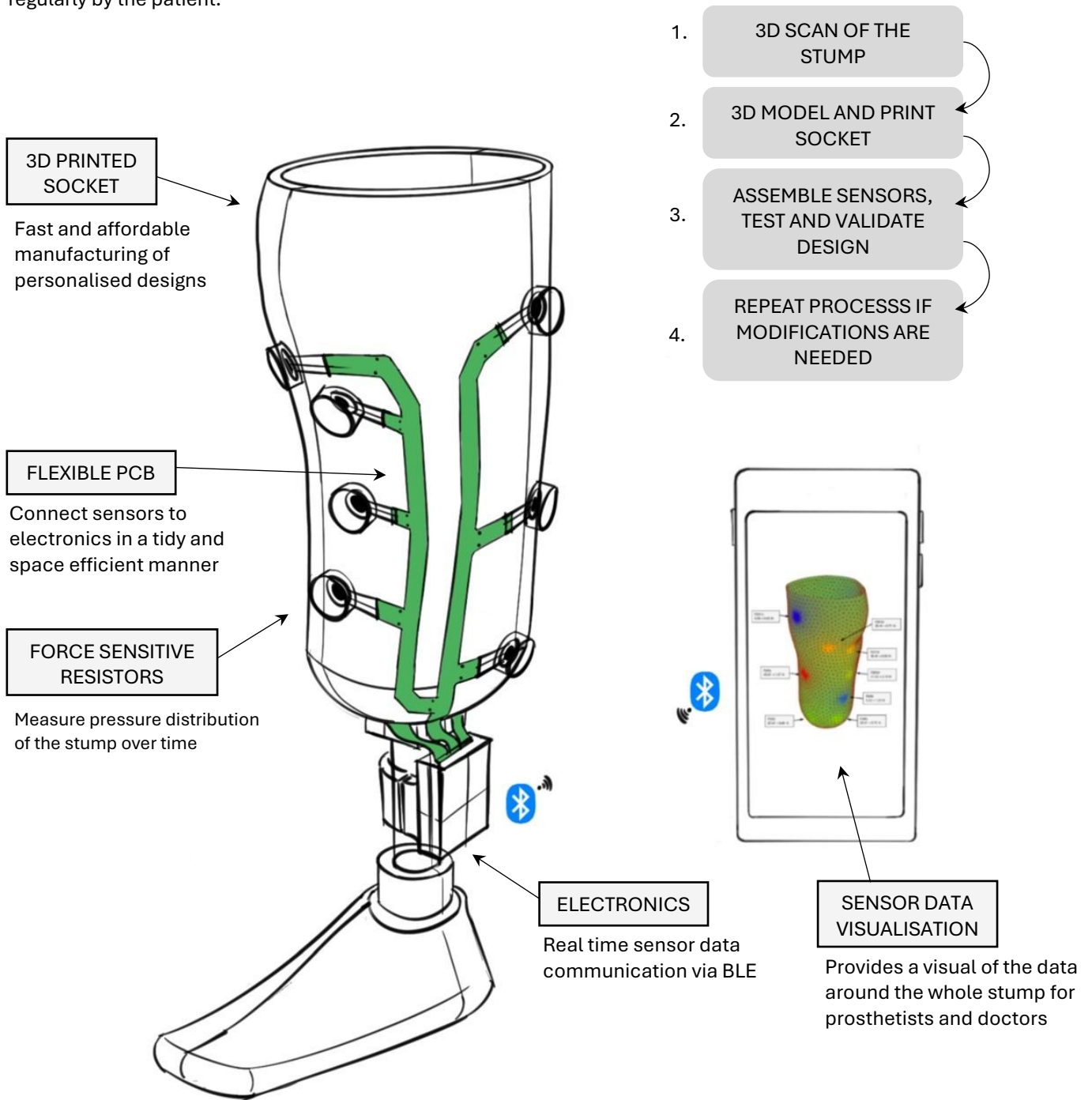


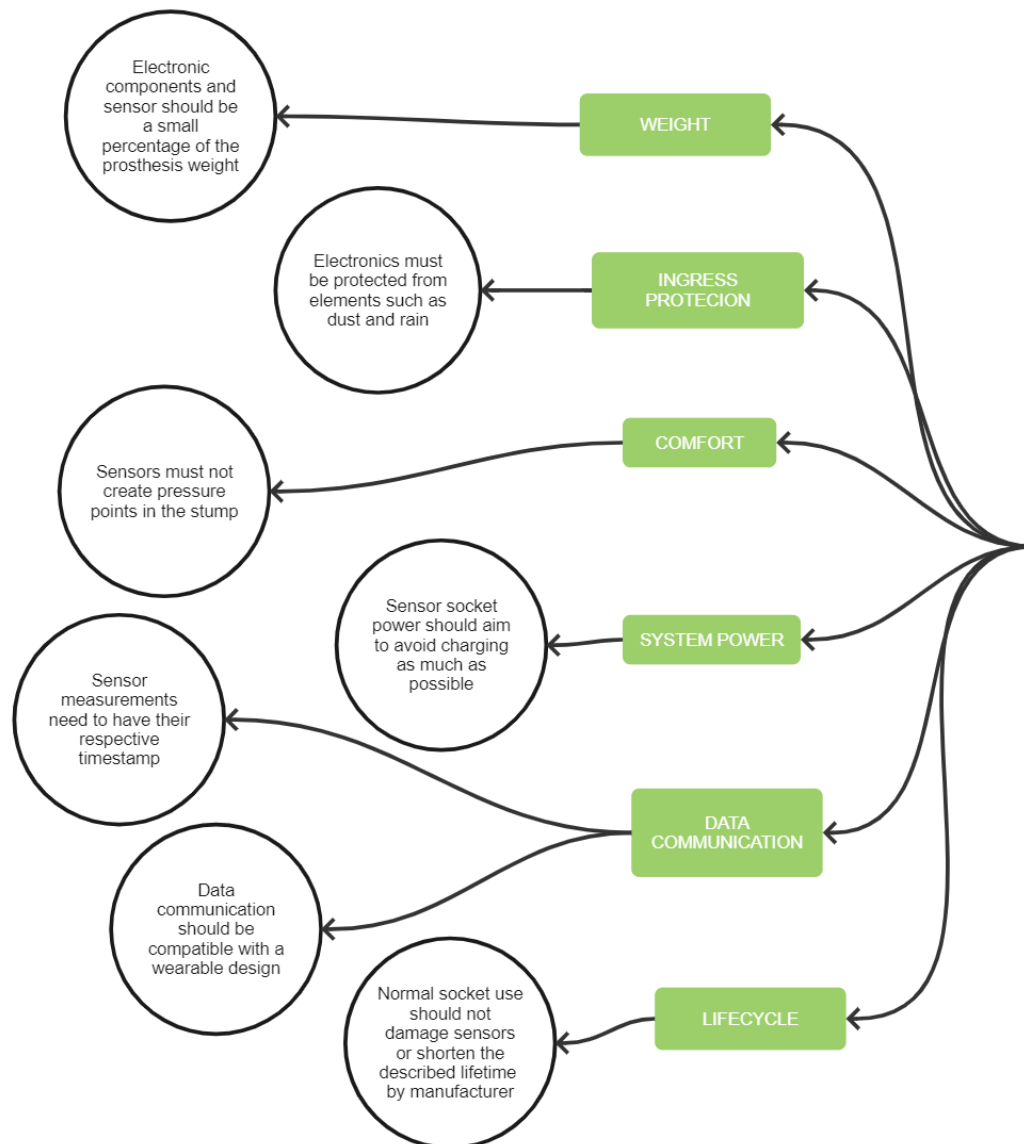
Figure 34. Conceptual design of 3D printed sensor socket to test socket fit and monitor stump over time

6.4.2. Requirements

Throughout the course of this project, various insights into the design goals and needs for a sensor-equipped prosthetic socket emerged and have been compiled into a set of requirements. These insights were gained through tasks such as assembling sensors into the socket and collecting data via a serial port reader. These and other similar tasks generated valuable thoughts on the essential functions and features for future prosthetic designs, forming the basis for this list of requirements.

Therefore, a list of requirements of a force sensing prosthetic socket has been created to state the important characteristics needed for it to be successful. These requirements describe design goals and criteria that can be used for selecting future promising ideas and design proposals and justifying the choices. This list can work as a reference for the future and is subjected to change based on new insights and developments, concrete requirements can be set over time when there is more information gathered concerning stakeholders and the design problem. Due to the stage of development that this project is at, requirements are described as wishes rather than demands, or requirements that must be met about specific number and parameters. So, aspects such as price, weight, lifetime and others are described vaguely described.

Figure 35 present a graphical overview of the list of requirements. In the Table 6 (page 28) the complete list of requirements along with a brief description and reasoning for each item is presented.



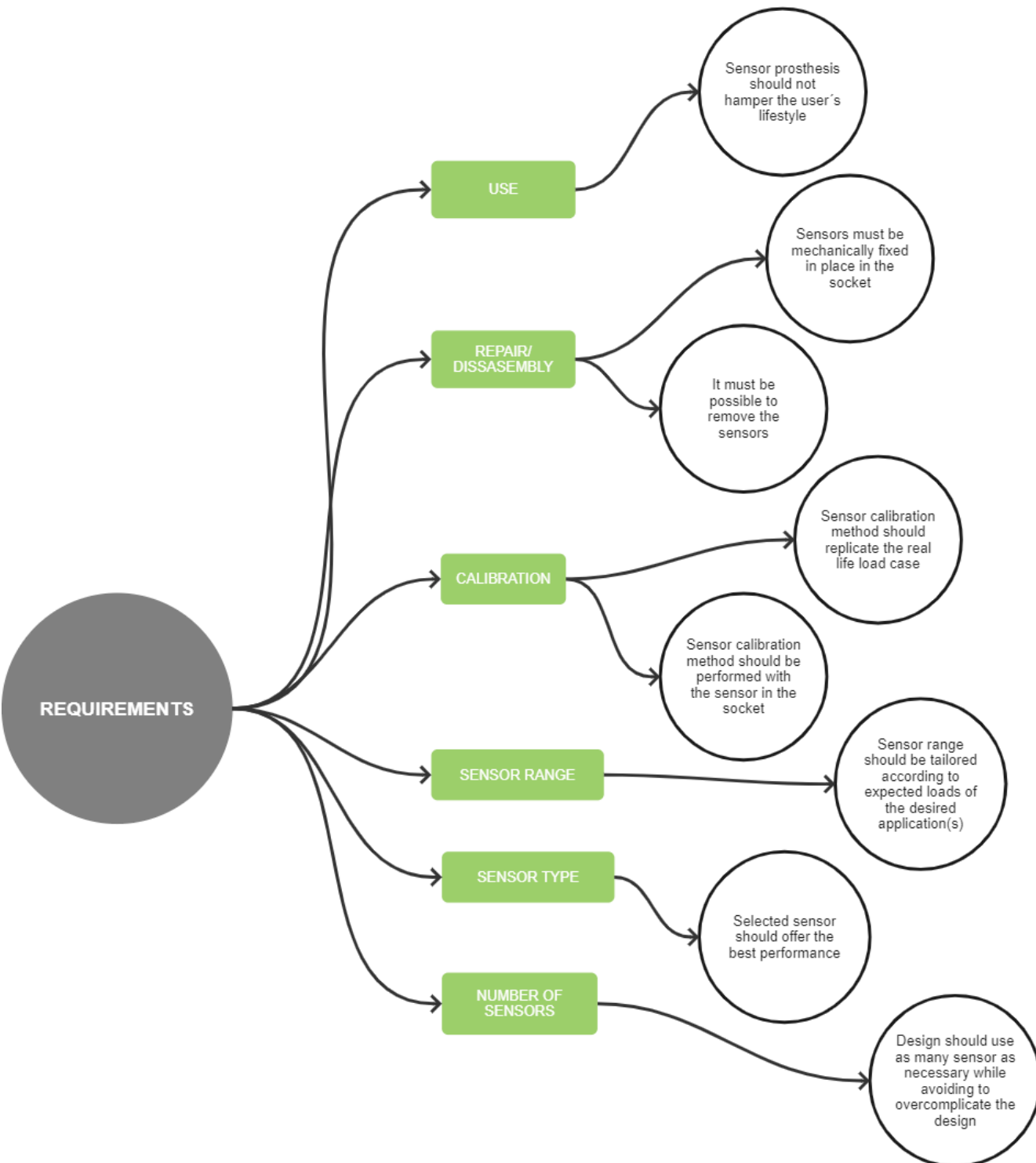


Figure 35. Diagram of requirements regarding the integration of sensors in a prosthetic socket to measure stump pressure

Table 6. List of requirements drawn from insights and observations on the application of FSR for below the knee prostheses

List of requirements

3D printed prosthetic socket equipped with pressure sensors to measure and visualize pressure distribution on the stump

Topic	Description	Reasoning
Use	Sensor prosthesis should not hamper user's lifestyle	Socket should enable the patients to do a "normal" lifestyle. Specific activities need to be further researched.
Comfort	Sensors must not create pressure points in the stump	Sensor integration creating pressure points must be avoided at all costs to ensure patient comfort.
Repair/ Dissassembly	Sensors must be mechanically fixed in place in the socket	Some part should be made to avoid the sensor from moving out of place (i.e.: a plate, layer of vacuum formed plastic).
	It must be possible to remove the sensors from the socket	Design must allow the sensors to be reused or replaced, either because the patient needs another socket, or a sensor is broken.
Calibration	Sensor calibration methods should replicate real life load case	The closest the sensor calibration methods are close to the sensor application, the closer the reading will be to the actual one.
	Sensor calibration method should be performed with the sensor in the socket	This way, patient would not need to take any action to calibrate sensors. Otherwise, this topic would become a barrier for the patient to use the prosthetic.
Disc for Sensor	The disc should not damage the sensor nor detach during use	Using epoxy glue to adhere the PU discs to the sensor might peel off or even damage the sensor, double sided tape does the job in the experiment, but it does not seem reliable when thinking about an user. Further exploration is needed to find an optimum solution
Sensor range	Sensor range should be tailored according to expected load of desired application(s)	Sensor range might be suitable for one type of activity activities, such as walking or jumping, due to their limited range. If it is a need to cover a wide range of activities, it might be that sensors of different ranges can be integrated in different locations depending on the expected load.
Sensor type	Selected sensor should offer the best performance	FSRs are explored in this study, but it might be the case that another sensor offers accurate reading of normal and shear stress. Sensor with better characteristics should be implemented.
Sensor location	Sensors should be strategically placed to monitor critical pressure points.	Proper sensor placement is crucial to ensure that all relevant pressure points are monitored, particularly those most prone to discomfort or injury.
Number of sensors	Design should use as many sensors as necessary while avoiding overcomplicating the design	Perhaps in the future, it is found through research that a smaller number of sensors is enough to output data of significance, which would simplify design and lower costs.

Sensor reading frequency	This should be sufficiently short to be able to measure pressure distribution over small time increments.	It might be that the sensor does not catch the instance where a significant load over a narrow time increment if the frequency is too large. The drawback is that a shorter frequency consumes more energy.
Weight	Electronic components and sensor should be a small percentage of the prosthesis weight	Electronics should not be too heavy that they become uncomfortable. A specific figure needs to be determined in the future.
Regulatory Compliance	The design should comply with relevant medical device regulations.	Adhering to regulatory standards ensures that the prosthetic is safe and effective for users.
Ease of Use	The prosthetic should be easy to don and doff.	The design should allow for easy and quick insertion and removal of the prosthetic, with especial regard for patients with limited mobility or dexterity.
Ingress Protection	Electronics must be protected from elements such as dust and rain	If the socket is worn outdoors, components such as flexible PCBs, electronics.
Cable management	Connection between sensors and PCB should aim neat and unobtrusive as possible.	For example, flexible PCB allow a flat and clean connection, but they might take more effort to design and produce; circular section can be cut to size rapidly, but they still add thickness to the design. This must be explored in the future.
Data communication	Sensor measurements need to have their respective timestamp	This outputs with an exact and know time that matches the sensor reading, key for the data processing. For example, using the Arduino delay as timestamp is not reliable as it might not reflect the accurate sensor reading time.
	Data communication should be compatible with a wearable design	The technology should allow user to do regular activities. In example, BLE would not need wires or more cable or connectors. In such way there is not extra weight that might be messy or heavy.
Lifecycle	Normal socket use should not damage sensors or shorten the described lifetime by manufacturer	Aspects such as socket assembly or regular socket use should not damage the sensors.

7. Future recommendations

The previous insights prompt design topics and tasks with significant potential for future development, aiming for a complete sensor integration in prosthetics for pressure monitoring and visualization. These recommendations extend beyond the project's focus on FSRs and testing procedures, addressing additional areas that were out of scope but can be built on the project's work. The future recommendations are outlined as follows:

- Systematically test FlexiForce sensors of different ranges, along other FSR models to compare their performance and determine the most suitable sensor.
- Investigate other types of sensors that could be used to measure pressure, such as capacitive sensors or strain gauges.

- Systematically test with other circuits, such as the non-inverting op-amp circuit adding to it the ADS 1115 module, or the 16-bit ADC voltage divider circuit (Appendix S).
- Perform tests with loading protocols of increasing level of complexity that mimic gait patterns. For example, in a sequence of steps: a sinusoidal loading pattern (Appendix T), then include load protocol form experimental data on joint load. Appendix I presents an example on the physiological condition from experimental data, extracted from Orthoload, a data repository that offers the load data on different joints and activities.
- Figure out a sensor calibration procedure that can be performed with the sensors integrated in the socket; this would be beneficial for the users since it would be less of a hassle for them in the future.
- Further develop the mechanical and electrical integration of the sensors in a 3D printed prosthetic socket.
- Figure system energy source. Energy harvesting is an attractive solution since it could use the gait potential energy while avoiding battery charging, which is less of a hassle for the user.
- Develop real time data communication and visualization. The aim is to have a wireless data communication without a delay between electronics and program, which displays the data in real time. The current version uses a Python script that reads a new row of csv with a delay.
- Perform user and product research. Stakeholder mapping and research to gather information stakeholders' needs and wishes. Conduct interviews with patients, organisations, medical practitioners and designers. Perform market research of 3D printed and smart prosthetic sockets through benchmark analysis or patent research.
- Once a satisfactory level of sensor development and a compelling integration is done, it would be ideal to test such prototype with a patient and implement the whole workflow from 3D scanning of the stump, modelling and manufacturing of the integrated socket, as well as user testing of the smart socket. This is a challenging topic since it to find a patient that is willing to be closely involved in the project, and it may require additional steps.
- Explore the implementation of actuation from the FSRs measurements.

Moreover, there are other ideas regarding smart prosthetics outside of FSR or pressure sensors that are worth mentioning:

- Smart prosthetic sensor with pneumatic actuation that uses air pressure sensors and air bladders to monitor, control and actuate upon the change of pressure in the stump.
- User liquid filled bladder to regulate pressure distribution. This is a more challenging project, but it can tackle both the pressure and the temperature regulation of the stump.
- A textile-based sensor that could read both normal and shear stress from the stretch of a conductive thread is a desirable solution due to a seamless integration on the prosthetic liner.

8. Conclusion

This study aimed to explore the potential of sensor integration in prosthetics for improving patient comfort and monitoring the residual limb. The results demonstrated that Force Sensitive Resistors are effective for measuring pressure distribution, which enable the improvement of prosthesis design through quantitative data. These findings suggest that integrating sensors into prosthetics could help advancing prosthetics by offering a monitoring and evaluation tool for the stump, therefore providing affordable and personalized patient comfort.

However, the study was limited by testing only one sensor type with a specific range and using simplified loading protocols, further research is needed to validate these findings in more complex scenarios. Future research should focus on testing additional sensor types of diverse ranges, refining the mechanical and electrical integration of the sensors in the socket, and conducting tests of increasing level of complexity that mimic patient gait to fully realize the potential of sensors for prosthetics. Ultimately, advancing sensor integration in prosthetics could enhance the quality of life for amputees, laying the foundations for future innovation on patient comfort and prosthesis with knowledge-based design.

9. References

- [1] S. Manz *et al.*, 'A review of user needs to drive the development of lower limb prostheses', *J. NeuroEngineering Rehabil.*, vol. 19, no. 1, p. 119, Nov. 2022, doi: 10.1186/s12984-022-01097-1.
- [2] T. Dillingham, P. Le, M. Ej, and B. Ar, 'Use and satisfaction with prosthetic devices among persons with trauma-related amputations: a long-term outcome study', *Am. J. Phys. Med. Rehabil.*, vol. 80, no. 8, Aug. 2001, doi: 10.1097/00002060-200108000-00003.
- [3] K. Ziegler-Graham, E. J. MacKenzie, P. L. Ephraim, T. G. Trivison, and R. Brookmeyer, 'Estimating the prevalence of limb loss in the United States: 2005 to 2050', *Arch. Phys. Med. Rehabil.*, vol. 89, no. 3, pp. 422–429, Mar. 2008, doi: 10.1016/j.apmr.2007.11.005.
- [4] C. L. McDonald, S. Westcott-McCoy, M. R. Weaver, J. Haagsma, and D. Kartin, 'Global prevalence of traumatic non-fatal limb amputation', *Prosthet. Orthot. Int.*, vol. 45, no. 2, pp. 105–114, Apr. 2021, doi: 10.1177/0309364620972258.
- [5] A. Esquenazi and R. DiGiacomo, 'Rehabilitation after amputation', *J. Am. Podiatr. Med. Assoc.*, vol. 91, no. 1, pp. 13–22, Jan. 2001, doi: 10.7547/87507315-91-1-13.
- [6] C. D. Murray, 'An interpretative phenomenological analysis of the embodiment of artificial limbs', *Disabil. Rehabil.*, vol. 26, no. 16, pp. 963–973, Aug. 2004, doi: 10.1080/09638280410001696764.
- [7] J. Sanders and S. Fatone, 'RESIDUAL LIMB VOLUME CHANGE: SYSTEMATIC REVIEW OF MEASUREMENT AND MANAGEMENT', *J. Rehabil. Res. Dev.*, vol. 48, no. 8, pp. 949–986, 2011.
- [8] M. Lilja and T. Öberg, 'Proper Time for Definitive Transtibial Prosthetic Fitting', *JPO J. Prosthet. Orthot.*, vol. 9, no. 2, p. 90, Spring 1997.
- [9] Jon Smith, *The Check Socket Fitting* | *limb-loss.org*, (Nov. 26, 2012). Accessed: Jul. 18, 2024. [Online Video]. Available: <https://www.youtube.com/watch?v=ol1cexkj b24>
- [10] C. McCloskey, J. Kenia, F. Shofer, J. Marschalek, and T. Dillingham, 'Improved Self-Reported Comfort, Stability, and Limb Temperature Regulation with an Immediate Fit, Adjustable Transtibial Prosthesis', *Arch. Rehabil. Res. Clin. Transl.*, vol. 2, no. 4, p. 100090, Dec. 2020, doi: 10.1016/j.arrct.2020.100090.
- [11] A. F. Mak, M. Zhang, and D. A. Boone, 'State-of-the-art research in lower-limb prosthetic biomechanics-socket interface: a review', *J. Rehabil. Res. Dev.*, vol. 38, no. 2, pp. 161–174, 2001.
- [12] W. C. Lee, M. Zhang, and A. F. Mak, 'Regional differences in pain threshold and tolerance of the transtibial residual limb: Including the effects of age and interface material', *Arch. Phys. Med. Rehabil.*, vol. 86, no. 4, pp. 641–649, Apr. 2005, doi: 10.1016/j.apmr.2004.08.005.
- [13] J. E. Sanders, D. S. Harrison, K. J. Allyn, and T. R. Myers, 'Clinical utility of in-socket residual limb volume change measurement: case study results', *Prosthet. Orthot. Int.*, vol. 33, no. 4, pp. 378–390, Dec. 2009, doi: 10.3109/03093640903214067.
- [14] W. J. Board, G. M. Street, and C. Caspers, 'A comparison of trans-tibial amputee suction and vacuum socket conditions', *Prosthet. Orthot. Int.*, vol. 25, no. 3, pp. 202–209, Dec. 2001, doi: 10.1080/03093640108726603.
- [15] C. Lake and T. J. Supan, 'The Incidence of Dermatological Problems in the Silicone Suspension Sleeve User', *JPO J. Prosthet. Orthot.*, vol. 9, no. 3, p. 97, Summer 1997.
- [16] K. Ghoseiri and M. R. Safari, 'Prevalence of heat and perspiration discomfort inside prostheses: Literature review', *J. Rehabil. Res. Dev.*, vol. 51, no. 6, pp. 855–868, 2014, doi: 10.1682/JRRD.2013.06.0133.
- [17] J. T. Peery, W. R. Ledoux, and G. K. Klute, 'Residual-limb skin temperature in transtibial sockets', *J. Rehabil. Res. Dev.*, vol. 42, no. 2, p. 147, 2005, doi: 10.1682/JRRD.2004.01.0013.
- [18] Y. Han, F. Liu, L. Zhao, and J. Zhe, 'An automatic and portable prosthetic cooling device with high cooling capacity based on phase change', *Appl. Therm. Eng.*, vol. 104, pp. 243–248, Jul. 2016, doi: 10.1016/j.applthermaleng.2016.05.074.
- [19] G. L. W. JR, J. P. Montez, D. K. Schultz, and A. J. Darius, 'Prosthesis cooling system', US20160030207A1, Feb. 04, 2016 Accessed: Feb. 22, 2024. [Online]. Available: <https://patents.google.com/patent/US20160030207A1/en>
- [20] Y. Han, F. Liu, G. Dowd, and J. Zhe, 'A thermal management device for a lower-limb prosthesis', *Appl. Therm. Eng.*, vol. 82, pp.

- 246–252, May 2015, doi: 10.1016/j.applthermaleng.2015.02.078.
- [21] K. Ghoseiri, Y. P. Zheng, L. L. T. Hing, M. R. Safari, and A. K. Leung, 'The prototype of a thermoregulatory system for measurement and control of temperature inside prosthetic socket', *Prosthet. Orthot. Int.*, vol. 40, no. 6, pp. 751–755, Dec. 2016, doi: 10.1177/0309364615588343.
- [22] J.-H. Seo *et al.*, 'A Prosthetic Socket with Active Volume Compensation for Amputated Lower Limb', *Sensors*, vol. 21, no. 2, p. 407, Jan. 2021, doi: 10.3390/s21020407.
- [23] K.-H. Lee *et al.*, 'A Pneumatically Controlled Prosthetic Socket for Transfemoral Amputees', *Sensors*, vol. 24, no. 1, p. 133, Dec. 2023, doi: 10.3390/s24010133.
- [24] J. E. Sanders, J. C. Cagle, D. S. Harrison, T. R. Myers, and K. J. Allyn, 'How does adding and removing liquid from socket bladders affect residual-limb fluid volume?', *J. Rehabil. Res. Dev.*, vol. 50, no. 6, pp. 845–860, 2013, doi: 10.1682/JRRD.2012.06.0121.
- [25] E. J. Weathersby, J. L. Garbini, B. G. Larsen, J. B. McLean, A. C. Vamos, and J. E. Sanders, 'Automatic Control of Prosthetic Socket Size for People With Transtibial Amputation: Implementation and Evaluation', *IEEE Trans. Biomed. Eng.*, vol. 68, no. 1, pp. 36–46, Jan. 2021, doi: 10.1109/TBME.2020.2992739.
- [26] M. Karamousadakis, A. Porichis, S. Ottikkutti, D. Chen, and P. Vartholomeos, 'A Sensor-Based Decision Support System for Transfemoral Socket Rectification', *Sensors*, vol. 21, no. 11, Art. no. 11, Jan. 2021, doi: 10.3390/s21113743.
- [27] J. C. Mertens *et al.*, 'A novel portable sensor to monitor bodily positions and activities in transtibial prosthesis users', *Clin. Biomech. Bristol Avon*, vol. 99, p. 105741, Oct. 2022, doi: 10.1016/j.clinbiomech.2022.105741.
- [28] 'Home | Limber P&O | 3d Printing Prosthetic | San Diego', Limber P&O. Accessed: Aug. 14, 2024. [Online]. Available: <https://www.limberprosthetics.com>
- [29] 'Quorum Prosthetics', Quorum Prosthetics. Accessed: Aug. 14, 2024. [Online]. Available: <https://www.quorumprosthetics.com>
- [30] 'R PRO 10 - Liquid silicone rubber for soft molds', www.reschimica.com. Accessed: Aug. 14, 2024. [Online]. Available: <https://www.reschimica.com/gb/silicone-rubbers/121-r-pro-10-liquid-silicone-rubber-for-soft-molds.html>
- [31] 'Overview | Adafruit HUZZAH32 - ESP32 Feather | Adafruit Learning System'. Accessed: Aug. 09, 2024. [Online]. Available: <https://learn.adafruit.com/adafruit-huzzah32-esp32-feather/overview>
- [32] 'HC4067 16-kanaals Analoge Multiplexer'. Accessed: Aug. 09, 2024. [Online]. Available: <https://www.tinytronics.nl/nl/communicatie-en-signalen/io-converters/hc4067-16-kanaals-analoge-multiplexer>
- [33] 'Best Practices in Mechanical Integration of the FlexiForce Sensor'. Tekscan. [Online]. Available: <https://www.tekscan.com/sites/default/files/FLX-Best-Practice-Mechanical-Integration-RevB.pdf>
- [34] 'Best Practices in Electrical Integration of FlexiForce Sensor'. Tekscan. [Online]. Available: <https://www.tekscan.com/sites/default/files/FLX-Best-Practice-Electrical-Integration-RevB.pdf>

Appendices

Appendix A. A201 FlexiForce Force Sensitive Resistor Datasheet	34
Appendix B. Physical components of the prosthesis prototype	37
Appendix C. Sensor calibration code	39
Appendix D. Calibrated code	42
Appendix E. ImportSerialAsCSV.py Python code	45
Appendix F. Python code to assign jet colour map to given Force values	47
Appendix G. Python code to interpolate the jet colour map over the mesh	49
Appendix H. Adjustment of material model to Load against Displacement curve from Experiment	52
Appendix I. Simulated gait pattern loading protocol reference from Orthoload	54
Appendix J. Sensor calibration test results scatter plots	56
Appendix K. Calibration curves from Sensor calibration test	59
Appendix L. Sensor calibration test results column charts and tables	62
Appendix M. Individual breakdown of Socket Sensor test results scatter plots	66
Appendix N. Individual breakdown of Socket sensor test results column charts	71
Appendix O. Combined data of Socket Sensor test results	77
Appendix P. Simulation results graph and table	80
Appendix Q. Socket Sensor Experiment and simulation results comparison	83
Appendix R. Sensor data visualization with Grasshopper of Socket Sensor test results	86
Appendix S. Non-Inverting Op-Amp and 16-bit ADC voltage divider circuits	90
Appendix T. Sinusoidal loading protocol test data	92
Appendix U. Modified BME simulation	94
Appendix V. Physiological loading conditions simulation	98
Appendix W. Prototype cost estimation	100
Appendix X. Graphical summary of the project	102
Appendix Y. Project brief	108

Appendix A.
A201 FlexiForce Force Sensitive Resistor Datasheet

FlexiForce™

Standard Model A201



The FlexiForce A201 is our standard sensor and meets the requirements of most customers. The A201 is a thin and flexible piezoresistive force sensor that is available off-the-shelf in a variety of lengths for easy proof of concept. These ultra-thin sensors are ideal for non-intrusive force and pressure measurement in a variety of applications. The A201 can be used with our test & measurement, prototyping, and embedding electronics, including the FlexiForce Sensor Characterization Kit, FlexiForce Prototyping Kit, FlexiForce Quickstart Board, and the ELF™ System*. You can also use your own electronics, or multimeter.

Benefits

- Thin and flexible
- Easy to use
- Convenient and affordable

✓ ROHS COMPLIANT

* Sensor will require an adapter/extender to connect to the ELF System. Contact your Tekscan representative for assistance.

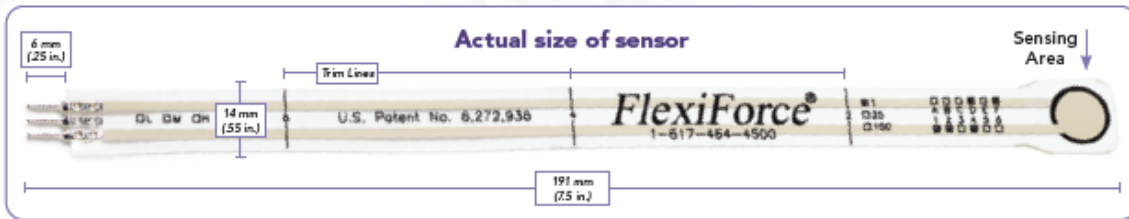
** Length does not include pins. Please add approximately 6 mm (0.25 in.) for pin length for a total length of approximately 197 mm (7.75 in.).

Physical Properties

Thickness	0.203 mm (0.008 in.)
Length	191 mm (7.5 in.)** (optional trimmed lengths: 152 mm (6 in.), 102 mm (4 in.), 51 mm (2 in.))
Width	14 mm (0.55 in.)
Sensing Area	9.53 mm (0.375 in.) diameter
Connector	3-pin Male Square Pin (center pin is inactive)
Substrate	Polyester
Pin Spacing	2.54 mm (0.1 in.)

	Typical Performance	Evaluation Conditions
Linearity (Error)	< ±3% of full scale	Line drawn from 0 to 50% load
Repeatability	< ±2.5%	Conditioned sensor, 80% of full force applied
Hysteresis	< 4.5% of full scale	Conditioned sensor, 80% of full force applied
Drift	< 5% per logarithmic time scale	Constant load of 111 N (25 lb)
Response Time	< 5µsec	Impact load, output recorded on oscilloscope
Operating Temperature	-40°C - 60°C (-40°F - 140°F)	Convection and conduction heat sources
Durability	≥ 3 million actuations	Perpendicular load, room temperature, 22 N (5 lb)
Temperature Sensitivity	0.36%/°C (± 0.2%/°F)	Conductive heating

***All data above was collected utilizing an Op Amp Circuit (shown on the next page). If your application cannot allow an Op Amp Circuit, visit www.tekscan.com/flexiforce-integration-guides, or contact a FlexiForce Applications Engineer.



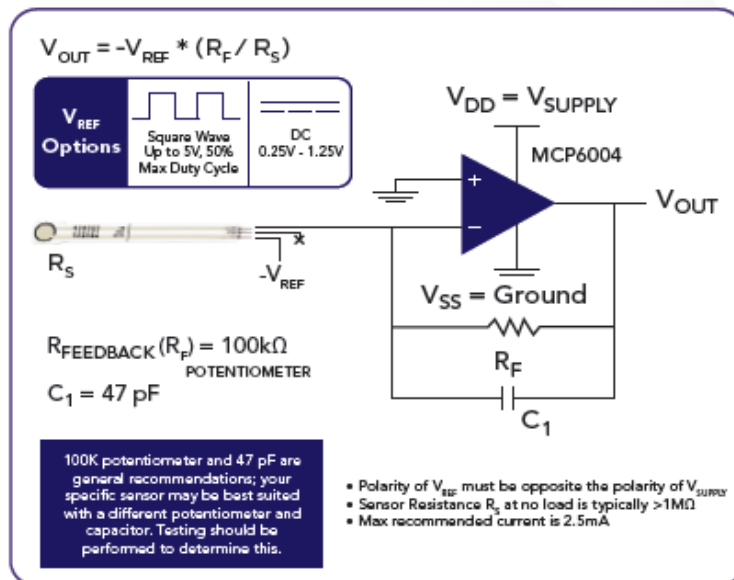
Standard Force Ranges as Tested with Circuit Shown

- 4.4 N (0 - 1 lb)
- 111 N (0 - 25 lb)
- 445 N (0 - 100 lb) †

† This sensor can measure up to 4,448 N (1,000 lb). In order to measure higher forces, apply a lower drive voltage (-0.5 V, -0.25 V, etc.) and reduce the resistance of the feedback resistor (1kΩ min.). To measure lower forces, apply a higher drive voltage and increase the resistance of the feedback resistor.

Sensor output is a function of many variables, including interface materials. Therefore, Tekscan recommends the user calibrate each sensor for the application.

Recommended Circuit



PURCHASE TODAY ONLINE AT WWW.TEKSCAN.COM/STORE



©Tekscan Inc., 2021. All rights reserved. Tekscan, the Tekscan logo, and FlexiForce are trademarks or registered trademarks of Tekscan, Inc.

+1.617.464.4283 | 1.800.248.3669 | info@tekscan.com | www.tekscan.com/flexiforce

Appendix B.
Physical components of the prosthesis prototype



Figure 36. Realistic stump made from casted silicone, on top the adaptor to the machine can be seen. Inside of the stump there is a cement core.

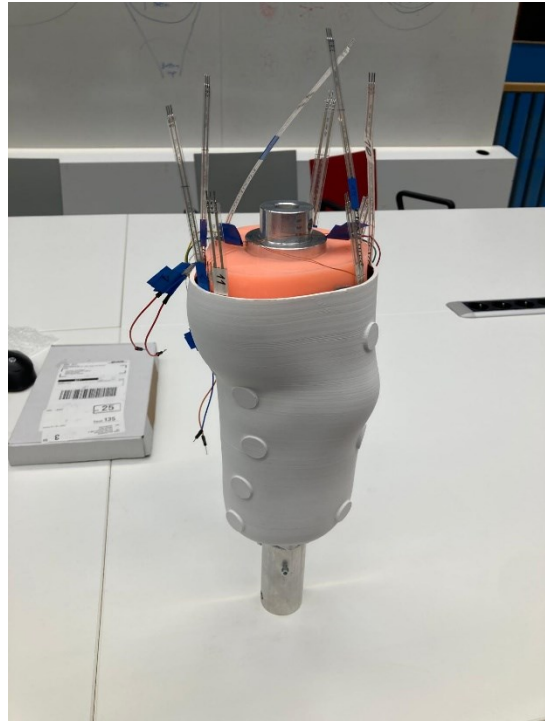


Figure 37. 3D printed prosthetic socket and FSRs integrated inside with stump in place.

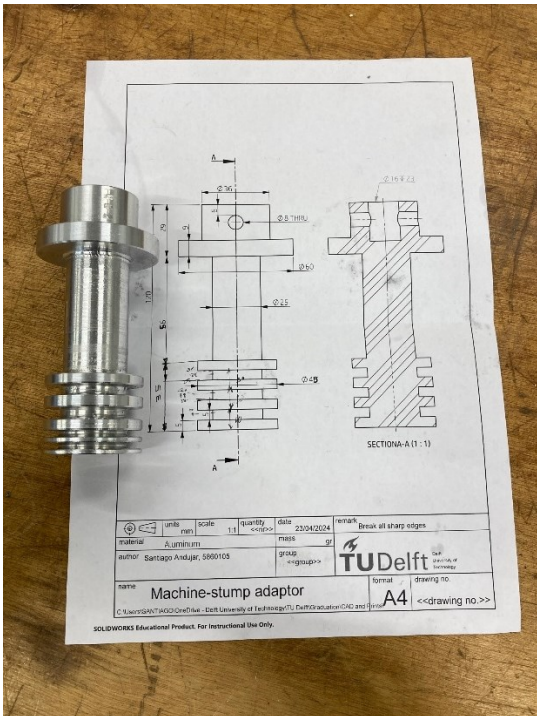


Figure 38. Machine-stump adaptor made from turned Al6061-T6.



Figure 39. Flexiforce A201 FSR sensors and PU discs

Appendix C.
Sensor calibration code

```

*
To be used for calibrating FSRs for 2 resistors.

This code connects SIG pin of MUX2 to 2 Channels of MUX2
This way we can find through testing which resistor covers best a particular load
range,
and confirm our guess for which resistor is best suitable.

Components:
1x Adafruit ESP32 Huzzah Feather
2x 16 Channel Analog Multiplexer
1x 10k ohm resistor
1x 100k ohm resistor
*/

int mux2_S0 = 33;
int mux2_S1 = 15;
int mux2_S2 = 32;
int mux2_S3 = 14;
int SIG2 = A5; // Reading from MUX2

int mux2ChannelNumber = 2; // Number of channels in MUX2

// Holds incoming values from 74HC4067 MUX2
int mux2Values[2] = {0, 0};

void setup() {
  Serial.begin(19200);

  pinMode(mux2_S0, OUTPUT);
  pinMode(mux2_S1, OUTPUT);
  pinMode(mux2_S2, OUTPUT);
  pinMode(mux2_S3, OUTPUT);
}

void selectMux2Channel(int channelNumber) {
  // Set the address bits based on the channel number for MUX2
  digitalWrite(mux2_S0, bitRead(channelNumber, 0));
  digitalWrite(mux2_S1, bitRead(channelNumber, 1));
  digitalWrite(mux2_S2, bitRead(channelNumber, 2));
  digitalWrite(mux2_S3, bitRead(channelNumber, 3));
}

void loop() {
  int j;
  String sensorData = ""; // String to store sensor readings

  // Connect to 3 channels of MUX2 and read values
  for (j = 0; j < mux2ChannelNumber; j++) { // Loop through channels 0, 1, and 2 of
MUX2

```

```
selectMux2Channel(j); // Select channel j on MUX2
delay(1);
mux2Values[j] = analogRead(SIG2); // Read the value from channel j of MUX2
sensorData += String(mux2Values[j]) + " "; // Concatenate sensor data
}

// Print the concatenated sensor data
Serial.println(sensorData);
delay(200);
}
```

Appendix D.
Calibrated code

```

/*
This code outputs the raw and calibrated value for 16 FSRs

Components:
1x Adafruit Huzzah ESP32 Feather
1x 16 Channel Analog Multiplexer
1x 100k Ohm Resistor

20240619 fix: extra comma at the end eliminated
20240627 edit: circuit uses only one multiplexer
*/
//Defined GPIO pins for MUX1
int mux1_S0 = 33;
int mux1_S1 = 15;
int mux1_S2 = 32;
int mux1_S3 = 14;

int SIG = A5; // Reading from MUX1
int mux1ChannelNumber = 16; // Number of channels in MUX1, 16 FSRs

// Define the x(known Loads) and y(respective values at known load) values for the
FSR calibration curves
float xValues[] = {0, 50, 250, 500, 750, 1000};
float yValues[][6] = {
  {0.000, 698.500, 2686.000, 3090.000, 3176.500, 3090.000}, // FSR1
  {0.000, 1215.000, 2759.333, 3134.000, 3205.000, 3111.000}, // FSR2
  {0.000, 722.165, 2717.000, 3204.335, 3332.670, 3359.000}, // FSR3
  {0.000, 1311.335, 2930.830, 3304.830, 3464.670, 3486.000}, // FSR4
  {0.000, 1623.500, 3043.670, 3388.335, 3480.500, 3423.500}, // FSR5
  {0.000, 1098.665, 2850.830, 3270.600, 3437.835, 3506.000}, // FSR6
  {0.000, 1028.892, 2770.420, 3190.372, 3351.032, 3414.387}, // FSR7
  {0.000, 1235.699, 2847.366, 3200.559, 3277.387, 3201.860}, // FSR8
  {0.000, 1570.000, 2930.000, 3285.290, 3454.330, 3555.840}, // FSR9
  {0.000, 1187.000, 2818.100, 3212.870, 3332.390, 3334.634}, // FSR10
  {0.000, 1224.670, 2810.118, 3211.935, 3371.882, 3446.470}, // FSR11
  {0.000, 1477.000, 2947.000, 3323.000, 3478.000, 3537.000}, // FSR12
  {0.000, 1623.000, 3017.850, 3373.700, 3511.450, 3545.160}, // FSR13
  {0.000, 1882.000, 3042.000, 3364.000, 3503.000, 3565.000}, // FSR14
  {0.000, 1712.500, 3075.000, 3427.770, 3590.000, 3675.000}, // FSR15
  {0.000, 1258.000, 2842.500, 3215.700, 3329.000, 3298.350} // FSR16
};

// Function to select the channel on MUX1
void selectMux1Channel(int channelNumber) {
  digitalWrite(mux1_S0, bitRead(channelNumber, 0));
  digitalWrite(mux1_S1, bitRead(channelNumber, 1));
  digitalWrite(mux1_S2, bitRead(channelNumber, 2));
  digitalWrite(mux1_S3, bitRead(channelNumber, 3));
}

```

```

// Function to perform linear interpolation
float linearInterpolate(float x[], float y[], int size, float value) {
  for (int i = 0; i < size - 1; i++) {
    if (value >= y[i] && value <= y[i + 1]) {
      return x[i] + (value - y[i]) * (x[i + 1] - x[i]) / (y[i + 1] - y[i]);
    }
  }
  return 0; // Return 0 if the value is out of range
}

void setup() {
  Serial.begin(19200);

  // Initialize pins for MUX1
  pinMode(mux1_S0, OUTPUT);
  pinMode(mux1_S1, OUTPUT);
  pinMode(mux1_S2, OUTPUT);
  pinMode(mux1_S3, OUTPUT);
}

void loop() {
  String outputString = "";

  // Loop through each channel on MUX1 (16 FSRs)
  for (int i = 0; i < 16; i++) {
    selectMux1Channel(i);
    delay(1);

    // Read the analog value from the selected FSR
    int analogValue = analogRead(SIG);

    // Interpolate the x value for the FSR and append values to output string
    float interpolatedValue = linearInterpolate(xValues, yValues[i], 6,
analogValue);

    outputString += String(analogValue) + "," + String(interpolatedValue);

    // Add a comma if it's not the last value
    if (i < 15) {
      outputString += ",";
    }
  }
  // Print the output string
  Serial.println(outputString);
  delay(200); // Adjust delay as necessary
}

```

Appendix E.
ImportSerialAsCSV.py Python code

```

# 20240619. This code establishes serial communication with the ESP32 and save the
sensor data in a .CSV file

import serial
import csv
import os
import time

def read_serial_and_save_to_csv(port, baud_rate=19200,
folder_path=r'C:\Users\SANTIAGO\OneDrive - Delft University of Technology\TU
Delft\Graduation\Data\20240618_SerialComESP32wGH', csv_file='20240620_data.csv'):
    # Create the folder if it does not exist
    if not os.path.exists(folder_path):
        os.makedirs(folder_path)

    # Full path to the CSV file
    csv_file_path = os.path.join(folder_path, csv_file)
    print(f"CSV file path: {csv_file_path}")

    ser = serial.Serial(port, baud_rate)

    # Header line for the CSV file
    header_line =
"FSR1,calFSR1,FSR2,calFSR2,FSR3,calFSR3,FSR4,calFSR4,FSR5,calFSR5,FSR6,calFSR6,FSR7
,calFSR7,FSR8,calFSR8,FSR9,calFSR9,FSR10,calFSR10,FSR11,calFSR11,FSR12,calFSR12,FSR
13,calFSR13,FSR14,calFSR14,FSR15,calFSR15,FSR16,calFSR16\n"

    with open(csv_file_path, 'w', newline='') as f:
        f.write(header_line) # Write header line

    while True:
        try:
            if ser.in_waiting > 0:
                data = ser.readline().decode('utf-8', errors='ignore').strip()
                f.write(data + '\n') # Write data with newline for each entry
                f.flush() # Ensure data is written immediately
                print(data) # Debug statement
            except UnicodeDecodeError as e:
                print("Decoding error: {}".format(e))
            except Exception as ex:
                print(f"Exception occurred: {ex}")

            time.sleep(0.2) # Adjust sleep time as necessary

# Read Serial data
port = 'COM10' # Add COM port
folder_path = r'C:\Users\SANTIAGO\OneDrive - Delft University of Technology\TU
Delft\Graduation\Data\20240618_SerialComESP32wGH' # Add desired folder path
csv_file = '20240620_data.csv' # Output CSV file name, modify as desired
read_serial_and_save_to_csv(port, 19200, folder_path, csv_file)

```

Appendix F.

Python code to assign jet colour map to given Force values

```

import Rhino.Geometry as rg
import System.Drawing as sd
import scriptcontext as sc

# Define the Jet color scheme
def jet_color(value):
    # Define the colors for Jet color scheme
    colors = [
        (0, 0, 255),    # Blue
        (0, 255, 255), # Cyan
        (0, 255, 0),   # Green
        (255, 255, 0), # Yellow
        (255, 0, 0)    # Red
    ]

    # Define the value range for mapping
    min_value = 0.0
    max_value = 1.0

    # Interpolate colors based on value
    if value <= min_value:
        return colors[0]
    elif value >= max_value:
        return colors[-1]
    else:
        # Calculate index and interpolation factor
        index = (len(colors) - 1) * (value - min_value) / (max_value - min_value)
        lower_index = int(index)
        upper_index = min(lower_index + 1, len(colors) - 1)
        fraction = index - lower_index

        # Interpolate between colors
        color = (
            int(colors[lower_index][0] * (1 - fraction) + colors[upper_index][0] * fraction),
            int(colors[lower_index][1] * (1 - fraction) + colors[upper_index][1] * fraction),
            int(colors[lower_index][2] * (1 - fraction) + colors[upper_index][2] * fraction)
        )

        return color

# Ensure input_value is not empty to avoid errors
if not input_pressure_value:
    raise ValueError("input_value is empty")

# Calculate the value range for normalization
min_value = min(input_pressure_value)
max_value = max(input_pressure_value)

# Normalize input values
values = [(each - min_value) / (max_value - min_value) for each in input_pressure_value]

# Map normalized values to Jet color scheme
colors = [jet_color(value) for value in values]

# Convert to System.Drawing.Color objects
output_colors = [sd.Color.FromArgb(color[0], color[1], color[2]) for color in colors]

# Output the colors to Grasshopper
output_value = output_colors

```

Appendix G.

Python code to interpolate the jet colour map over the mesh

```

import Rhino.Geometry as rg
import System.Drawing as sd
import rhinoscriptsyntax as rs

def interpolate_color(mesh, vertex_index, known_colors, known_indices, threshold):
    if not known_indices:
        return sd.Color.Black

    # Initialize variables for weighted color sum
    r, g, b = 0, 0, 0
    total_weight = 0

    # Loop over known vertices and use their colors
    for i, known_index in enumerate(known_indices):
        known_vertex = mesh.Vertices[known_index]
        distance = mesh.Vertices[vertex_index].DistanceTo(known_vertex)

        # If the vertex is within the threshold distance, return the color directly
        if distance <= threshold:
            return known_colors[i]

        weight = 1.0 / (distance + 1e-6)
        color = known_colors[i]
        r += color.R * weight
        g += color.G * weight
        b += color.B * weight
        total_weight += weight

    # Compute the weighted average color
    if total_weight > 0:
        r = int(r / total_weight)
        g = int(g / total_weight)
        b = int(b / total_weight)
    else:
        # Default to black if no known vertices are found
        r, g, b = 0, 0, 0

    return sd.Color.FromArgb(r, g, b)

# Main interpolation function
def interpolate_mesh_colors(mesh, known_colors, known_indices, threshold):
    interpolated_colors = []

    for i in range(mesh.Vertices.Count):
        if i in known_indices:
            interpolated_colors.append(known_colors[known_indices.index(i)])
        else:
            interpolated_color = interpolate_color(mesh, i, known_colors, known_indices,
threshold)
            interpolated_colors.append(interpolated_color)

    return interpolated_colors

def closest_vertex_index(mesh, point):
    # Get the closest point on the mesh to the input point
    mesh_point = mesh.ClosestMeshPoint(point, 0.0)
    if mesh_point is None:
        raise ValueError("Could not find the closest point on the mesh.")

    # Get the face index where the closest point is located

```

```

face_index = mesh_point.FaceIndex
if face_index == -1:
    raise ValueError("Invalid face index found.")

# Get the vertex indices of the face containing the closest point
face = mesh.Faces[face_index]
face_vertex_indices = [face.A, face.B, face.C, face.D]

# Filter out any -1 indices (which can occur if the face is a triangle)
face_vertex_indices = [i for i in face_vertex_indices if i != -1]

# Initialize the closest vertex
closest_vertex_index = face_vertex_indices[0]
closest_vertex = mesh.Vertices[closest_vertex_index]
closest_distance = point.DistanceTo(closest_vertex)

# Iterate over the vertices to find the closest one
for index in face_vertex_indices:
    vertex = mesh.Vertices[index]
    distance = point.DistanceTo(vertex)
    if distance < closest_distance:
        closest_vertex_index = index
        closest_distance = distance

return closest_vertex_index

# Inputs from Grasshopper
# mesh: The input mesh
# measured_vertex_position: List of points where we have known colors
# measured_vertex_color: List of colors corresponding to these points
# distance_threshold: Slider value for the distance threshold

anchor_points = [rg.Point3d(p) for p in measured_vertex_position]

# Now we try to find the index of these points regarding the input mesh
vertex_indices = []

for each in anchor_points:
    temp_index = closest_vertex_index(mesh, each)
    vertex_indices.append(temp_index)

vertex_colors = measured_vertex_color # This should be a list of System.Drawing.Color
corresponding to the points

# Call the function to interpolate colors
interpolated_colors = interpolate_mesh_colors(mesh, vertex_colors, vertex_indices,
distance_threshold)

# Assign the interpolated colors to the mesh
if len(interpolated_colors) == mesh.Vertices.Count:
    mesh.VertexColors.Clear()
    for color in interpolated_colors:
        mesh.VertexColors.Add(color)

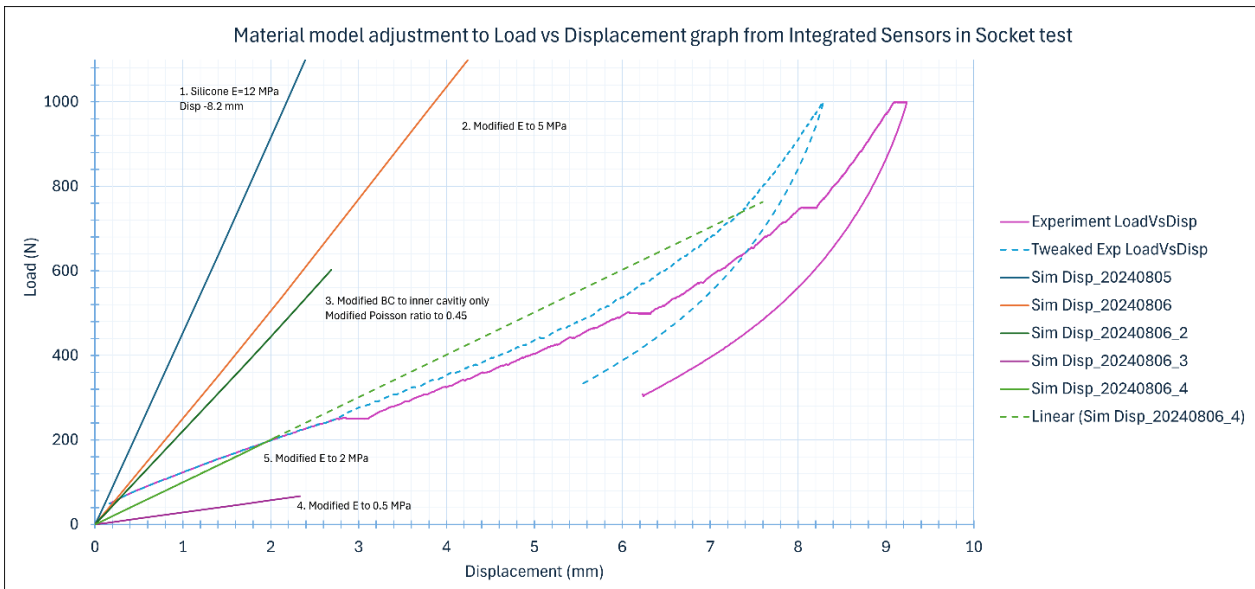
# Output the mesh with vertex colors
color_mesh = mesh

```

Appendix H.
Adjustment of material model to Load
against Displacement curve from Experiment

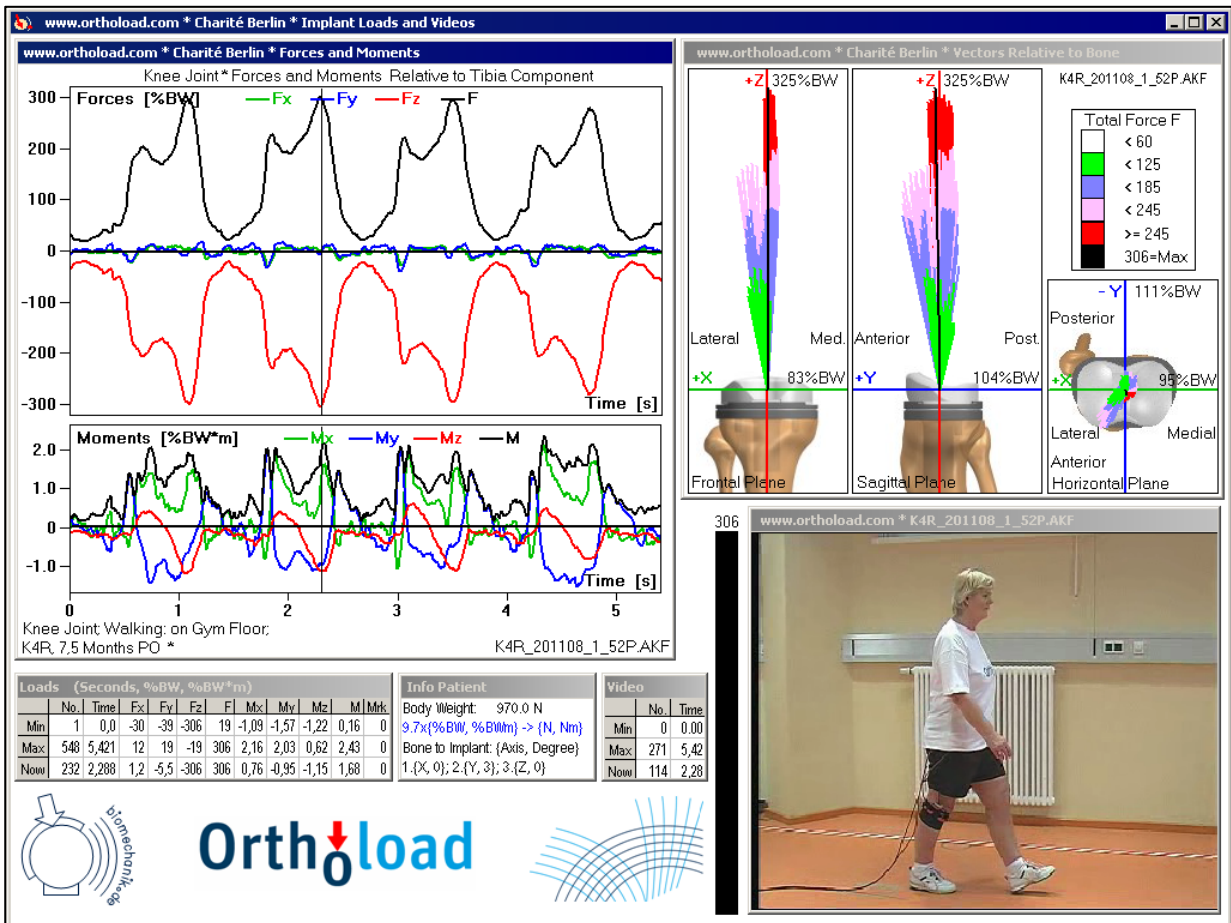
The image on the top shows the Load against Displacement curve from the Integrated Sensors test. Since the test was performed with steps, the curve is modified to eliminate this to show the behaviour under a constant load application.

The image below shows the iteration process to adjust the mechanical properties input in the simulation for the silicone material so that it is comparable to the Load against displacement curve from the experiment. An input of 2 MPa for the Young's Modulus and 0.45 for the Poisson ratio shows a comparable Load against Displacement curve in the simulation to the experiment one.



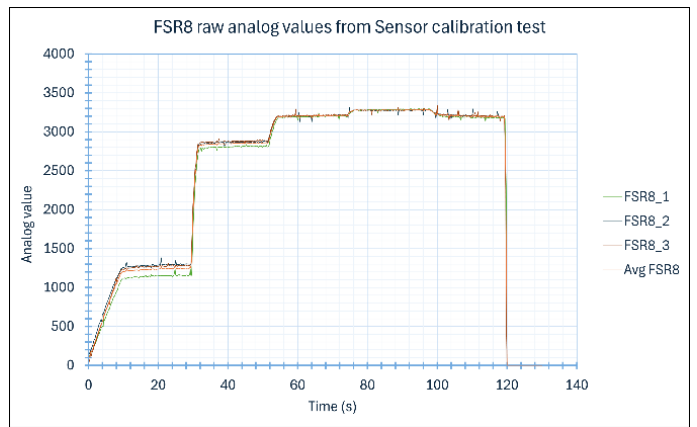
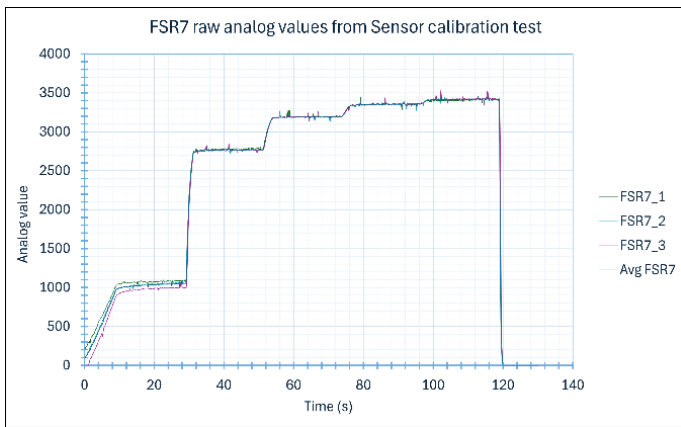
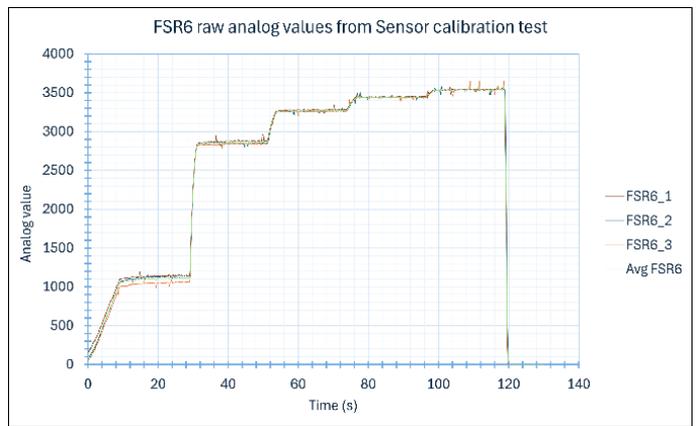
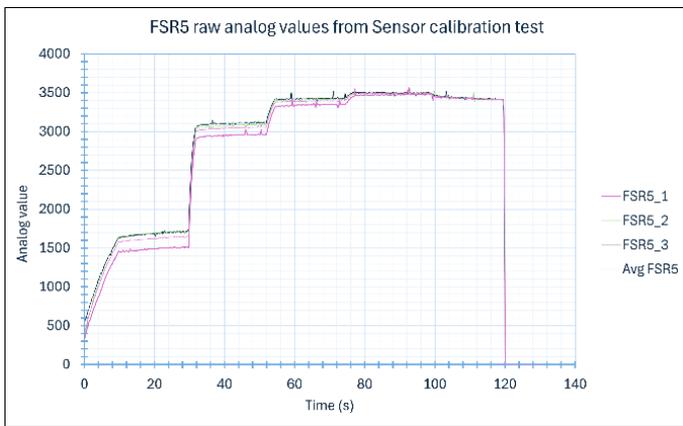
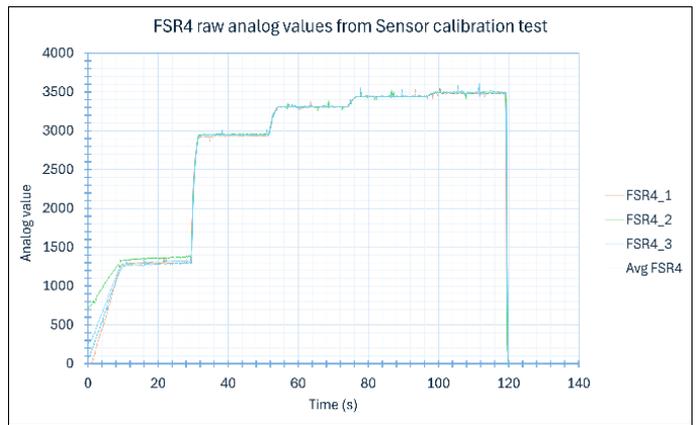
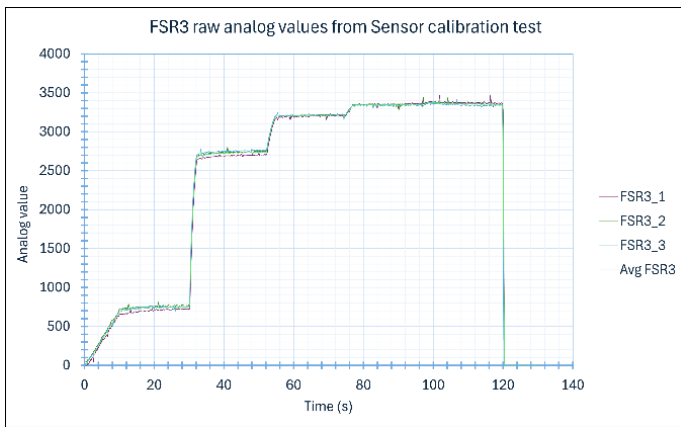
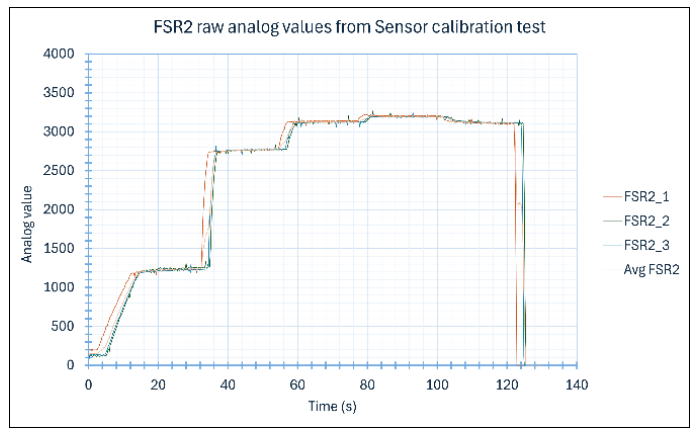
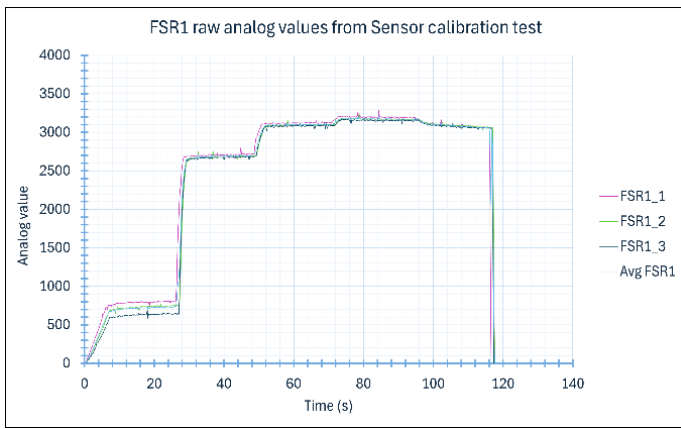
Appendix I.

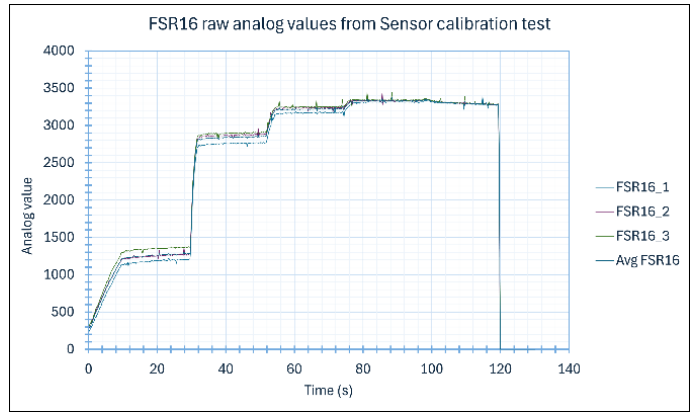
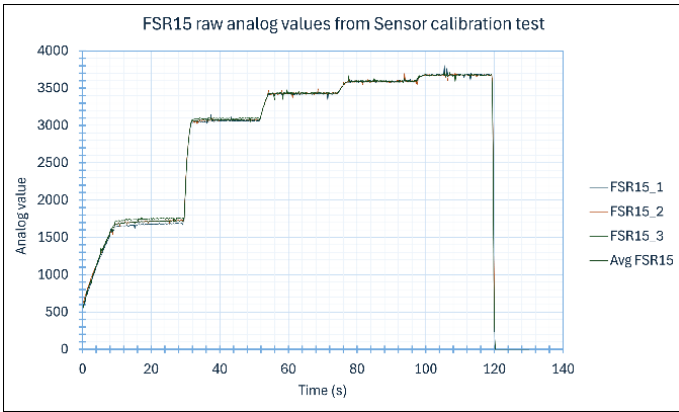
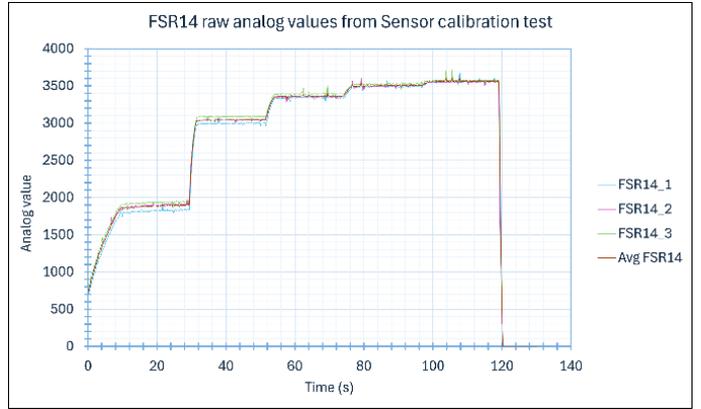
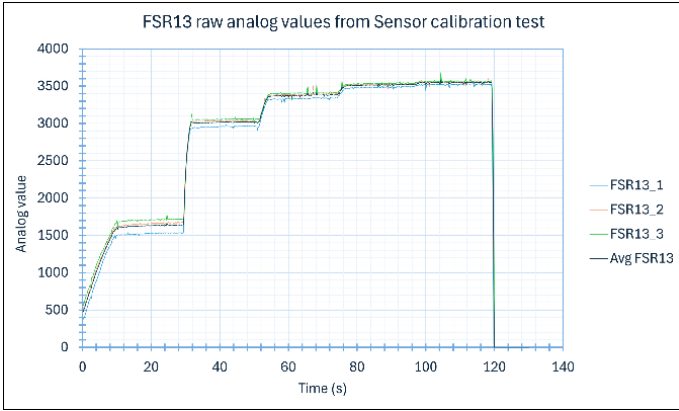
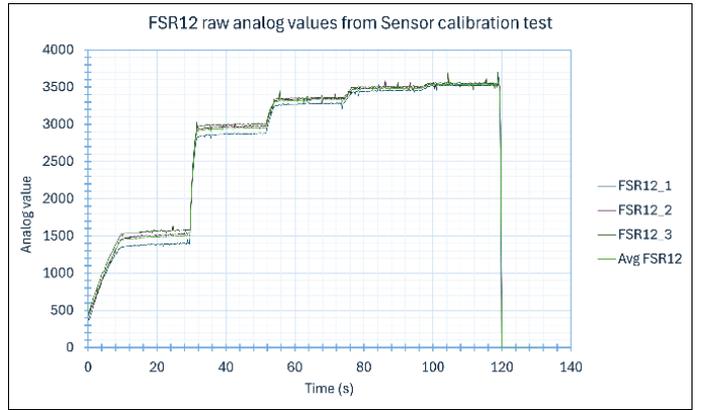
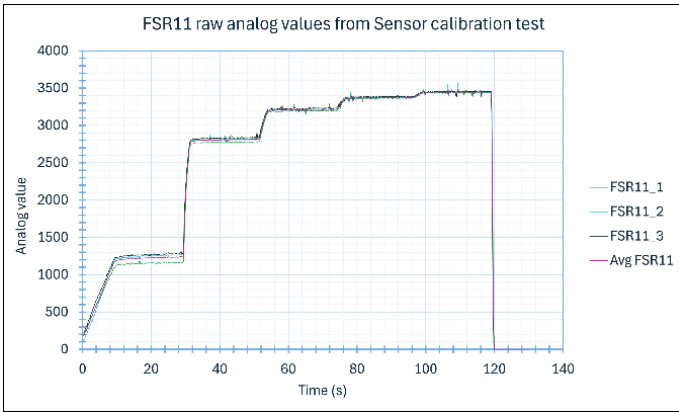
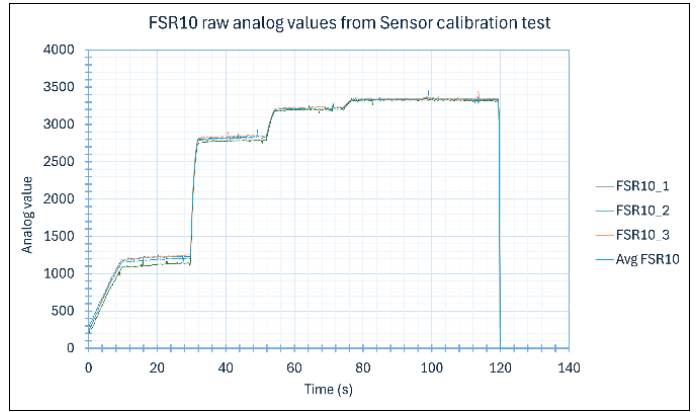
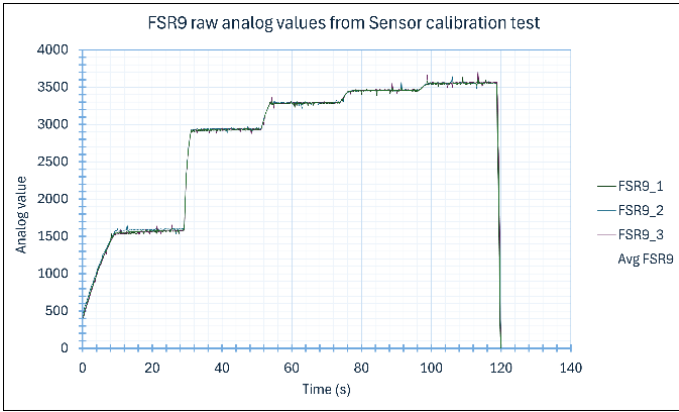
Simulated gait pattern loading protocol reference from Orthoload



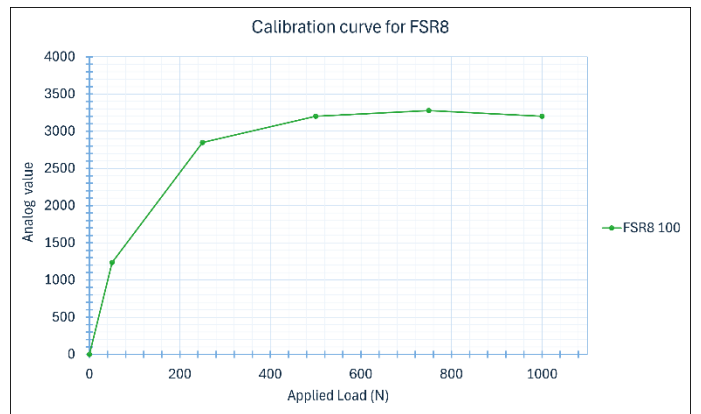
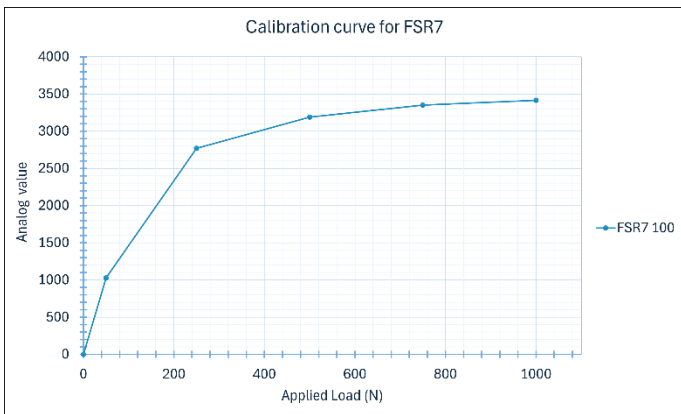
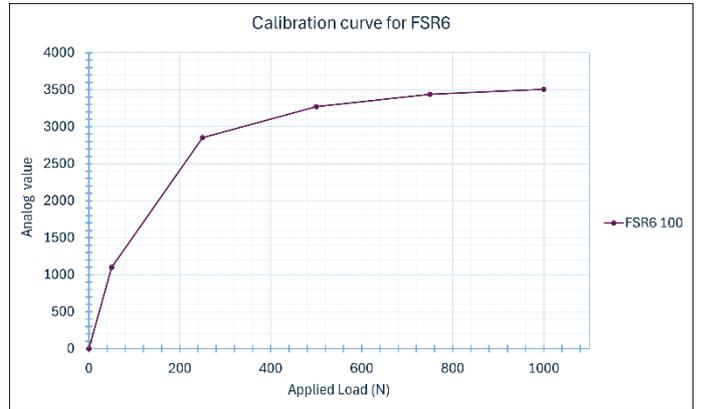
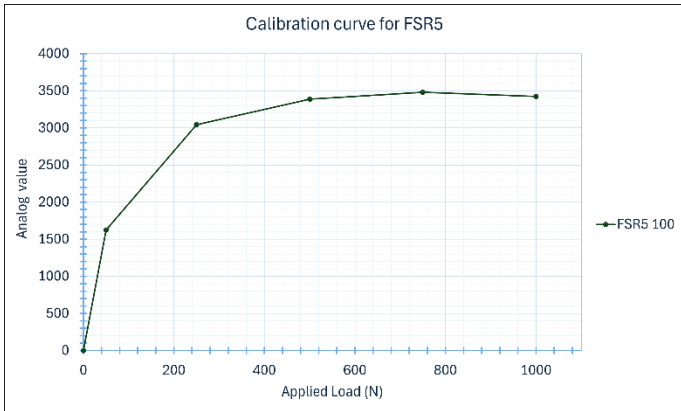
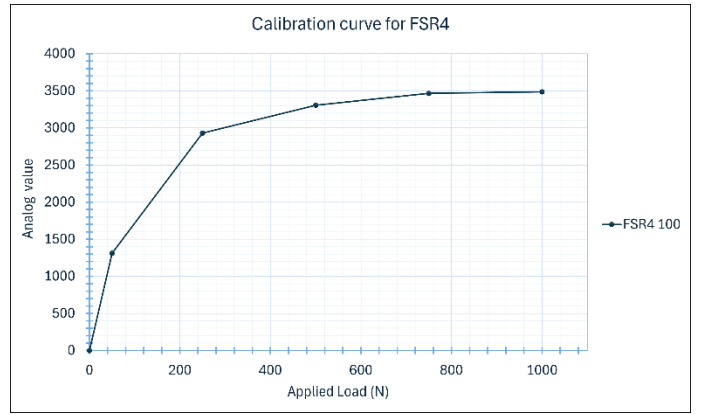
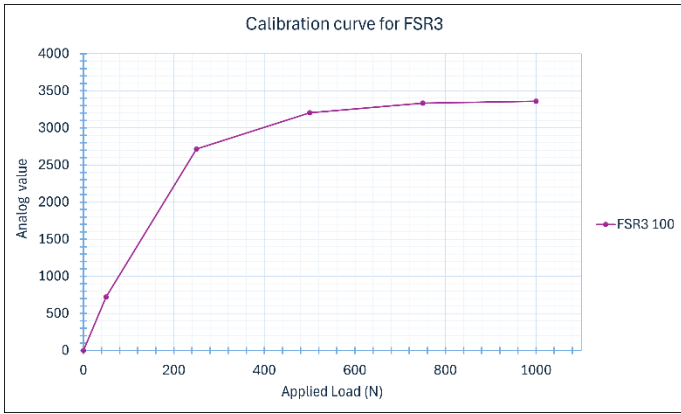
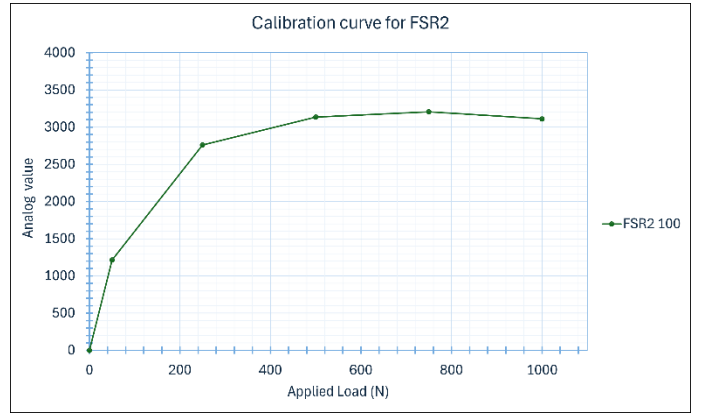
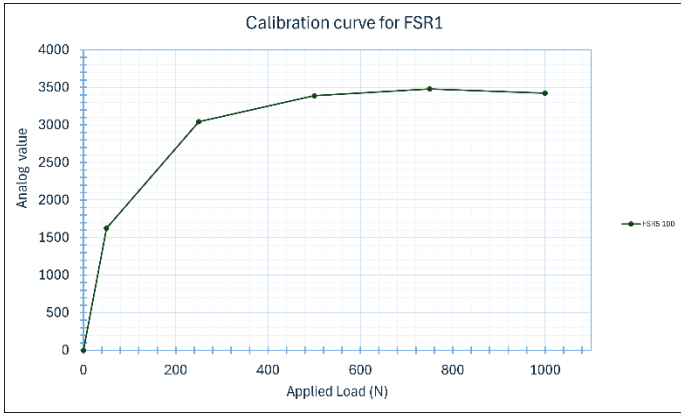
[Link to data repository](#)

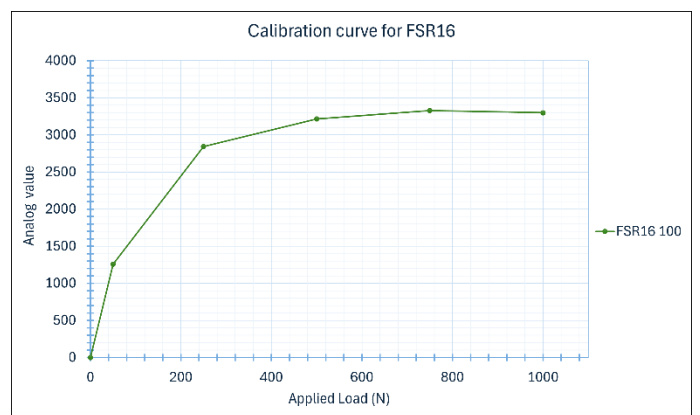
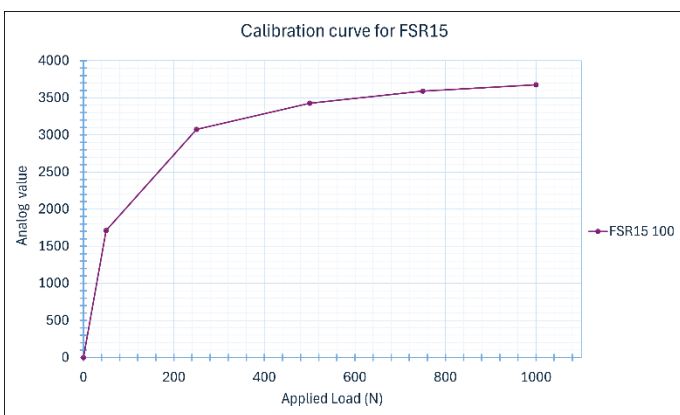
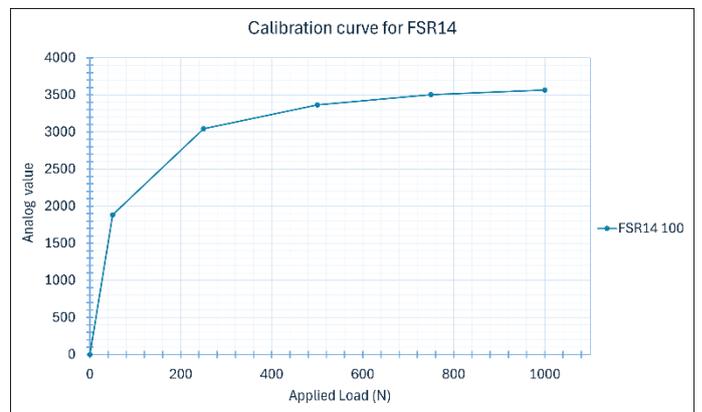
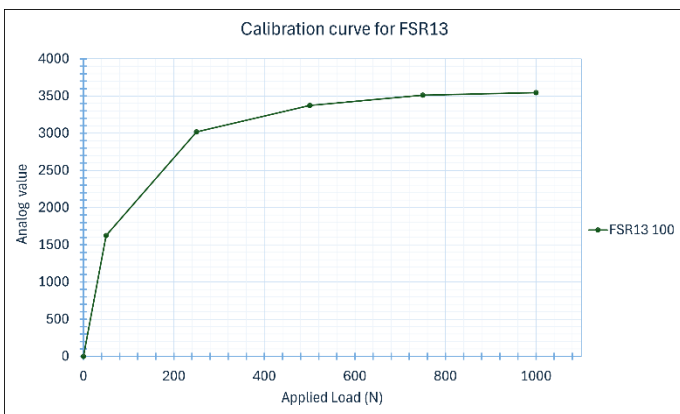
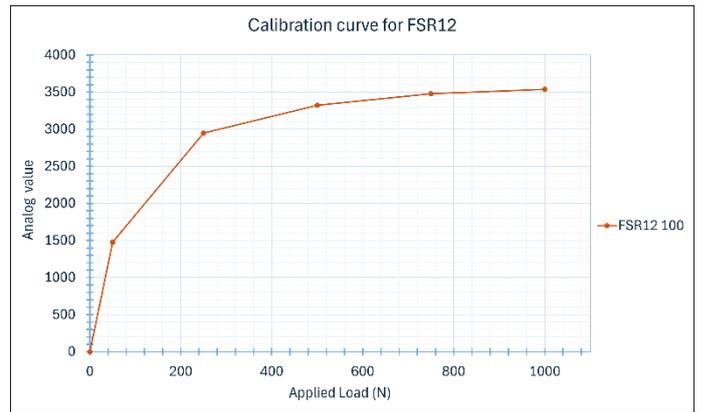
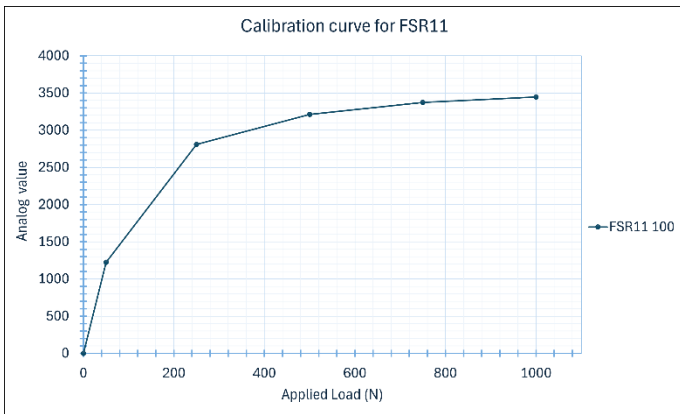
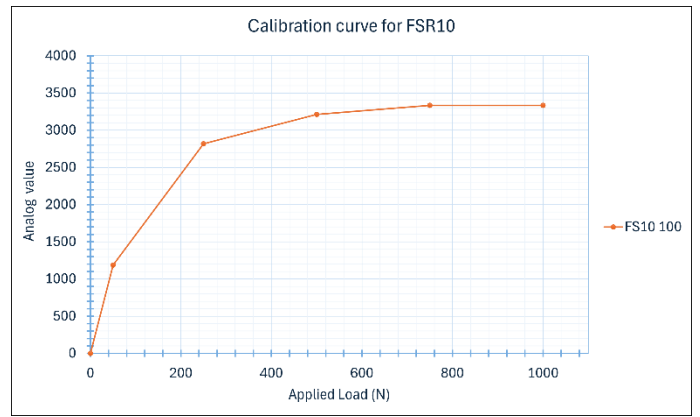
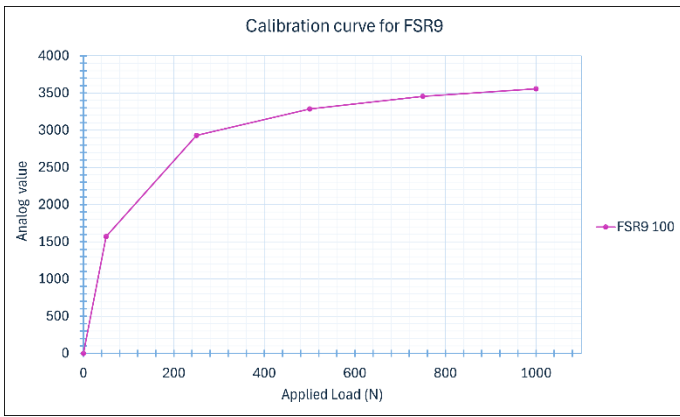
Appendix J.
Sensor calibration test results scatter plots.
FSR raw analog value against time





Appendix K.
Calibration curves from Sensor calibration test





Appendix L.

Sensor calibration test results column charts and tables.

FSR analog value grouped by applied load

FSR1	<i>Applied Load</i>	<i>AvgFSR1_1</i>	<i>AvgFSR1_2</i>	<i>AvgFSR1_3</i>	<i>AvgFSR1</i>	<i>SD</i>
	50	787.92	725.31	624.67	712.63	67.25
	250	2700.47	2681.06	2665.94	2682.49	14.13
	500	3123.04	3095.65	3085.00	3101.23	16.02
	750	3196.41	3170.04	3153.90	3173.45	17.52
	1000	3091.14	3094.24	3078.16	3087.84	6.97
FSR2	<i>Applied Load</i>	<i>AvgFSR2_1</i>	<i>AvgFSR2_2</i>	<i>AvgFSR2_3</i>	<i>AvgFSR2</i>	<i>SD</i>
	50	1219.92	1233.88	1215.00	1222.93	8.00
	250	2764.80	2762.40	2767.46	2764.89	2.07
	500	3135.02	3119.94	3120.22	3125.06	7.04
	750	3205.12	3192.30	3189.56	3195.66	6.78
	1000	3112.58	3118.98	3119.54	3117.03	3.16
FSR3	<i>Applied Load</i>	<i>AvgFSR3_1</i>	<i>AvgFSR3_2</i>	<i>AvgFSR3_3</i>	<i>AvgFSR3</i>	<i>SD</i>
	50	695.84	750.84	743.86	730.18	24.45
	250	2693.70	2738.74	2751.98	2728.14	24.95
	500	3191.92	3209.52	3209.20	3203.55	8.22
	750	3350.98	3350.18	3338.36	3346.51	5.77
	1000	3376.56	3366.44	3348.28	3363.76	11.70
FSR4	<i>Applied Load</i>	<i>AvgFSR4_1</i>	<i>AvgFSR4_2</i>	<i>AvgFSR4_3</i>	<i>AvgFSR4</i>	<i>SD</i>
	50	1298.46	1357.06	1278.70	1311.41	33.27
	250	2924.64	2954.20	2946.92	2941.92	12.58
	500	3304.52	3306.40	3313.18	3308.03	3.72
	750	3439.64	3440.02	3446.00	3441.89	2.91
	1000	3479.18	3482.86	3500.74	3487.59	9.42
FSR5	<i>Applied Load</i>	<i>AvgFSR5_1</i>	<i>AvgFSR5_2</i>	<i>AvgFSR5_3</i>	<i>AvgFSR5</i>	<i>SD</i>
	50	1479.64	1687.08	1679.74	1615.49	96.10
	250	2945.18	3071.28	3099.88	3038.78	67.21
	500	3342.20	3406.80	3422.96	3390.65	34.89
	750	3471.56	3497.26	3497.76	3488.86	12.23
	1000	3429.24	3438.30	3439.82	3435.79	4.67
FSR6	<i>Applied Load</i>	<i>AvgFSR6_1</i>	<i>AvgFSR6_2</i>	<i>AvgFSR6_3</i>	<i>AvgFSR6</i>	<i>SD</i>
	50	1133.42	1122.92	1044.48	1100.27	39.68
	250	2871.44	2849.32	2835.04	2851.93	14.97
	500	3276.92	3261.20	3260.10	3266.07	7.68
	750	3445.94	3442.06	3437.76	3441.92	3.34
	1000	3538.04	3537.00	3539.22	3538.09	0.91
FSR7	<i>Applied Load</i>	<i>AvgFSR7_1</i>	<i>AvgFSR7_2</i>	<i>AvgFSR7_3</i>	<i>AvgFSR7</i>	<i>SD</i>
	50	1069.58	1037.70	980.22	1029.17	36.98
	250	2774.08	2757.70	2768.80	2766.86	6.83
	500	3194.82	3185.60	3193.58	3191.33	4.09
	750	3351.02	3351.14	3358.62	3353.59	3.55
	1000	3403.44	3415.92	3420.26	3413.21	7.13
FSR8	<i>Applied Load</i>	<i>AvgFSR8_1</i>	<i>AvgFSR8_2</i>	<i>AvgFSR8_3</i>	<i>AvgFSR8</i>	<i>SD</i>
	50	1144.08	1286.28	1269.92	1233.43	63.53
	250	2803.24	2861.20	2875.04	2846.49	31.10
	500	3194.02	3199.94	3210.26	3201.41	6.71
	750	3284.00	3273.72	3276.76	3278.16	4.31
	1000	3188.94	3211.08	3212.30	3204.11	10.74

	Applied Load	AvgFSR9_1	AvgFSR9_2	AvgFSR9_3	AvgFSR9	SD
FSR9	50	1553.96	1588.84	1564.34	1569.05	14.62
	250	2921.64	2939.20	2931.18	2930.67	7.18
	500	3280.18	3289.14	3289.10	3286.14	4.21
	750	3451.40	3456.90	3460.78	3456.36	3.85
	1000	3546.30	3557.68	3555.32	3553.10	4.90

	Applied Load	AvgFSR10_1	AvgFSR10_2	AvgFSR10_3	AvgFSR10	SD
FSR10	50	1113.18	1218.56	1219.64	1183.79	49.93
	250	2774.64	2816.86	2835.10	2808.87	25.32
	500	3198.00	3215.26	3223.84	3212.37	10.75
	750	3324.10	3335.28	3342.84	3334.07	7.70
	1000	3323.26	3337.88	3346.42	3335.85	9.56

	Applied Load	AvgFSR11_1	AvgFSR11_2	AvgFSR11_3	AvgFSR11	SD
FSR11	50	1151.50	1249.36	1265.94	1222.27	50.50
	250	2775.56	2810.16	2829.60	2805.11	22.35
	500	3196.40	3213.98	3225.92	3212.10	12.12
	750	3363.10	3373.88	3385.32	3374.10	9.07
	1000	3438.34	3449.72	3449.50	3445.85	5.31

	Applied Load	AvgFSR12_1	AvgFSR12_2	AvgFSR12_3	AvgFSR12	SD
FSR12	50	1380.44	1504.88	1558.18	1481.17	74.47
	250	2863.50	2963.46	2991.04	2939.33	54.79
	500	3277.90	3338.96	3350.40	3322.42	31.82
	750	3452.74	3491.44	3503.26	3482.48	21.58
	1000	3520.70	3538.86	3554.54	3538.03	13.83

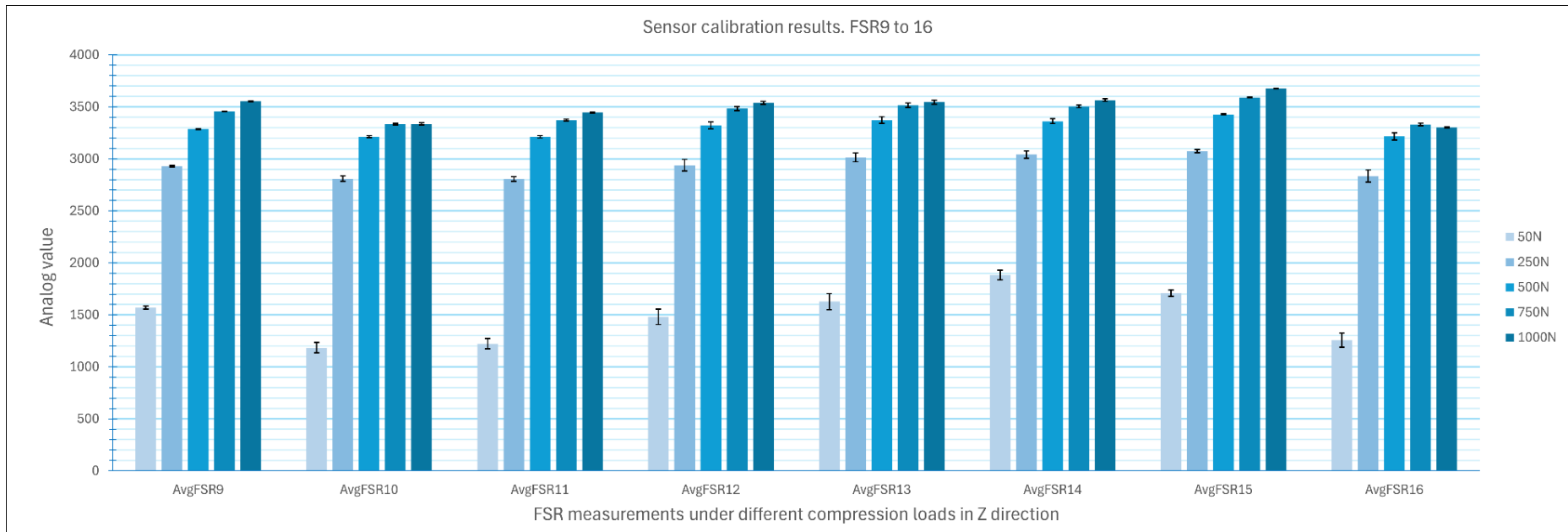
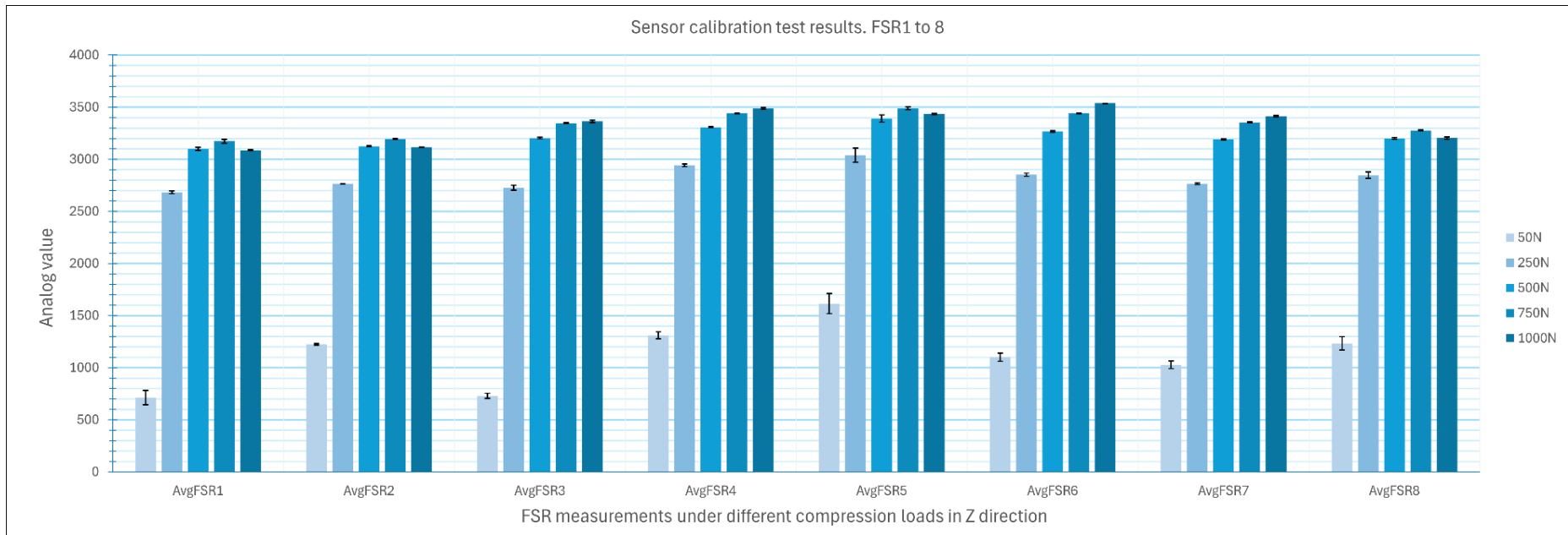
	Applied Load	AvgFSR13_1	AvgFSR13_2	AvgFSR13_3	AvgFSR13	SD
FSR13	50	1520.56	1654.80	1706.00	1627.12	78.19
	250	2953.34	3032.66	3053.26	3013.09	43.08
	500	3330.72	3385.48	3405.04	3373.75	31.45
	750	3484.48	3522.58	3535.00	3514.02	21.49
	1000	3519.64	3552.50	3566.08	3546.07	19.50

	Applied Load	AvgFSR14_1	AvgFSR14_2	AvgFSR14_3	AvgFSR14	SD
FSR14	50	1670.50	1711.38	1746.44	1709.44	31.03
	250	3056.44	3068.82	3093.78	3073.01	15.53
	500	3421.16	3428.50	3434.88	3428.18	5.61
	750	3588.90	3586.76	3594.20	3589.95	3.13
	1000	3680.86	3673.14	3674.74	3676.25	3.33

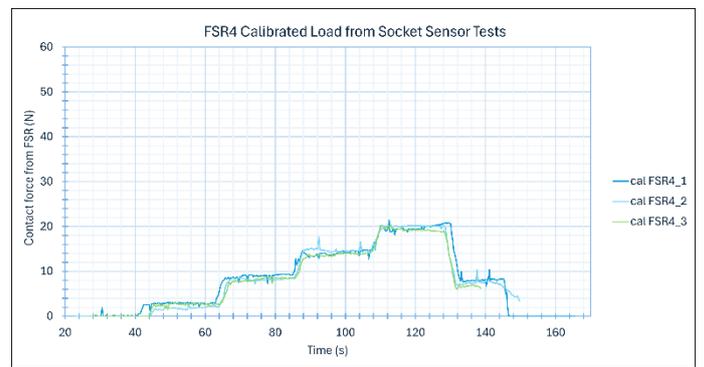
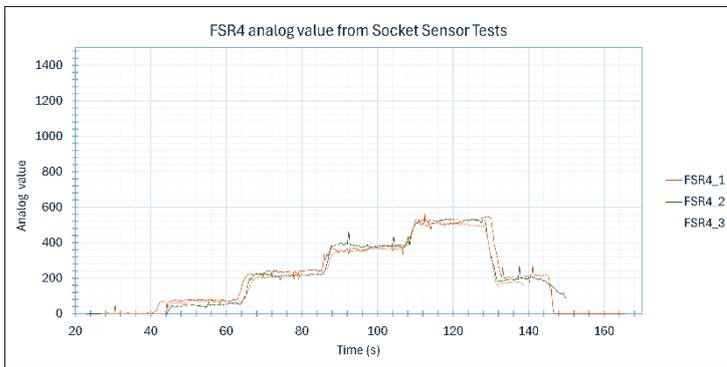
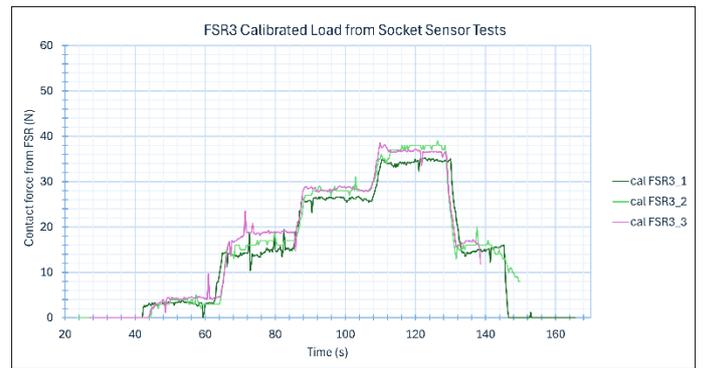
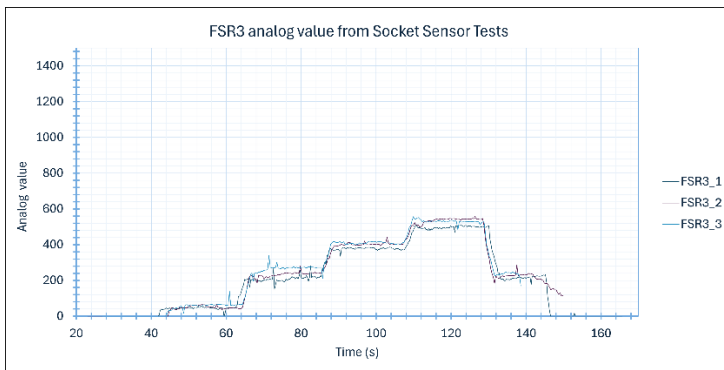
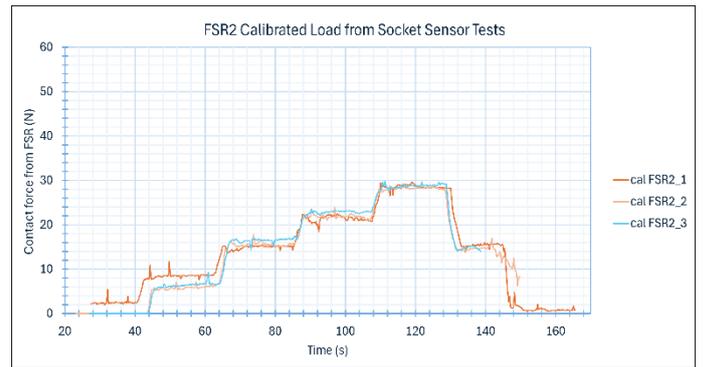
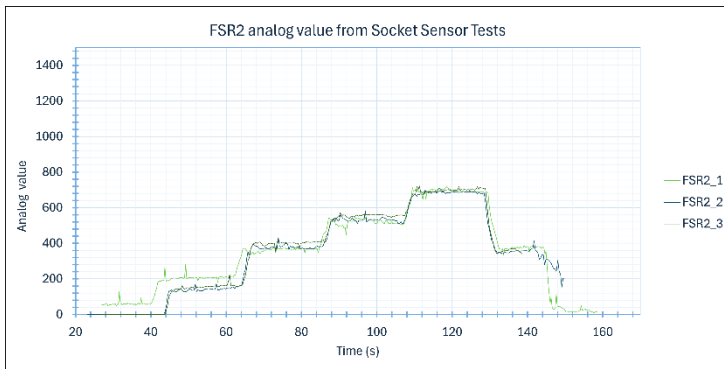
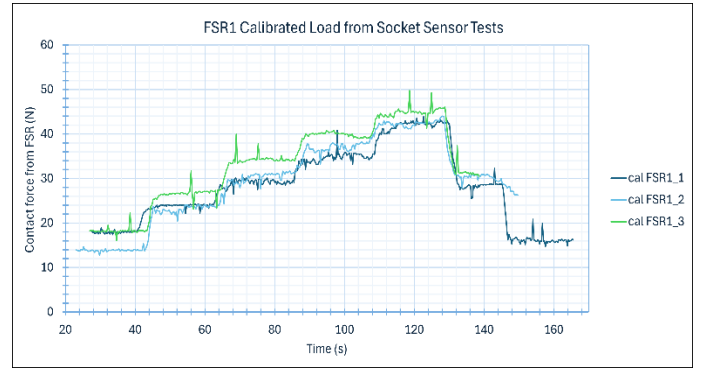
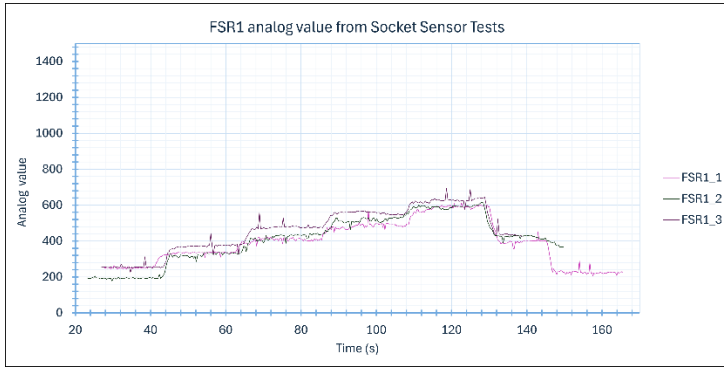
	Applied Load	AvgFSR15_1	AvgFSR15_2	AvgFSR15_3	AvgFSR15	SD
FSR15	50	1670.50	1711.38	1746.44	1709.44	31.03
	250	3056.44	3068.82	3093.78	3073.01	15.53
	500	3421.16	3428.50	3434.88	3428.18	5.61
	750	3588.90	3586.76	3594.20	3589.95	3.13
	1000	3680.86	3673.14	3674.74	3676.25	3.33

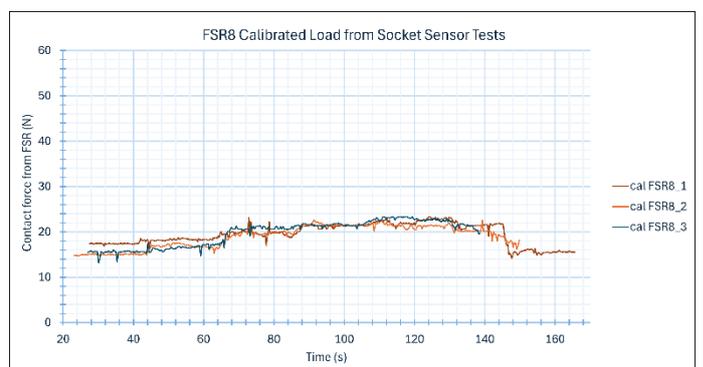
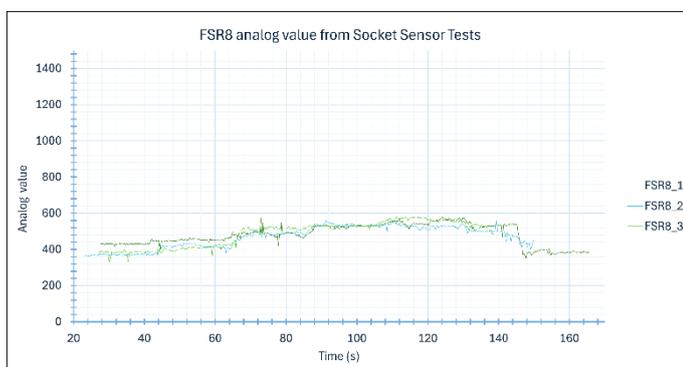
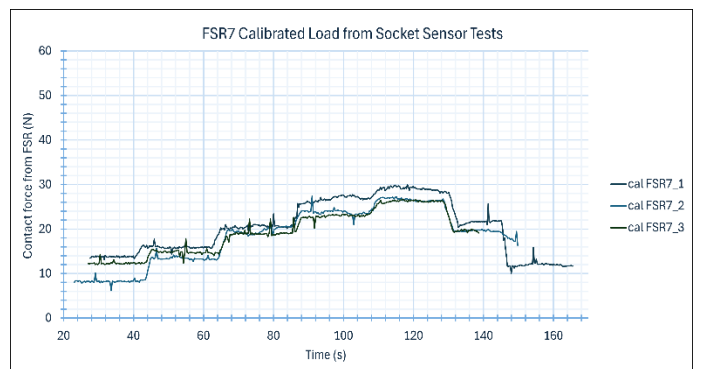
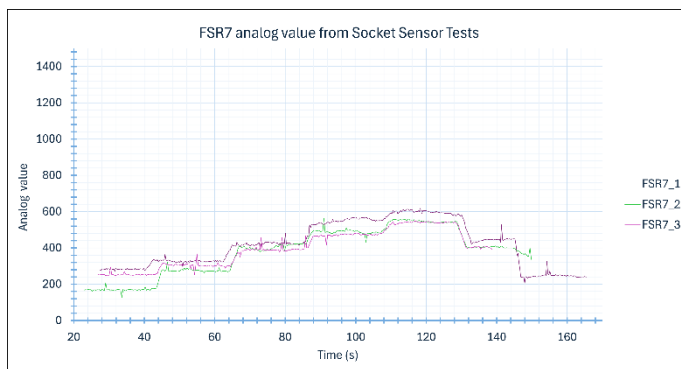
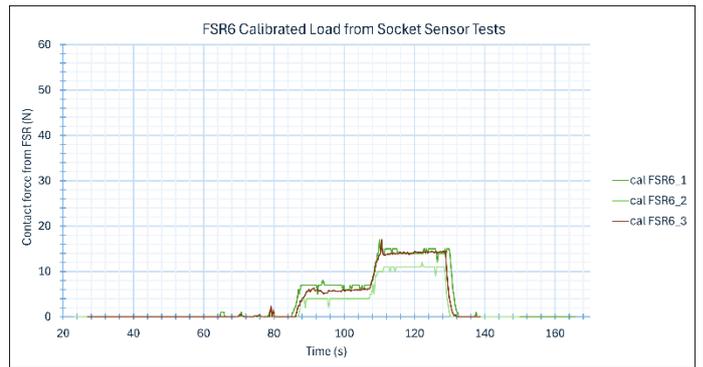
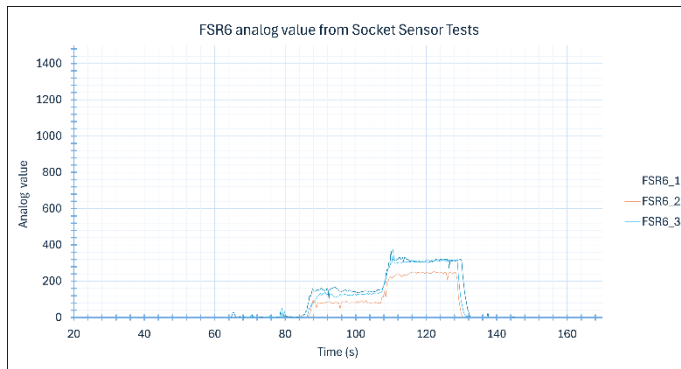
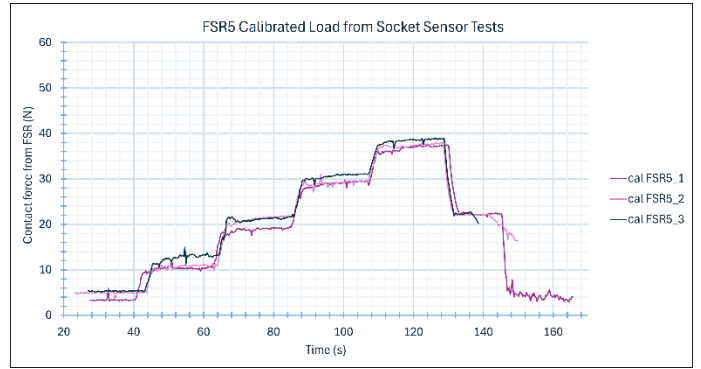
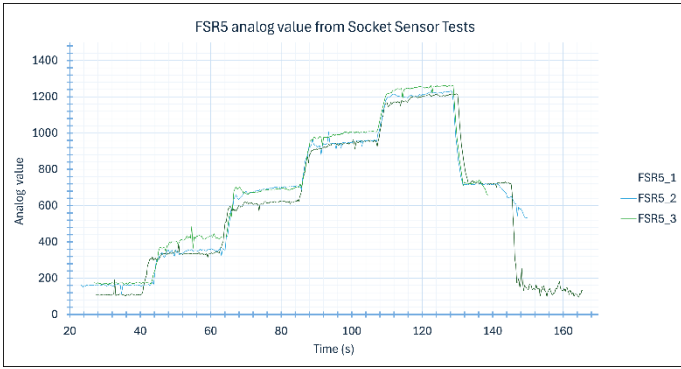
	Applied Load	AvgFSR16_1	AvgFSR16_2	AvgFSR16_3	AvgFSR16	SD
FSR16	50	1176.64	1247.08	1344.36	1256.03	68.76
	250	2752.66	2862.04	2888.56	2834.42	58.82
	500	3168.20	3231.54	3248.32	3216.02	34.50
	750	3313.24	3332.04	3345.16	3330.15	13.10
	1000	3294.94	3302.96	3308.08	3301.99	5.41

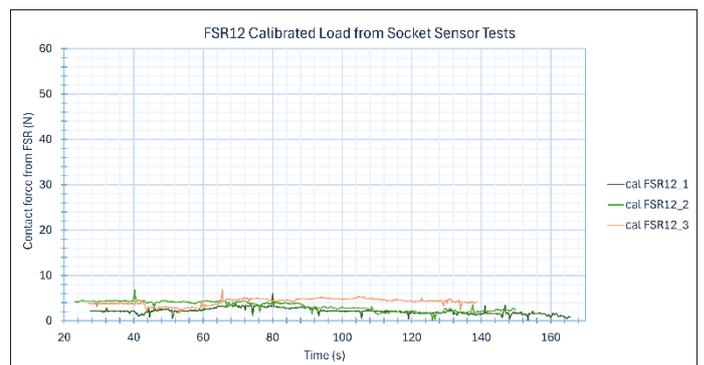
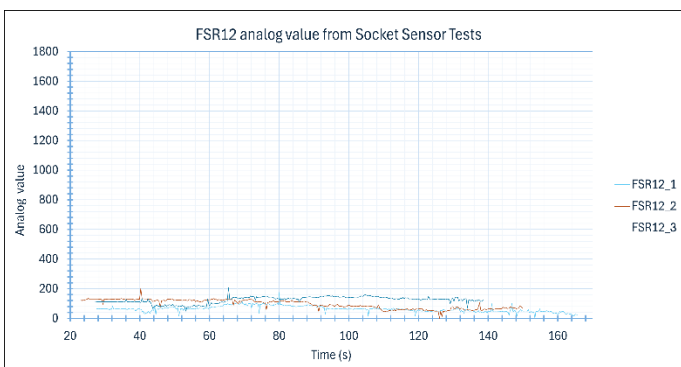
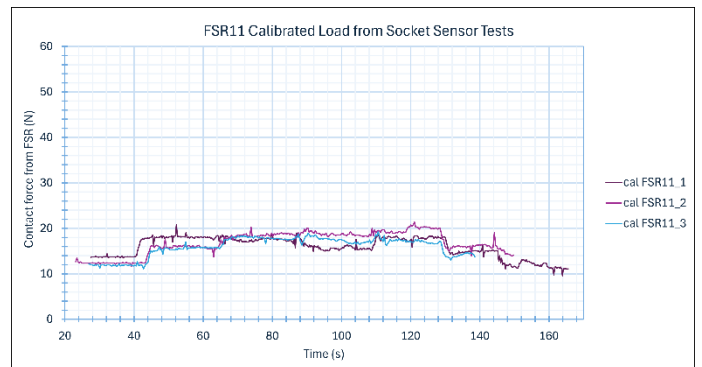
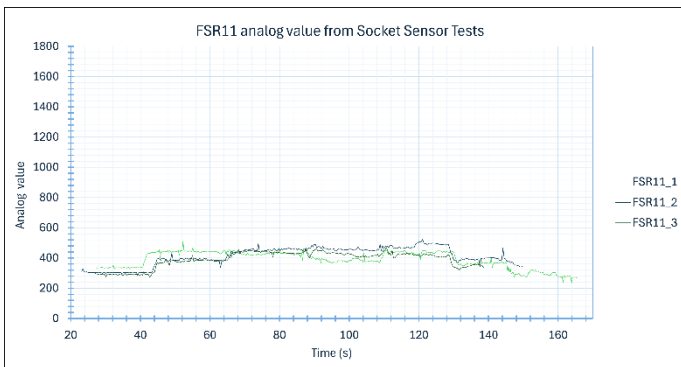
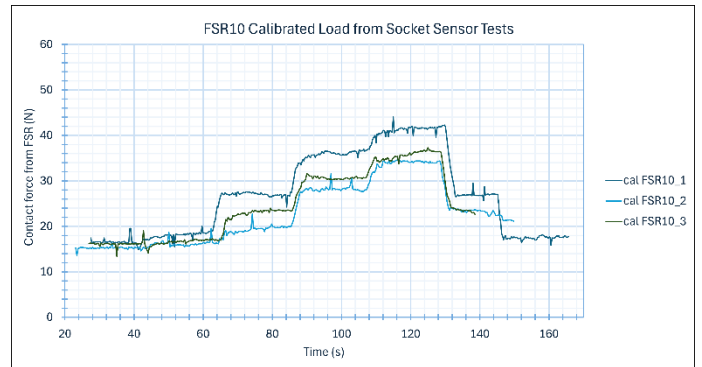
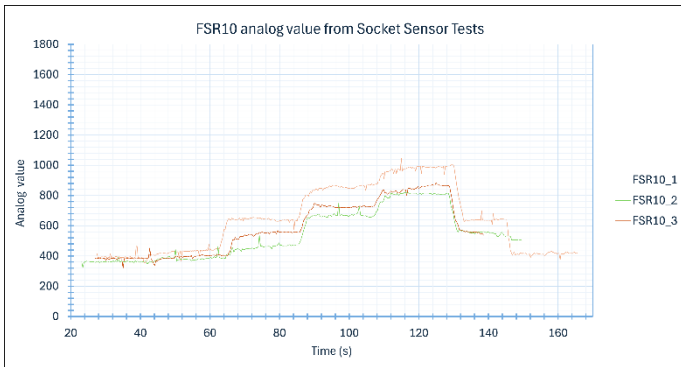
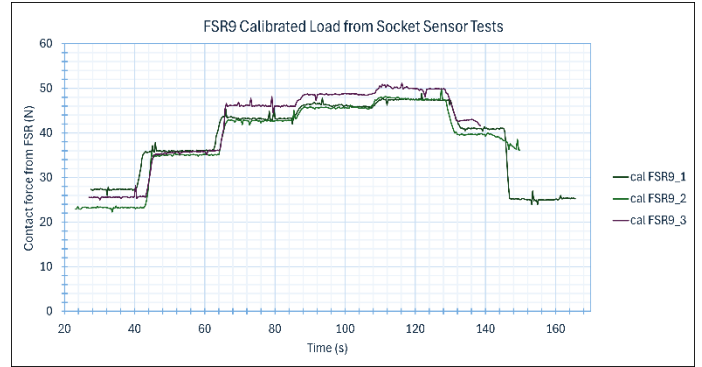
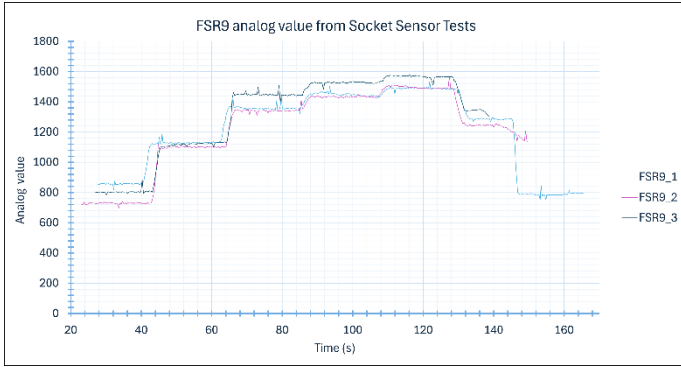
Applied Load units in Newton
Sensor results are analog value

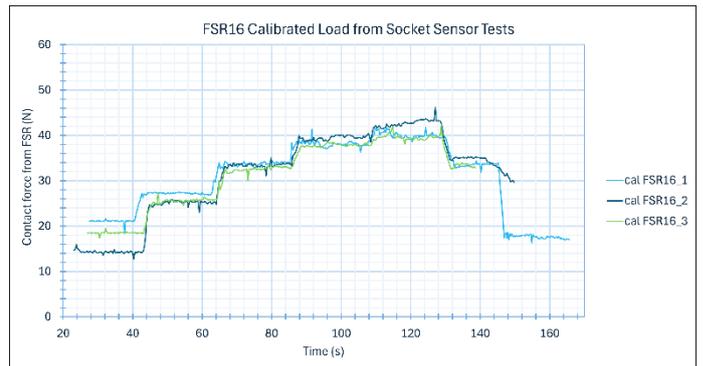
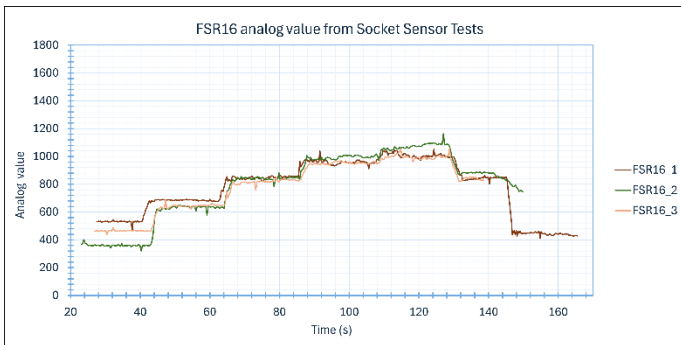
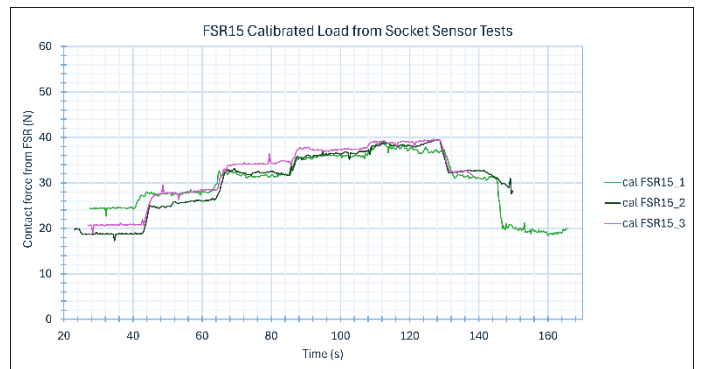
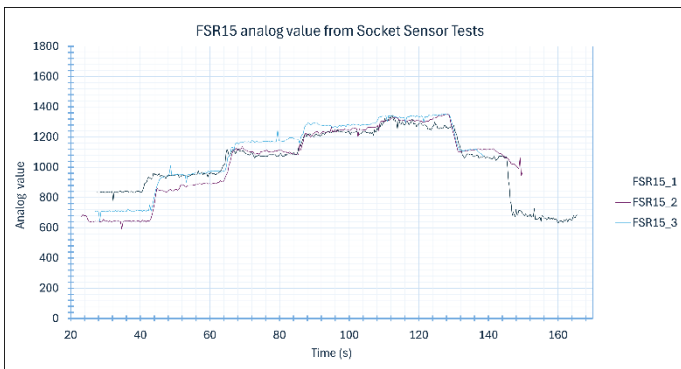
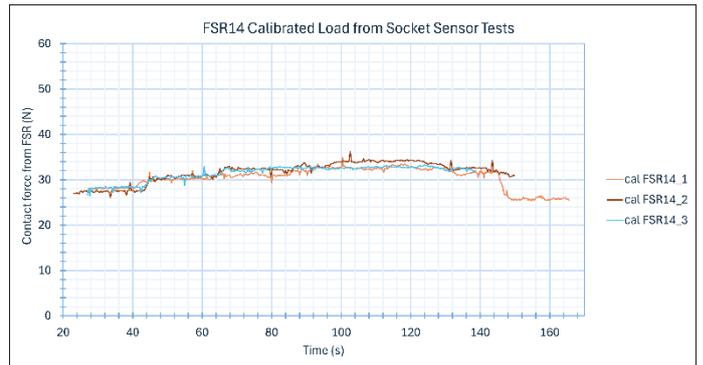
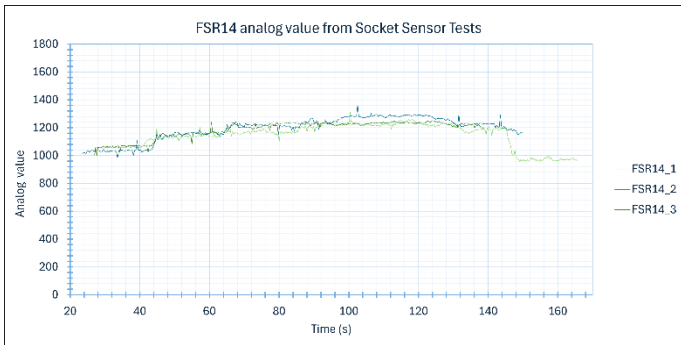
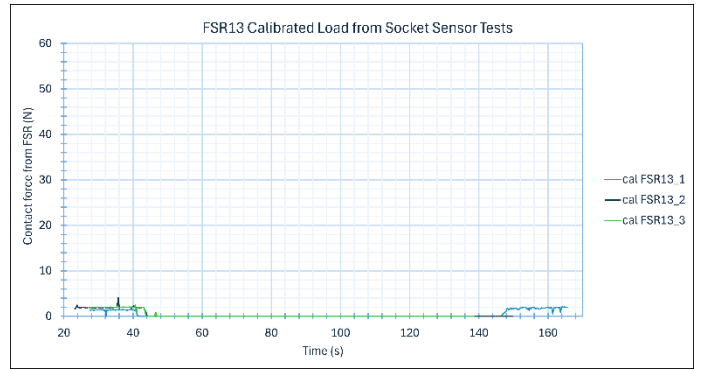
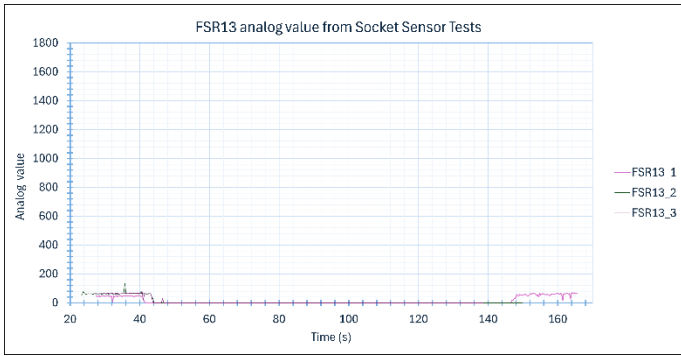


Appendix M.
Individual breakdown of Socket Sensor test results scatter plots









Appendix N.

Individual breakdown of Socket sensor test results column charts.
Calibrated Load sensor output grouped by applied load

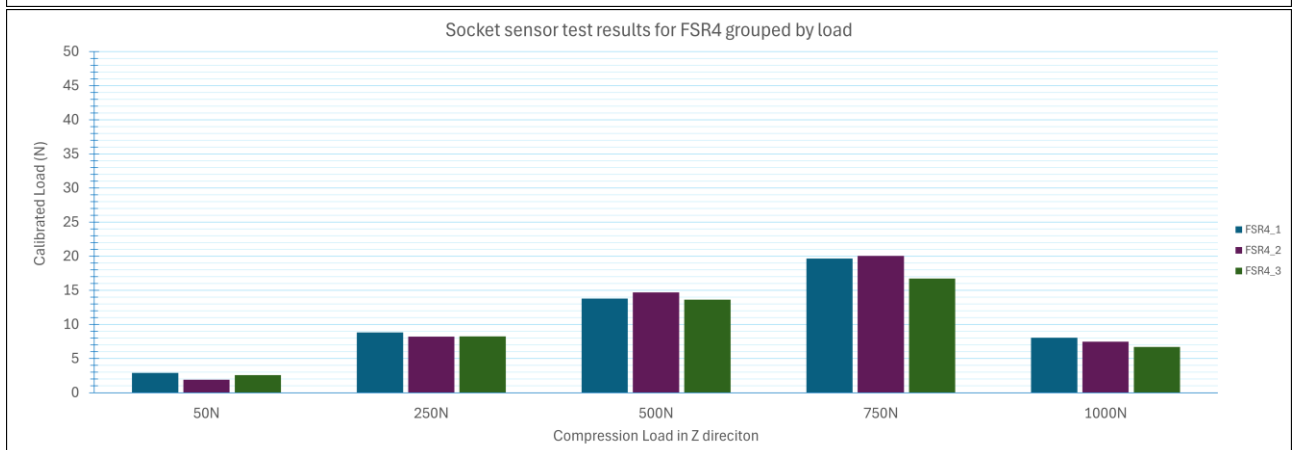
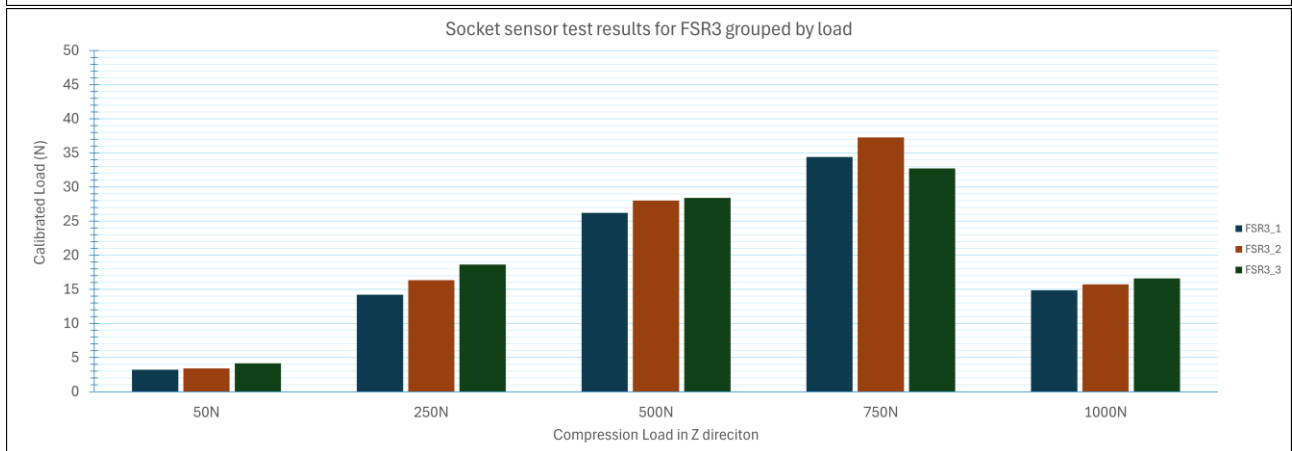
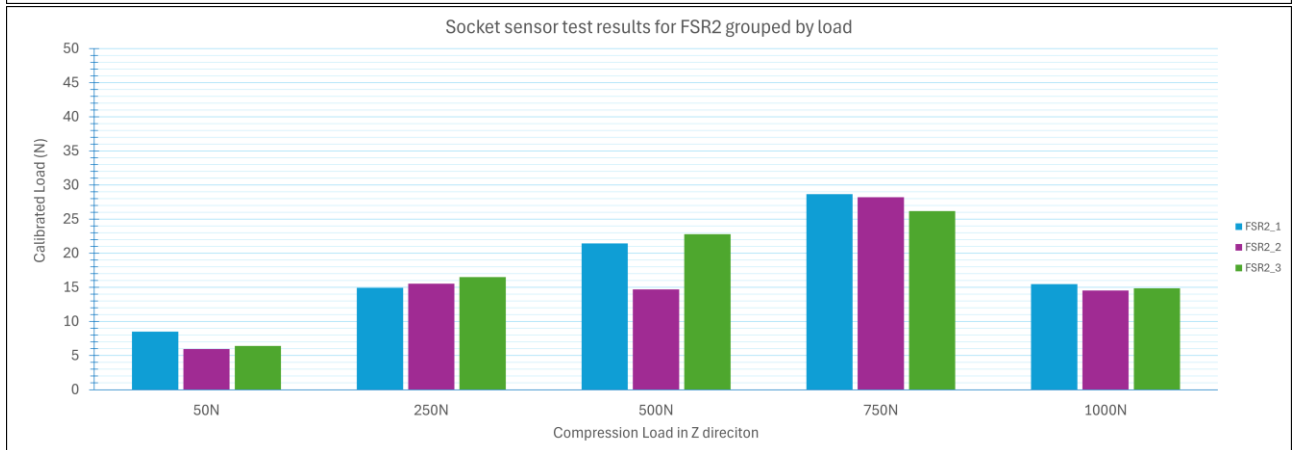
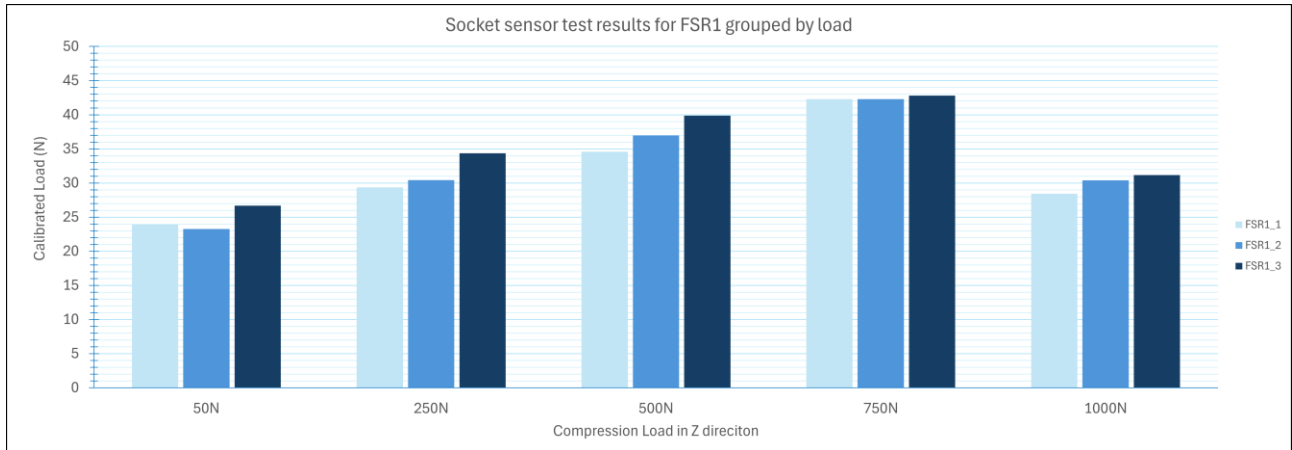
Applied Load	FSR1_1	FSR1_2	FSR1_3	FSR2_1	FSR2_2	FSR2_3	FSR3_1	FSR3_2	FSR3_3	FSR4_1	FSR4_2	FSR4_3
50	23.90	23.27	26.67	8.50	5.95	6.40	3.22	3.40	4.17	2.89	1.89	2.58
250	29.36	30.42	34.35	14.94	15.53	16.51	14.23	16.34	18.64	8.84	8.23	8.26
500	34.58	36.97	39.89	21.44	14.70	22.78	26.22	28.02	28.39	13.79	14.70	13.65
750	42.29	42.29	42.80	28.66	28.20	26.17	34.41	37.26	32.74	19.67	20.05	16.72
1000	28.42	30.40	31.16	15.48	14.53	14.85	14.85	15.74	16.61	8.07	7.48	6.71

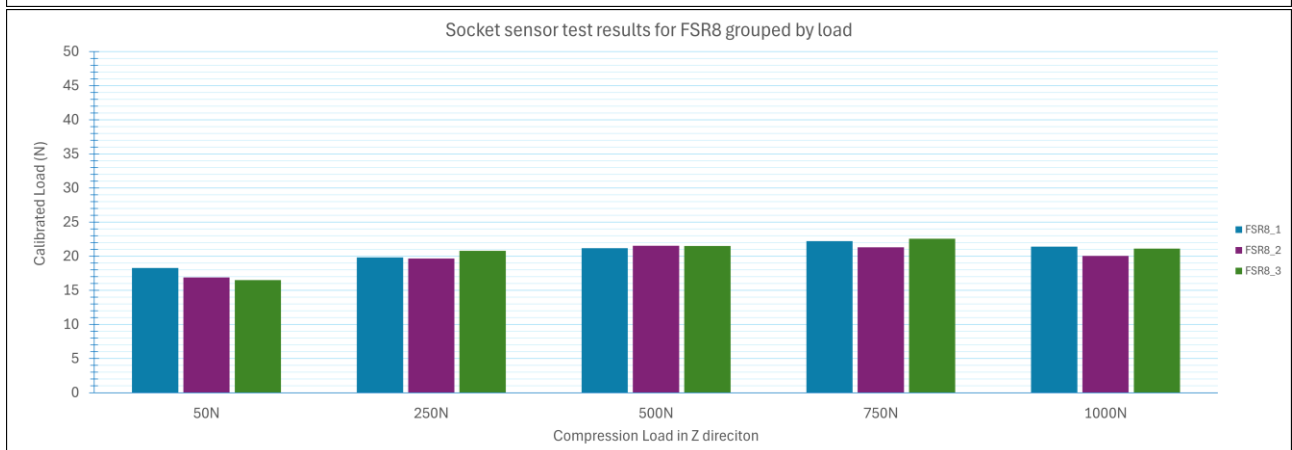
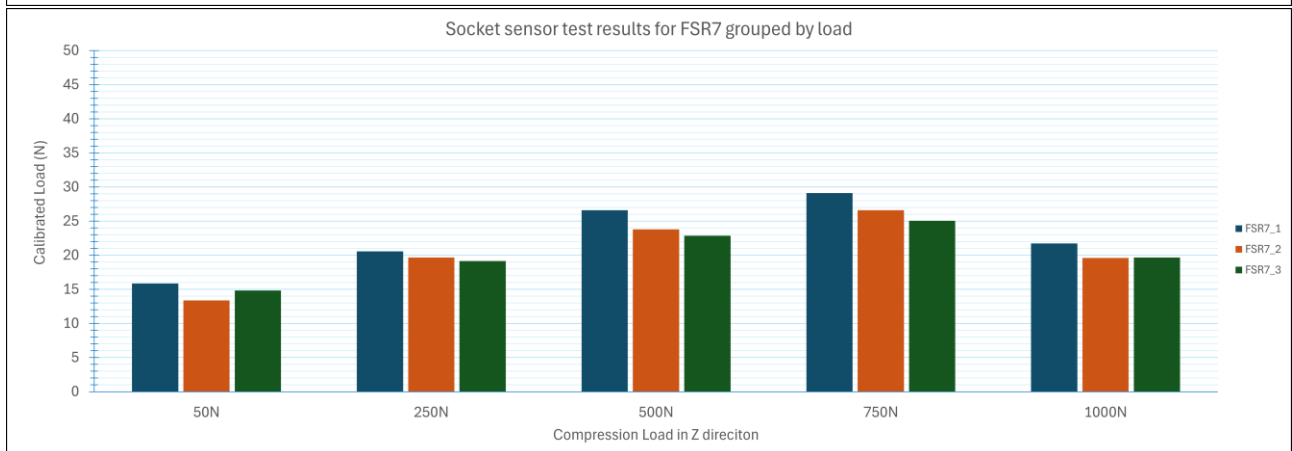
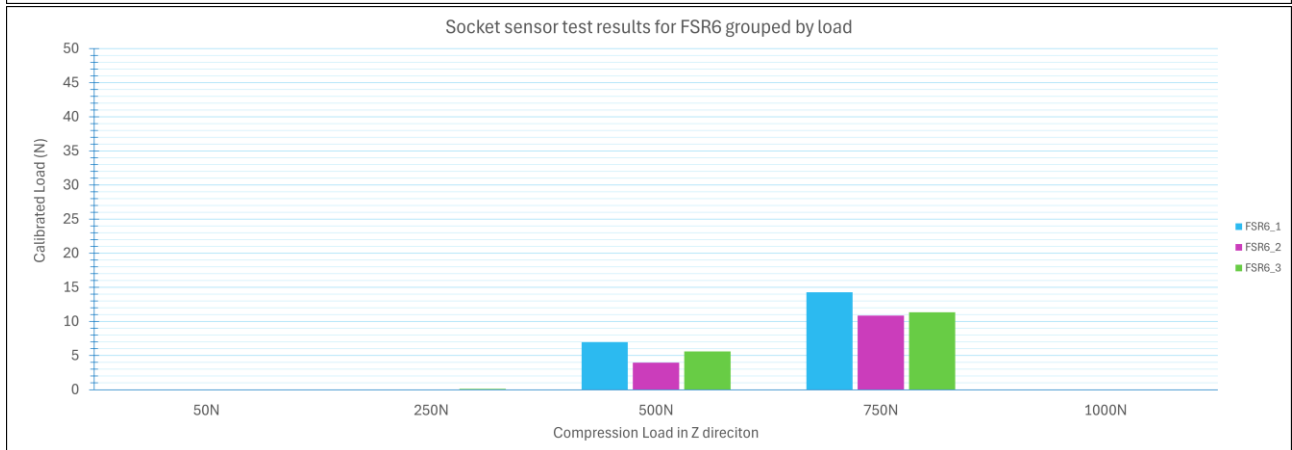
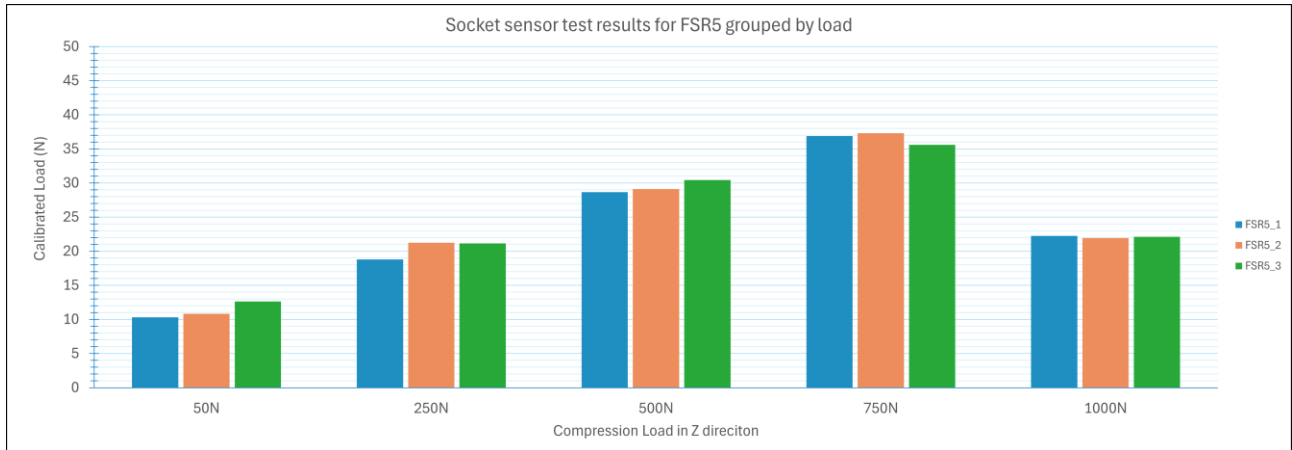
Applied Load	FSR5_1	FSR5_2	FSR5_3	FSR6_1	FSR6_2	FSR6_3	FSR7_1	FSR7_2	FSR7_3	FSR8_1	FSR8_2	FSR8_3
50	10.33	10.83	12.65	0.00	0.00	0.00	15.88	13.38	14.82	18.27	16.89	16.50
250	18.81	21.26	21.14	0.04	0.00	0.14	20.58	19.67	19.15	19.83	19.67	20.80
500	28.67	29.12	30.44	6.98	3.96	5.62	26.61	23.79	22.86	21.20	21.55	21.49
750	36.90	37.32	35.60	14.28	10.88	11.35	29.13	26.61	25.06	22.23	21.32	22.56
1000	22.25	21.93	22.12	0.03	0.00	0.00	21.72	19.60	19.68	21.42	20.06	21.11

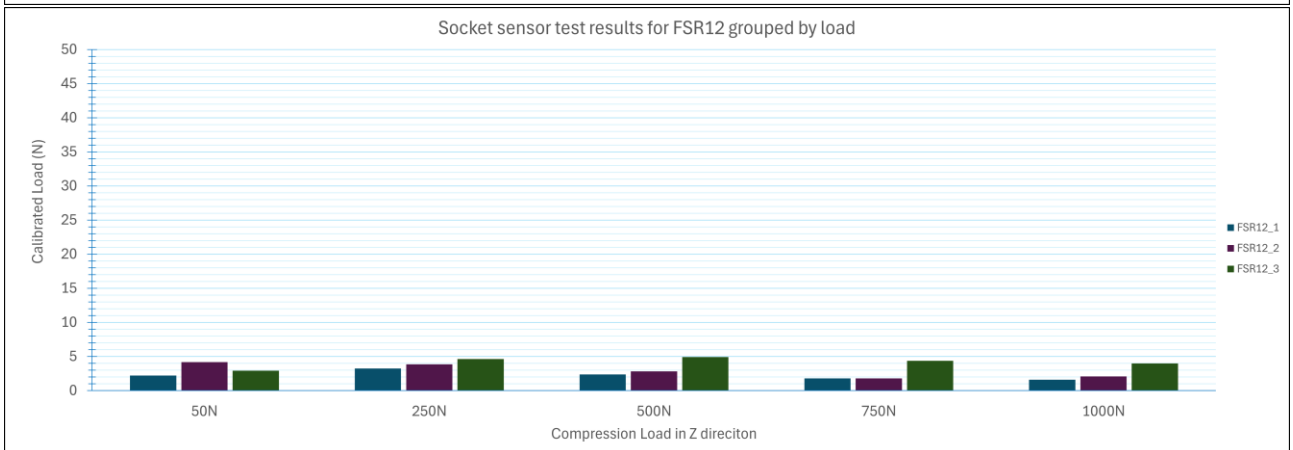
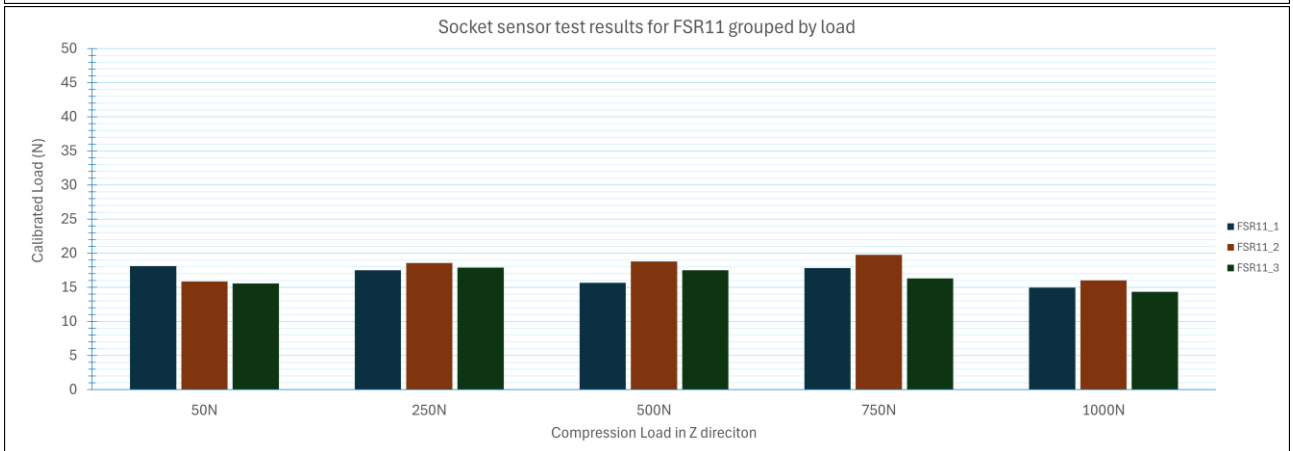
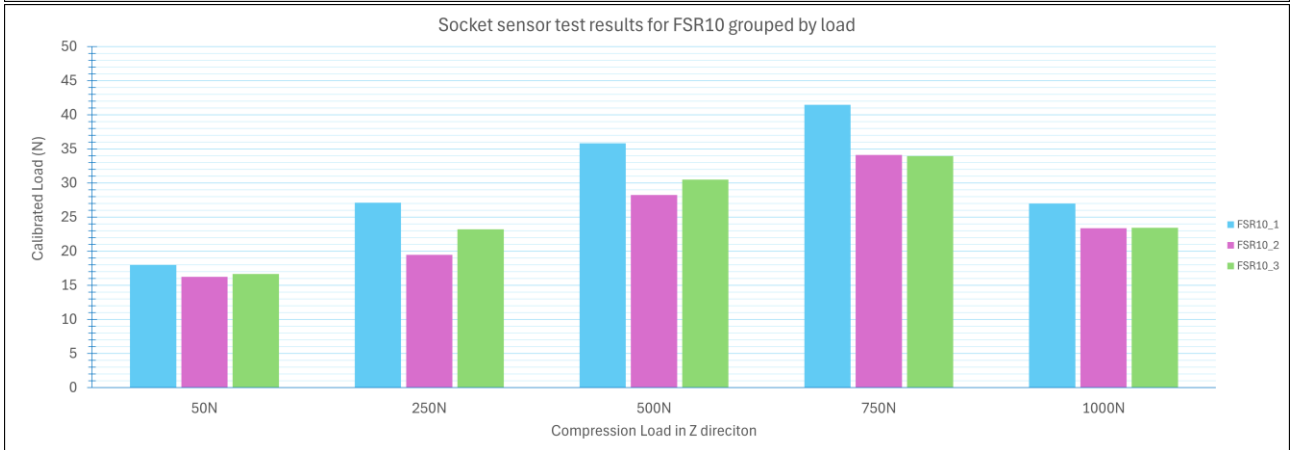
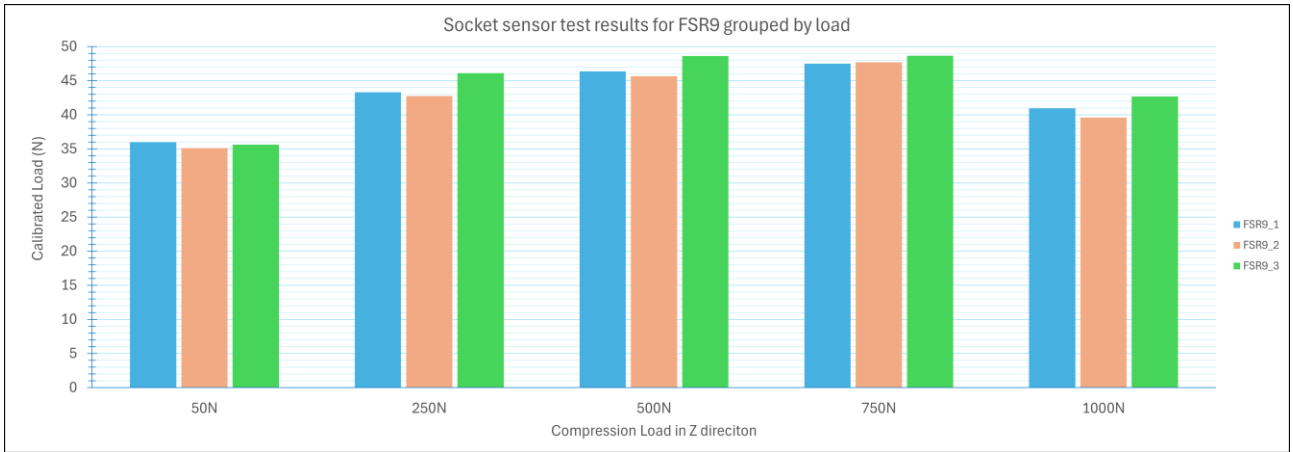
Applied Load	FSR9_1	FSR9_2	FSR9_3	FSR10_1	FSR10_2	FSR10_3	FSR11_1	FSR11_2	FSR11_3	FSR12_1	FSR12_2	FSR12_3
50	35.98	35.11	35.62	17.97	16.23	16.66	18.11	15.87	15.55	2.23	4.17	2.92
250	43.28	42.75	46.12	27.13	19.48	23.20	17.51	18.55	17.88	3.25	3.85	4.65
500	46.35	45.64	48.62	35.83	28.25	30.50	15.66	18.79	17.50	2.38	2.83	4.93
750	47.48	47.69	48.65	41.45	34.10	33.95	17.84	19.74	16.32	1.78	1.80	4.38
1000	40.95	39.59	42.70	26.99	23.38	23.44	14.95	16.03	14.33	1.61	2.08	4.00

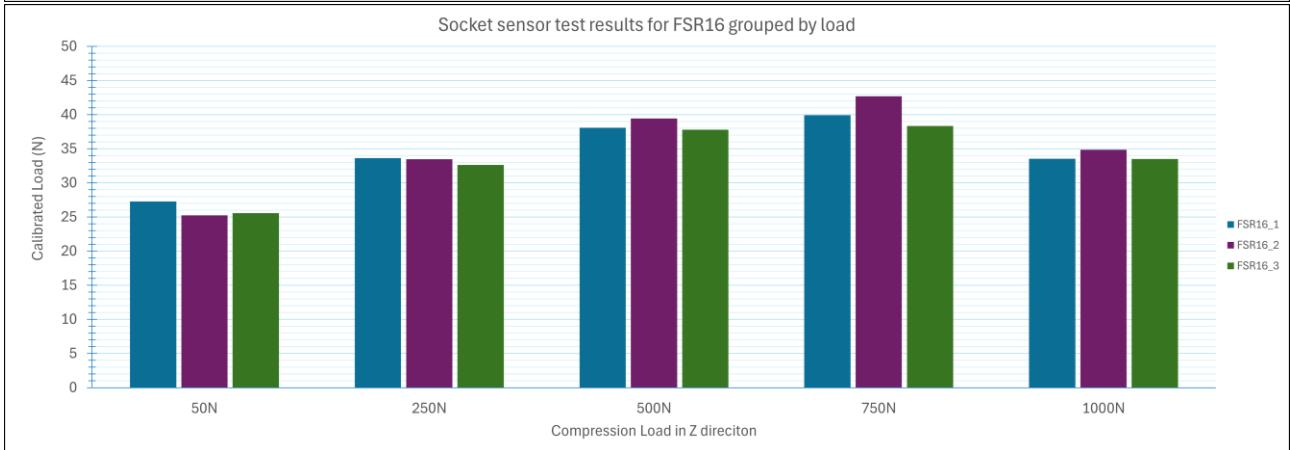
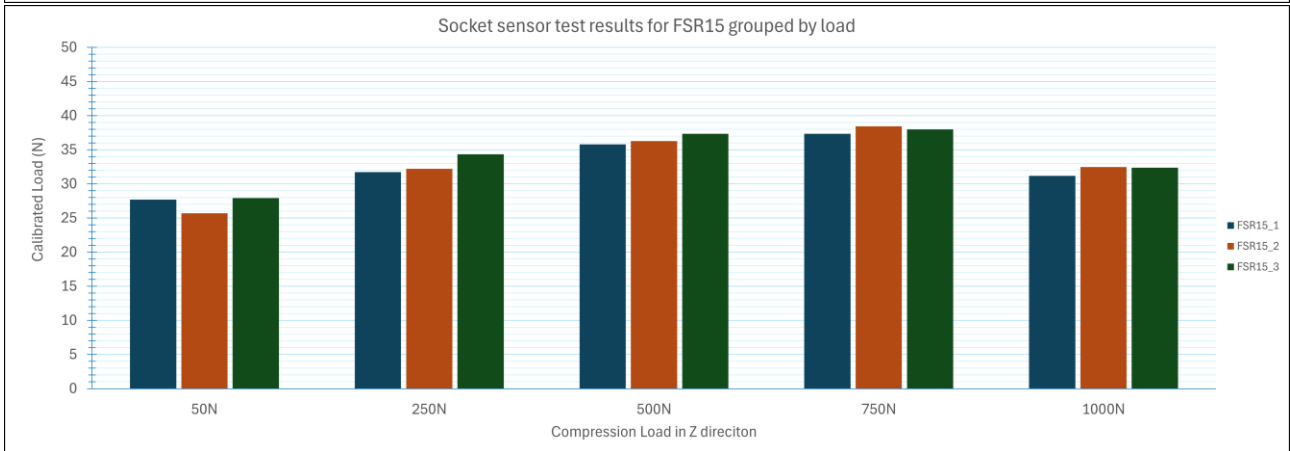
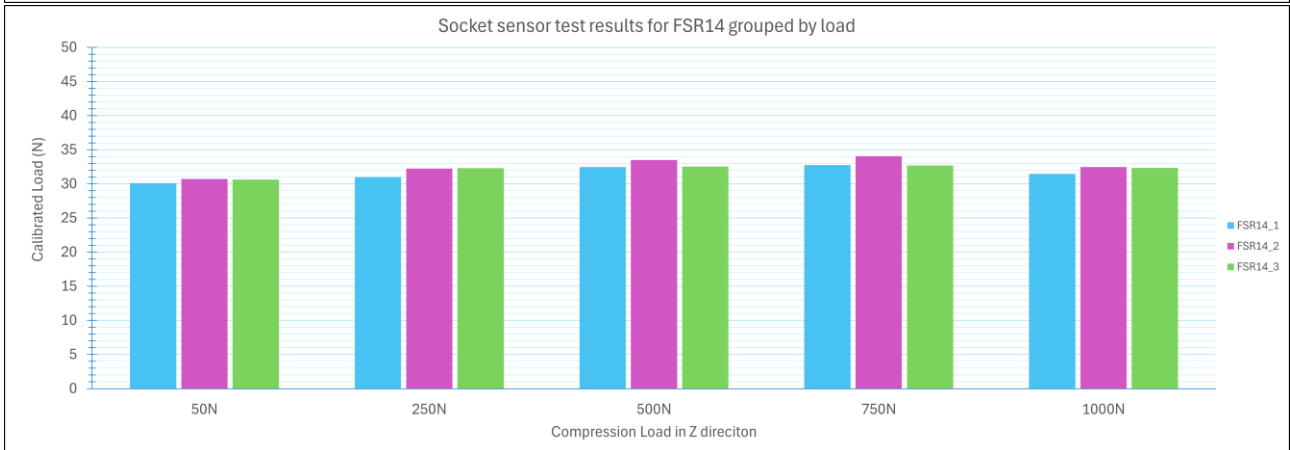
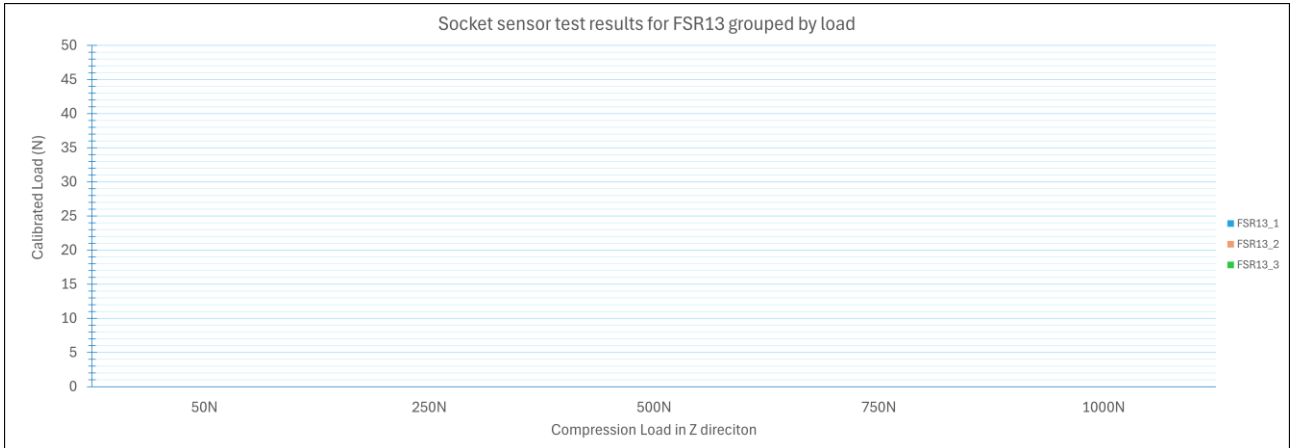
Applied Load	FSR13_1	FSR13_2	FSR13_3	FSR14_1	FSR14_2	FSR14_3	FSR15_1	FSR15_2	FSR15_3	FSR16_1	FSR16_2	FSR16_3
50	0.00	0.00	0.02	30.12	30.73	30.64	27.69	25.71	27.91	27.27	25.25	25.59
250	0.00	0.00	0.00	30.98	32.26	32.31	31.72	32.21	34.33	33.63	33.46	32.63
500	0.00	0.00	0.00	32.47	33.51	32.55	35.81	36.29	37.36	38.09	39.43	37.80
750	0.00	0.00	0.00	32.75	34.04	32.70	37.34	38.43	37.99	39.92	42.71	38.33
1000	0.00	0.00	0.00	31.46	32.48	32.35	31.19	32.46	32.39	33.55	34.85	33.49

Units in Newtons



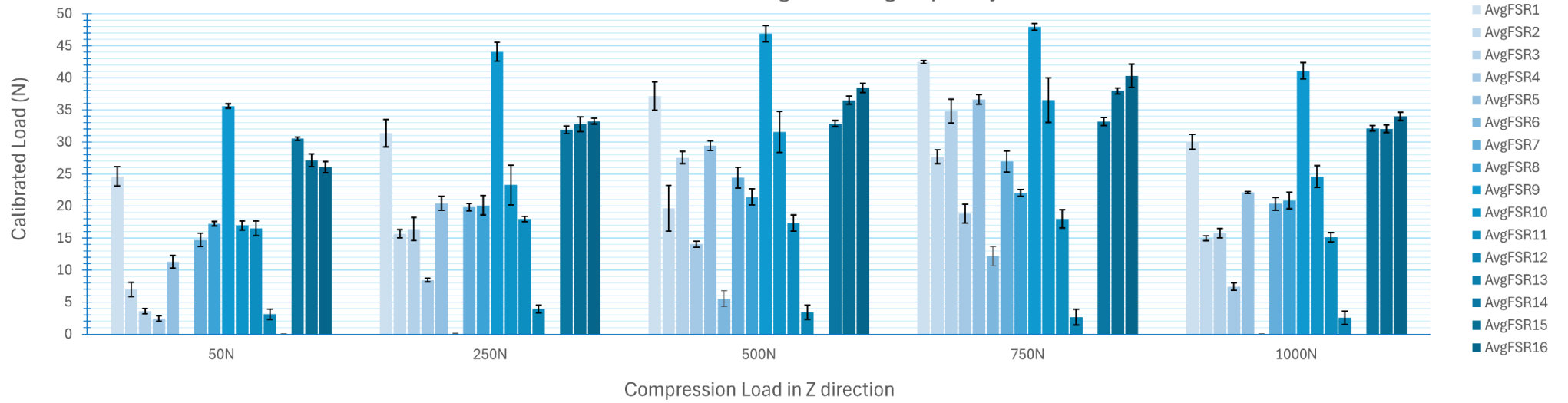






Appendix O.
Combined data of Socket Sensor test results.
Averaged Calibrated Load grouped by applied load

Socket sensor test average results grouped by load



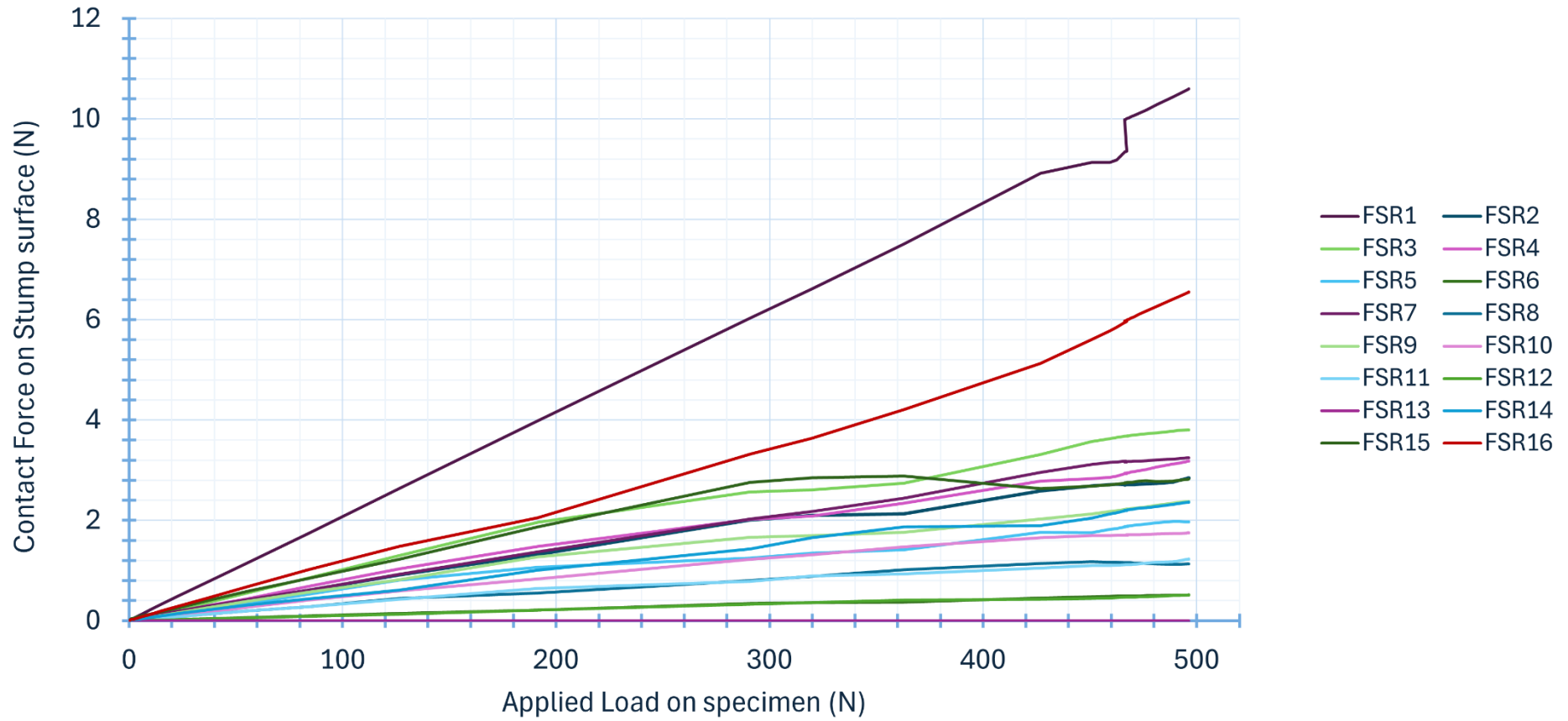
Applied Load	FSR1		FSR2		FSR3		FSR4		FSR5		FSR6		FSR7		FSR8	
	Avg Val	SD														
50N	24.61	1.48	6.95	1.11	3.59	0.41	2.45	0.42	11.27	1.00	0.00	0.00	14.69	1.02	17.22	0.36
250N	31.38	2.15	15.66	0.65	16.40	1.80	8.44	0.28	20.40	1.13	0.06	0.06	19.80	0.59	20.10	1.48
500N	37.14	2.17	19.64	3.53	27.54	0.95	14.05	0.47	29.41	0.75	5.52	1.23	24.42	1.60	21.41	1.27
750N	42.46	0.24	27.68	1.08	34.80	1.87	18.81	1.49	36.61	0.73	12.17	1.50	26.93	1.68	22.04	0.51
1000N	29.99	1.15	14.95	0.39	15.74	0.72	7.42	0.56	22.10	0.13	0.01	0.01	20.33	0.98	20.86	1.27

Applied Load	FSR9		FSR10		FSR11		FSR12		FSR13		FSR14		FSR15		FSR16	
	Avg Val	SD														
50N	35.57	0.36	16.95	0.74	16.51	1.14	3.11	0.80	0.01	0.01	30.50	0.27	27.11	0.99	26.04	0.88
250N	44.05	1.48	23.27	3.12	17.98	0.43	3.92	0.57	0.00	0.00	31.85	0.61	32.75	1.13	33.24	0.44
500N	46.87	1.27	31.53	3.18	17.32	1.29	3.38	1.11	0.00	0.00	32.85	0.47	36.48	0.65	38.44	0.71
750N	47.94	0.51	36.50	3.50	17.97	1.40	2.65	1.22	0.00	0.00	33.17	0.62	37.92	0.45	40.32	1.81
1000N	41.08	1.27	24.60	1.69	15.10	0.70	2.56	1.03	0.00	0.00	32.10	0.45	32.01	0.58	33.96	0.63

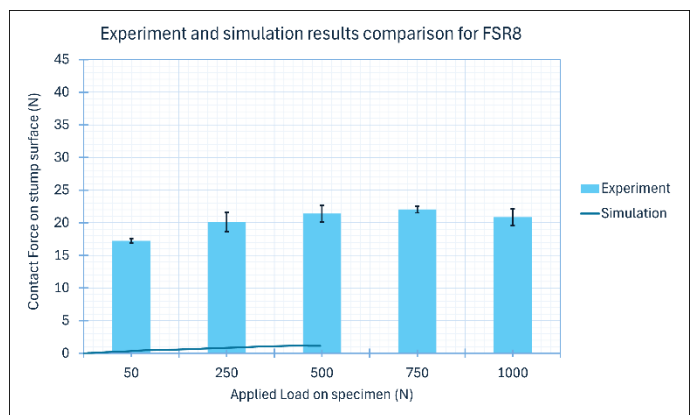
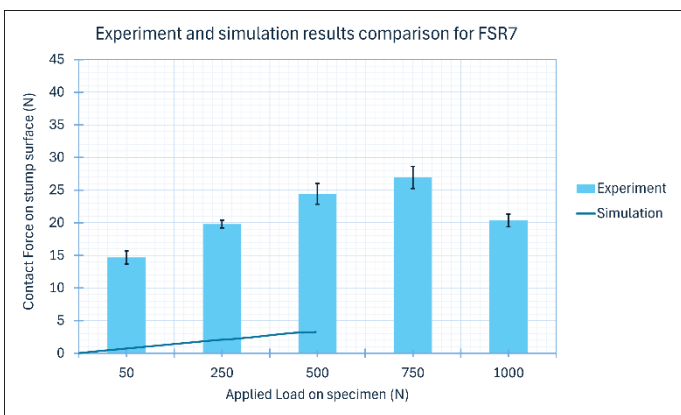
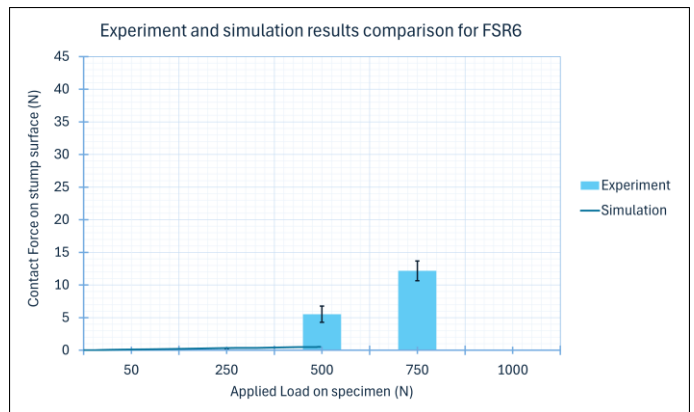
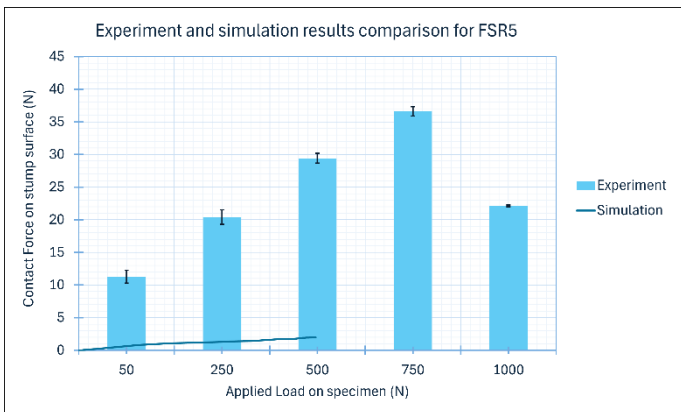
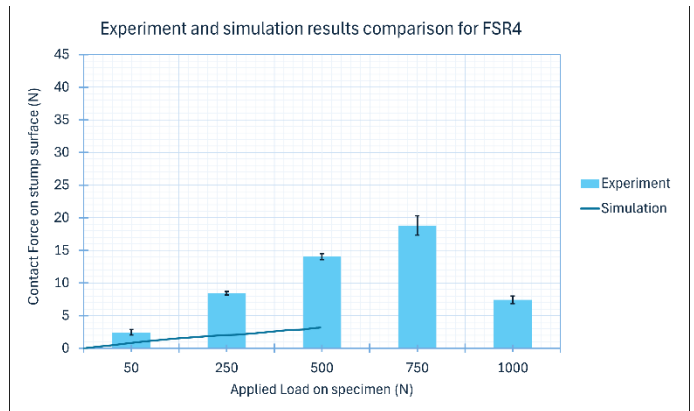
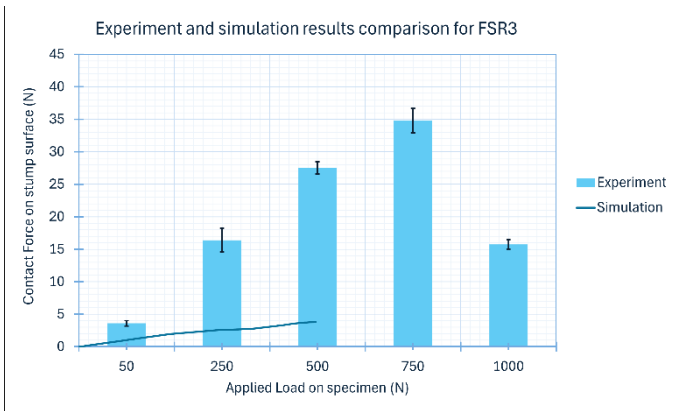
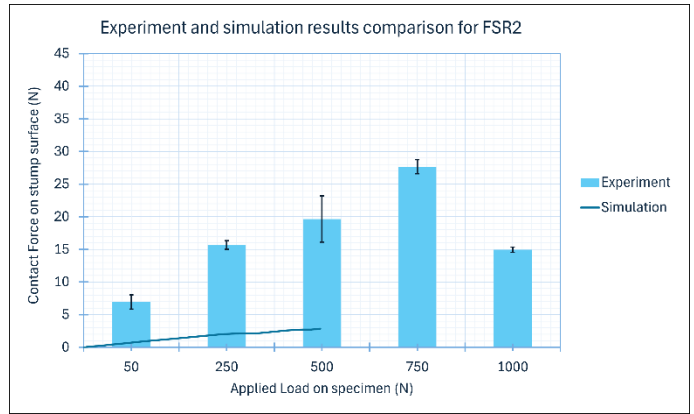
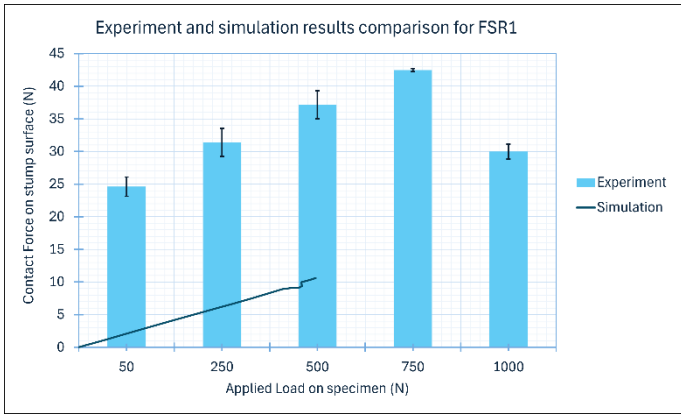
Units in Newtons

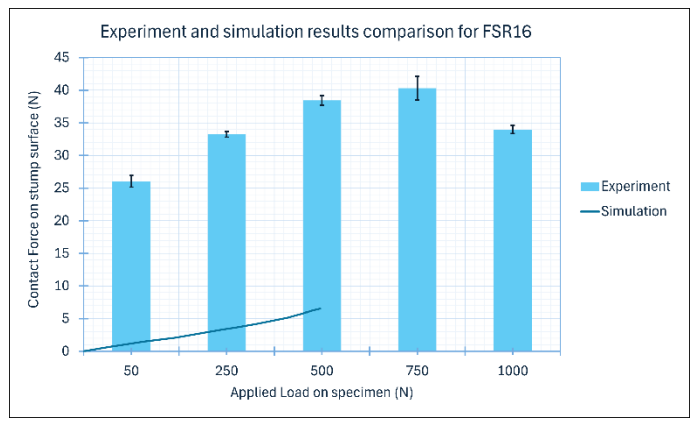
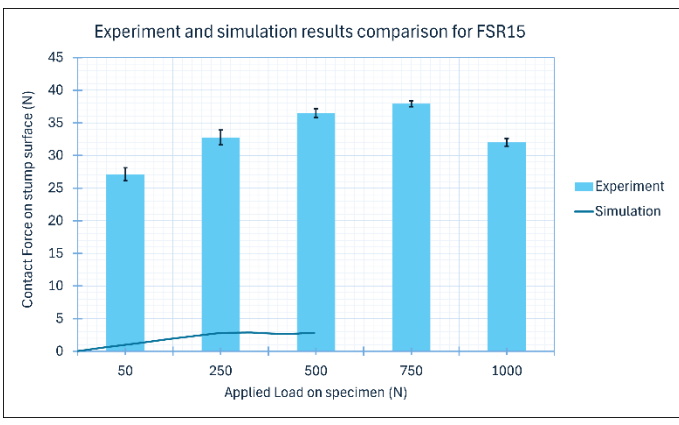
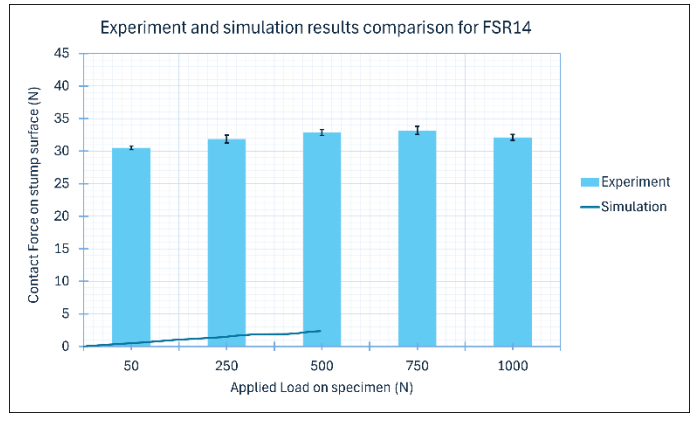
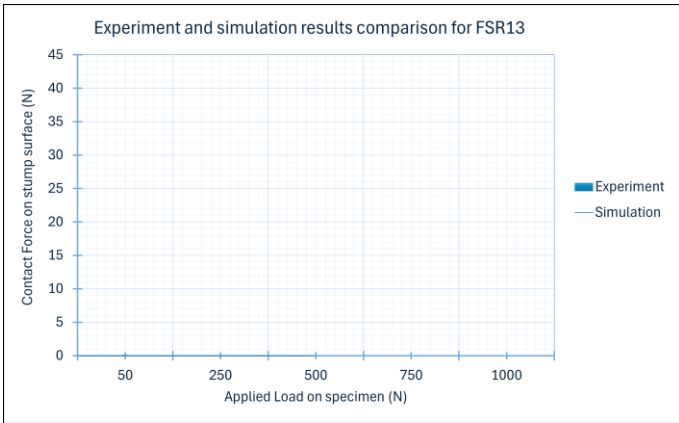
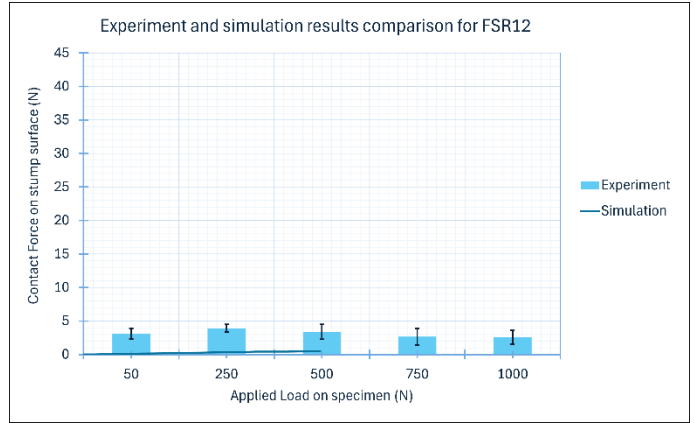
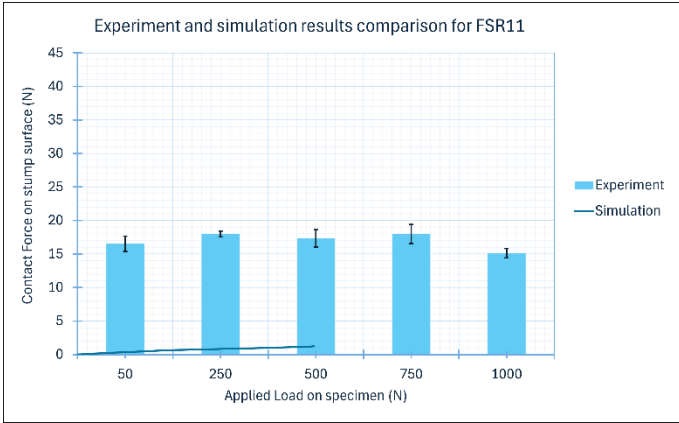
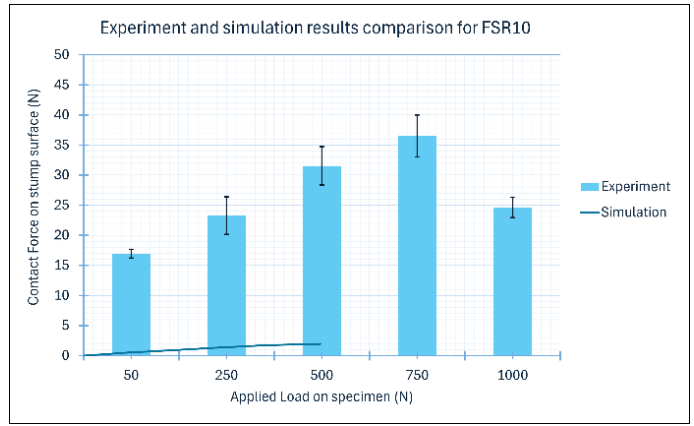
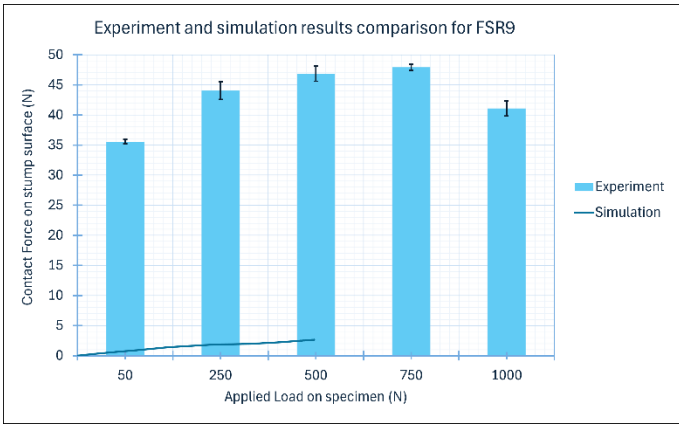
Appendix P.
Simulation results graph and table

Simulation results

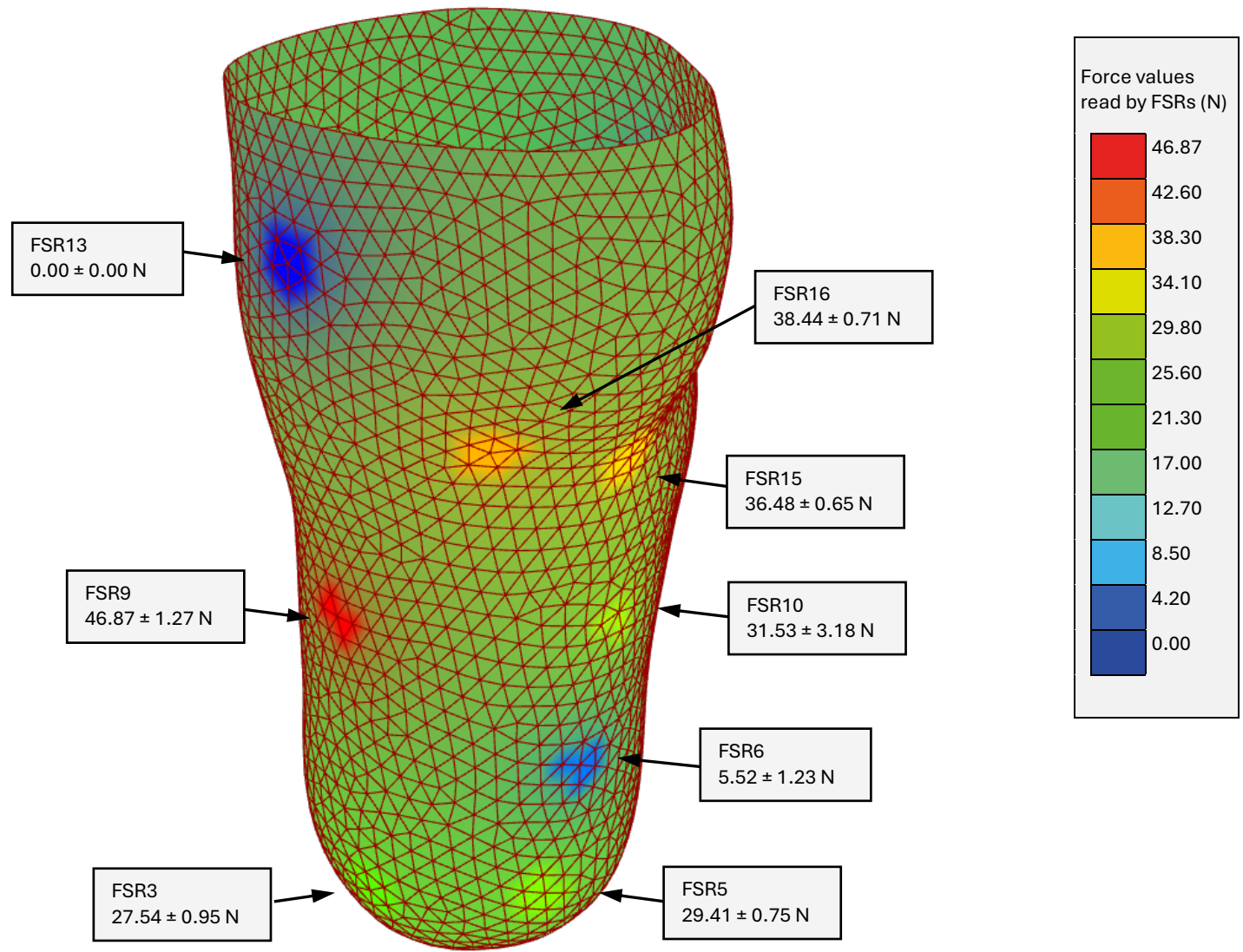


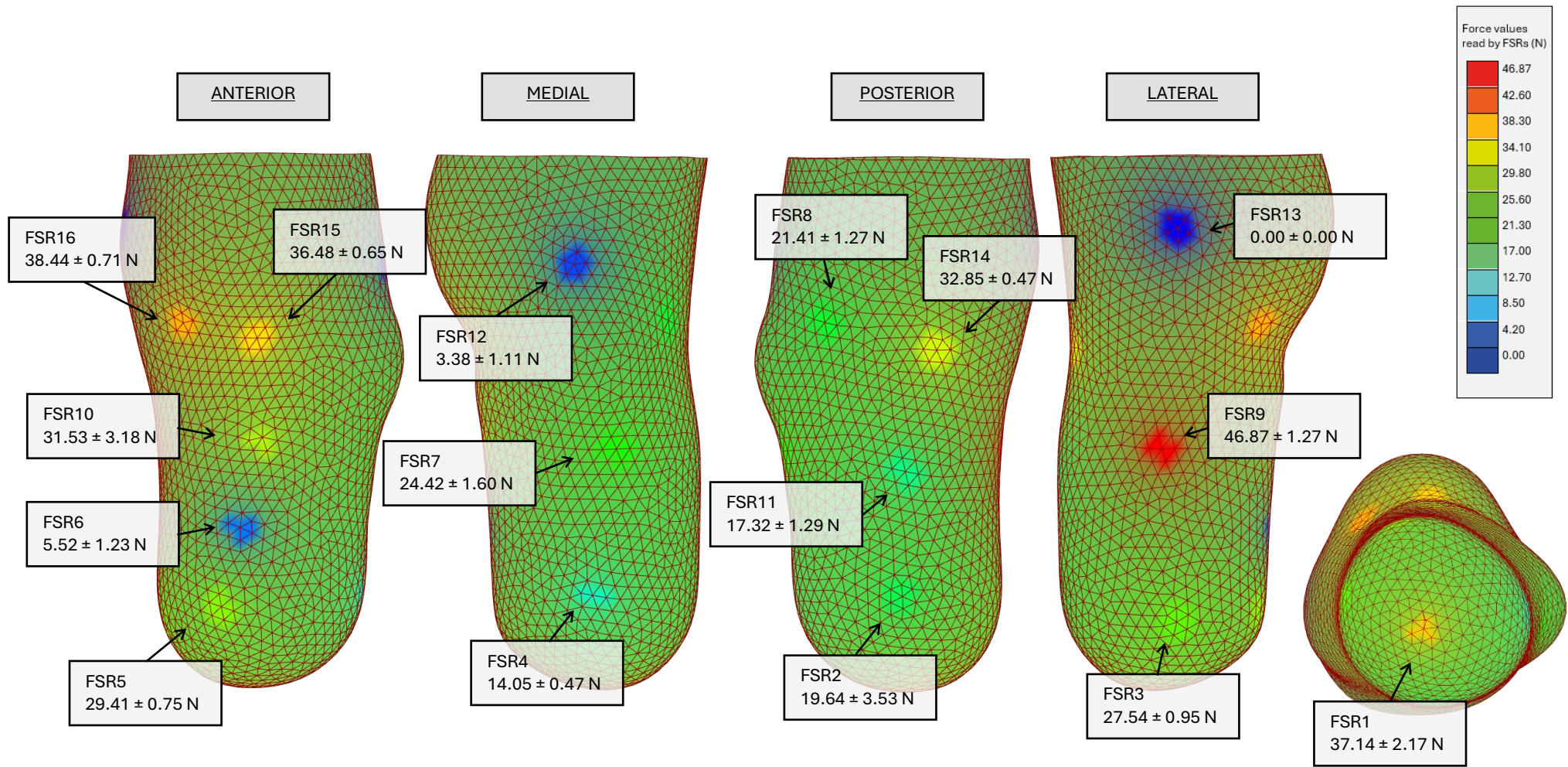
Appendix Q.
Socket Sensor Experiment and simulation results comparison

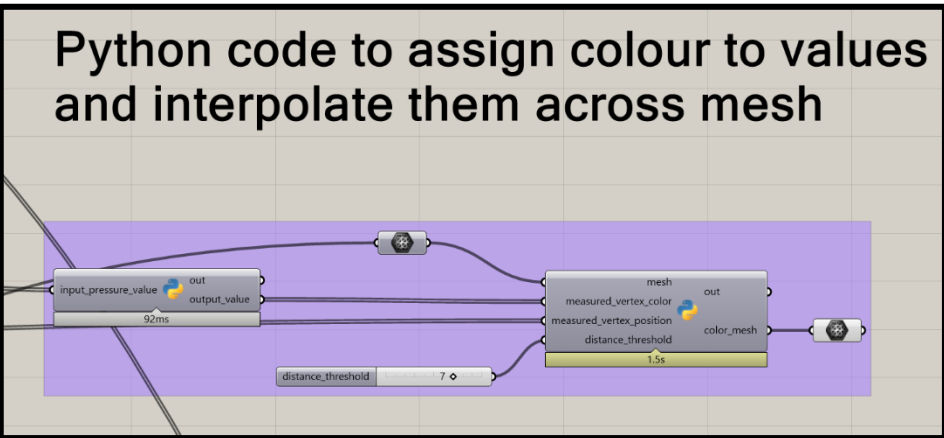
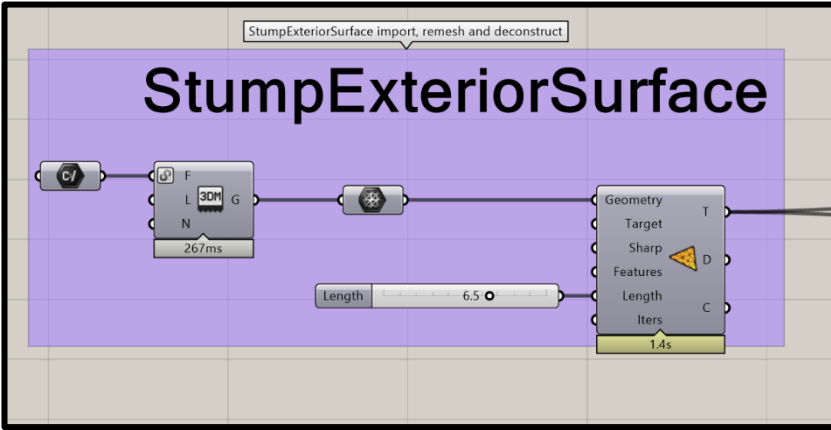
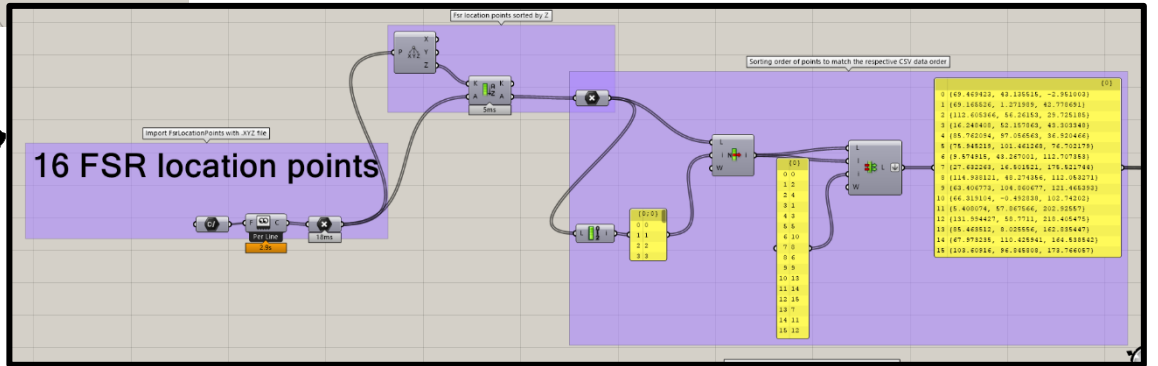
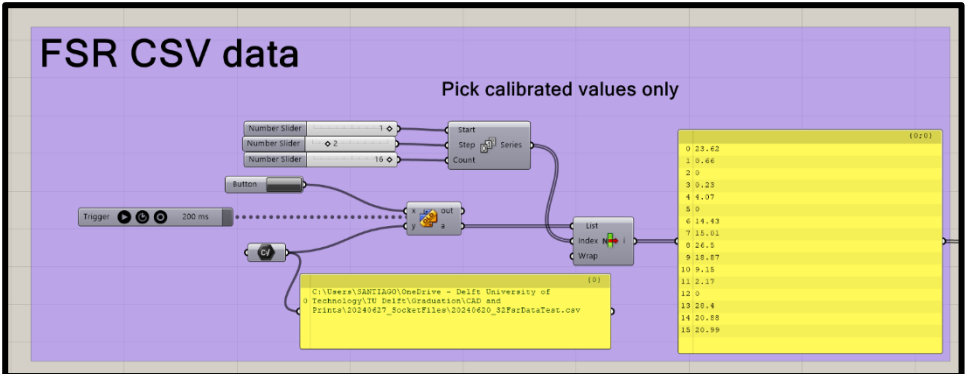
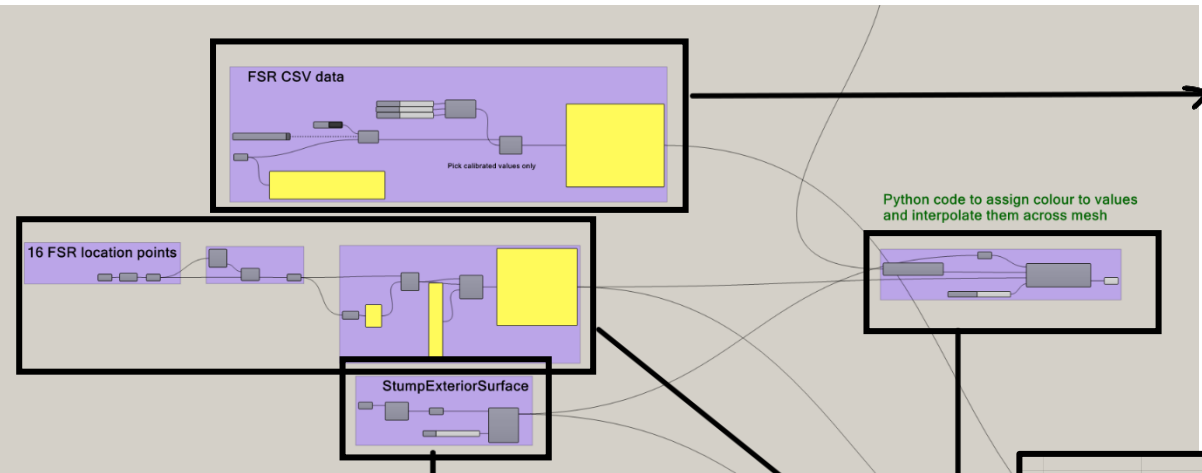




Appendix R.
Sensor data visualization with Grasshopper
of Socket Sensor test results







Appendix S.
Non-Inverting Op-Amp and 16-bit ADC voltage divider circuits

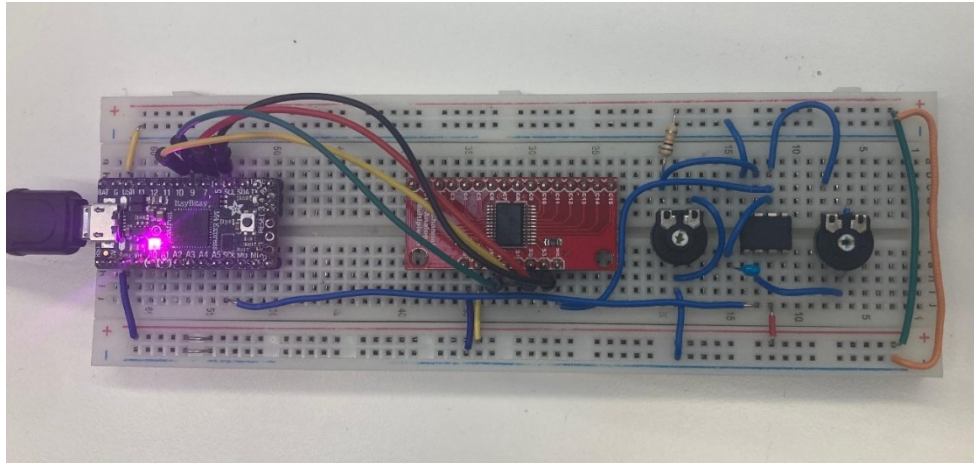


Figure 40. Non-inverting op-amp circuit

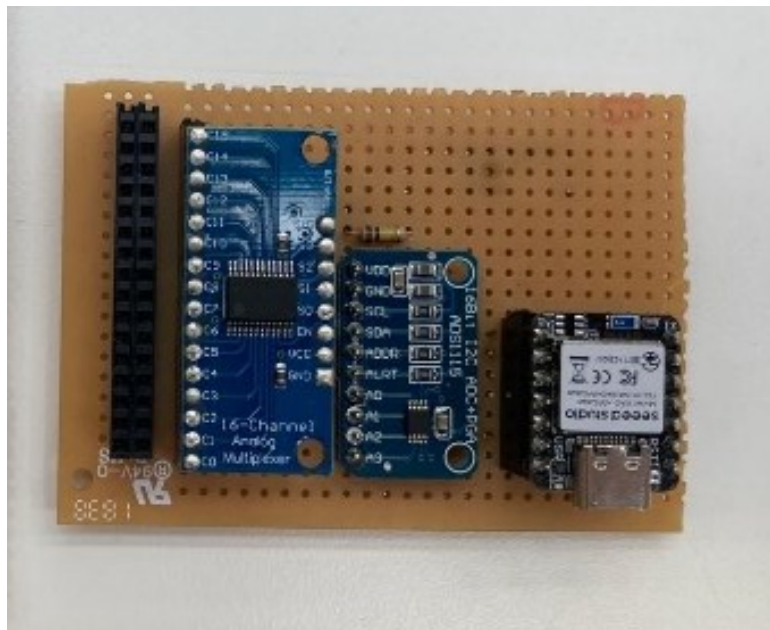
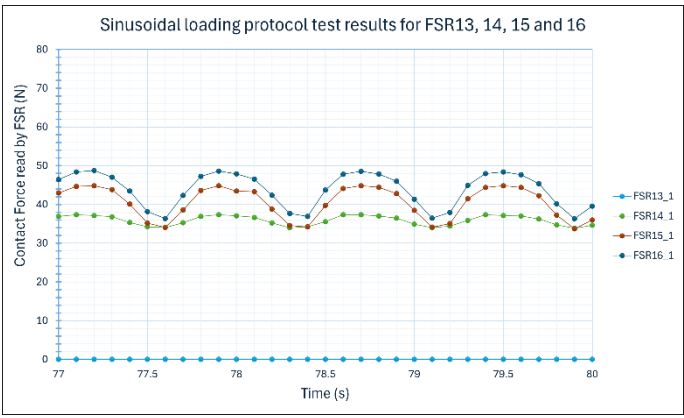
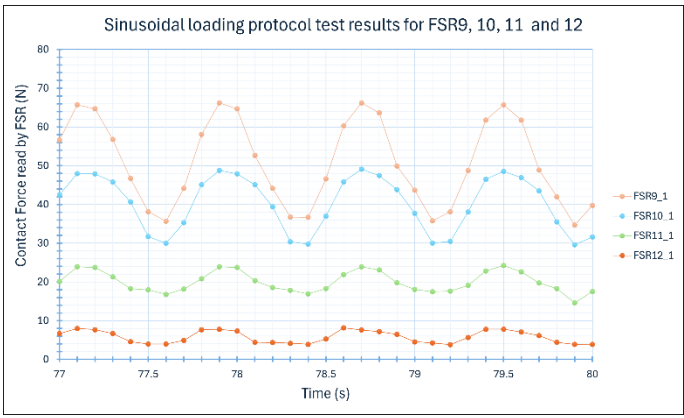
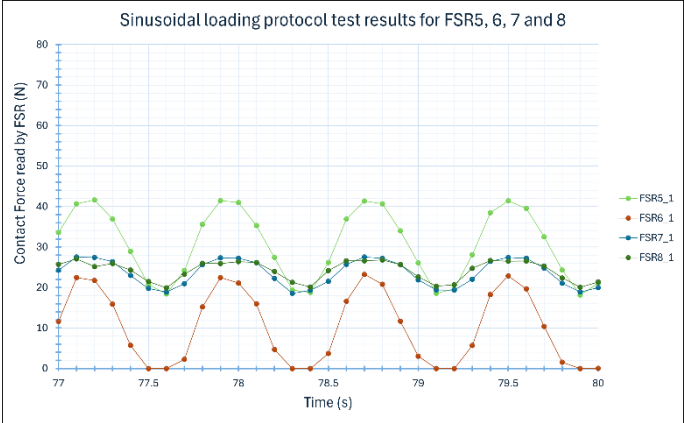
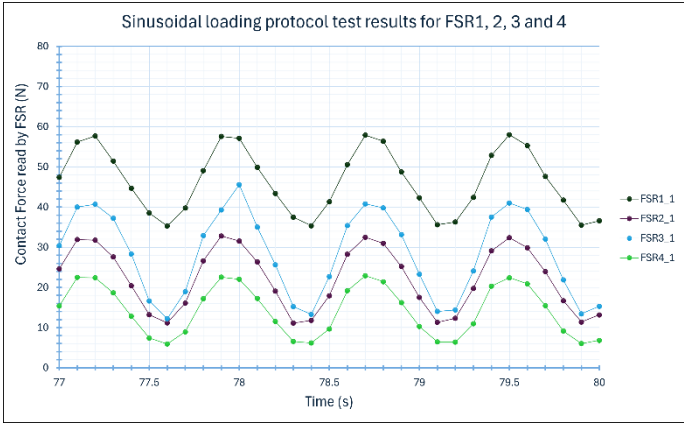
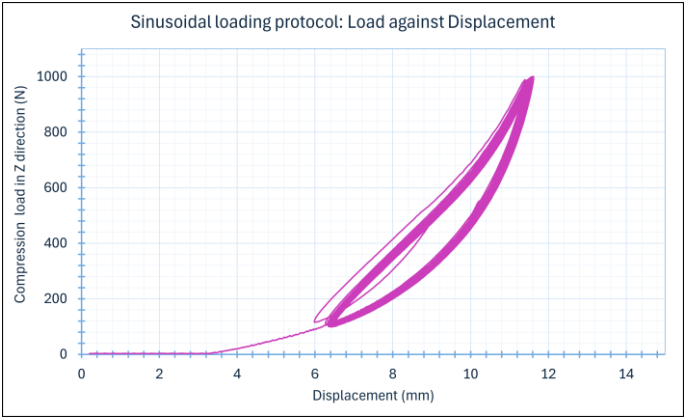
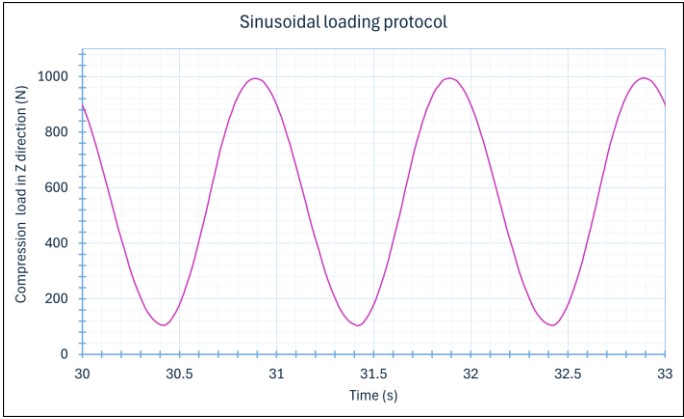


Figure 41. Voltage divider circuit with ADS 1115 module and Seeeduino XIAO microcontroller

Appendix T.
Sinusoidal loading protocol test data



Appendix U.
Modified BME simulation

Simulation setup

This model (further referred to as Modified BME simulation) provided by V. Moosabeiki aims to simulate the physiological conditions of the prosthesis and stump interaction to provide a topology optimised prosthetic socket. The simulation setup is modified slightly to compare the results from this simulation with the experiment results and find out if there is a correlation, pattern and differences.

Materials

- Bone. The Mechanical Elastic tab requires two inputs:
 - Young’s Modulus: 16000 units (16000 MPa).
 - Poisson ratio: 0,3.
- Stump:
 - Young’s Modulus: 5 units (5 MPa).
 - Poisson’s ratio: 0.45.
- Socket:
 - Young’s Modulus: 1650 units (1650 MPa).
 - Poisson ratio: 0,4.

Parts

- Bone. 3D deformable solid part, assigned the “Bone” section.
- Stump. 3D deformable solid part, assigned the “Stump” material
- Socket. 3D deformable solid part, assigned the “Socket” material.

Steps

- Step-1. Static (General) step after Initial Step:
 - Maximum number of increments: 10000.
 - Increment size: 0.1; 1E-05; 1.

Interaction

- Contact Property.
 - Tangential Behavior. Friction formulation: Penalty; Directionality: Isotropic; Friction Coefficient: 0,7.
 - Normal Behavior. Pressure-Overclosure: “Hard” contact; Constraint enforcement method: Default. Allow separation after contact.
 - Geometric Properties.

Constraints, Boundary Conditions and Loads

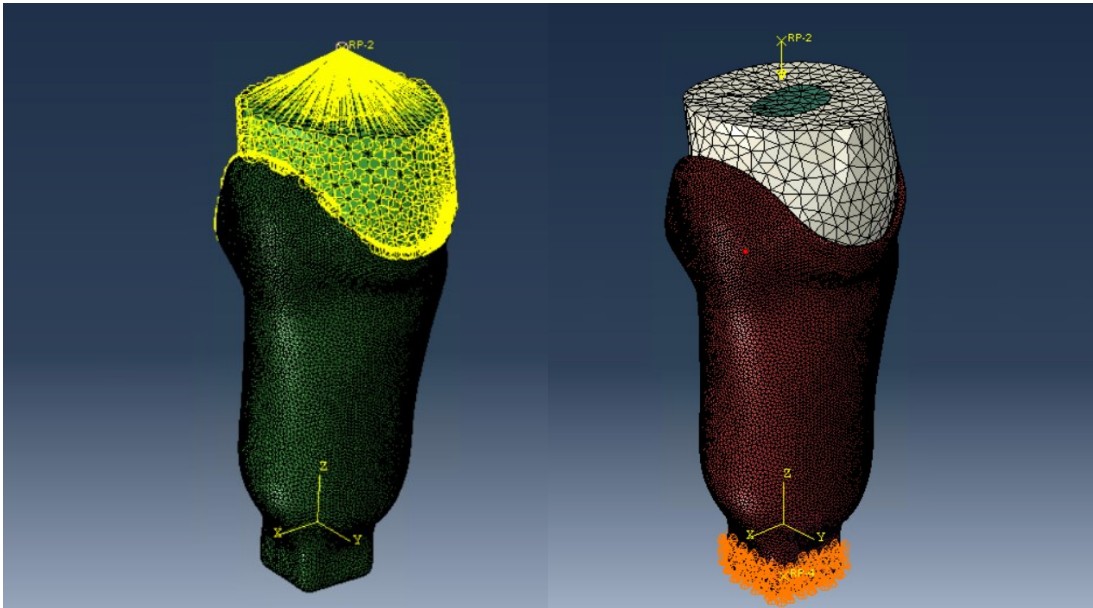
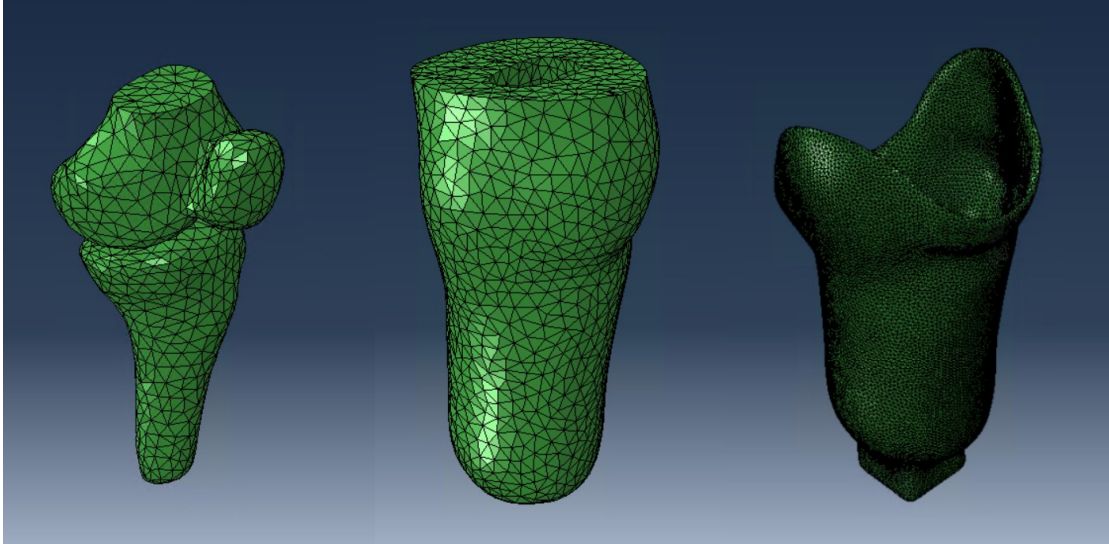
- Encastrate Boundary Condition in the socket bottom.
- Reference Point in 0,0,290 (X, Y, Z).
- Coupling between Reference Point and top surface of leg.
- Tie constraint between the bone outer surface (main surface) and internal stump surface (secondary surface).
- Tie constraint between the interior socket surface (main surface) and the stump exterior surface (secondary surface).
- Load of -750 N in the Z direction, applied from the Reference Point.

Mesh

The parts are imported as meshes from another software; the parameters are not modifiable. Using the probe tool, the distance between nodes for the socket is around 2.5 mm and around 6 mm for the stump.

Results

The results have been measured on the interior surface of the socket. The highest values are below the knee and in the posterior side of the leg, corresponding to FSR8 and FSR 15 of 0,3 and 0,4 MPa respectively. FSR1, 2, 3, and 4 show similar values around 0,1 MPa and FSR13, 16, 5, 7 registered low values around 0,05 MPa. Besides that, FSR12 and FSR9 present negative values, this negative pressure means that the socket is “pulling away” from the socket.



FSR	1	2	3	4	5	6	7	8	9	10	11	12	13	14	15	16
Pressure (MPa)	0.113	0.198	0.155	0.095	0.038	0.045	0.073	0.314	-0.110	0.152	0.201	-0.187	0.019	0.181	0.404	0.064

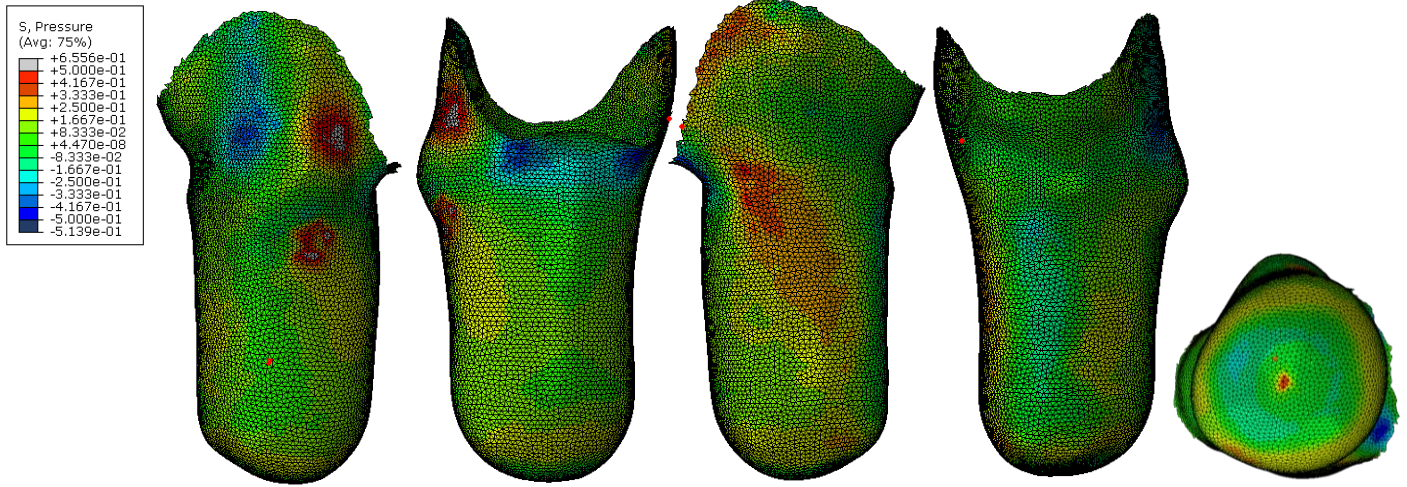


Figure 43. Physiological conditions simulation results visualisation (from left to right: front, left, back, right and bottom) and table of averaged pressure values in the respective FSRs nodes

FSR	1	2	3	4	5	6	7	8	9	10	11	12	13	14	15	16
Simulation (MPa)	0.113	0.198	0.155	0.095	0.038	0.045	0.073	0.314	-0.110	0.152	0.201	-0.187	0.019	0.181	0.404	0.064
Experiment (MPa)	0.276	0.180	0.226	0.122	0.238	0.079	0.175	0.143	0.311	0.237	0.117	0.017	0.000	0.215	0.246	0.262

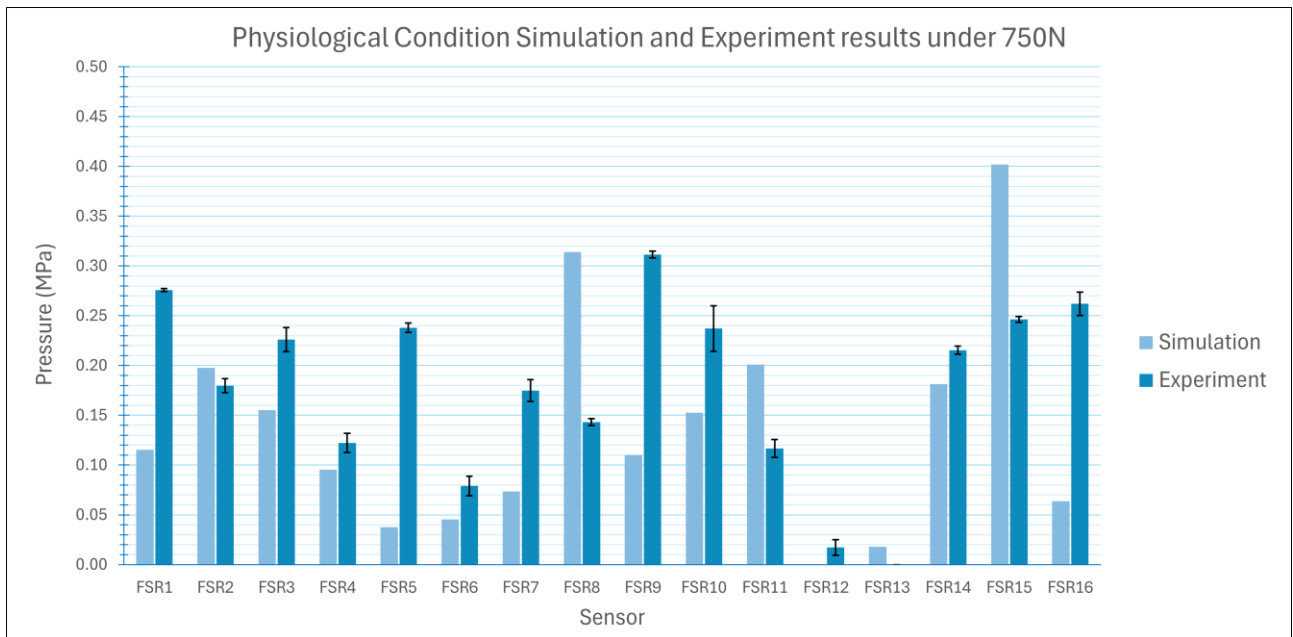
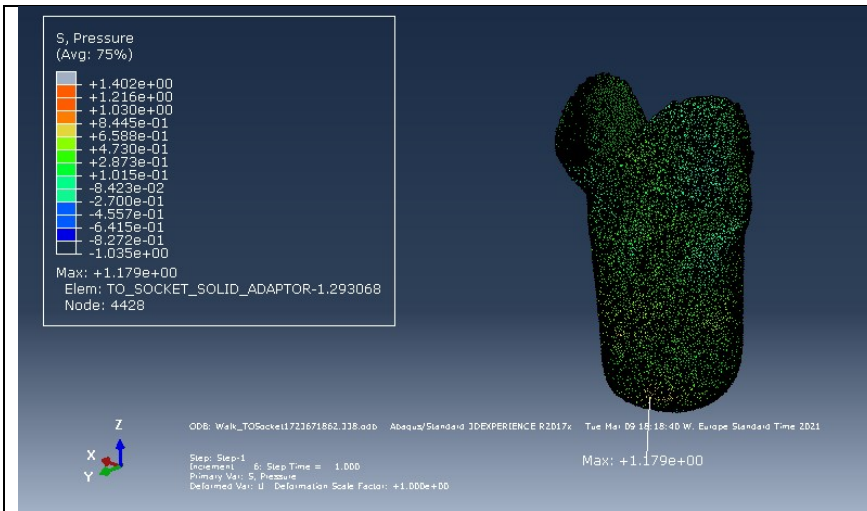


Figure 42. Modified BME and experimental data comparison in MPa

Appendix V.
Physiological loading conditions simulation



Walk

Force (x,y,z): 7,46;49.11;1811.04

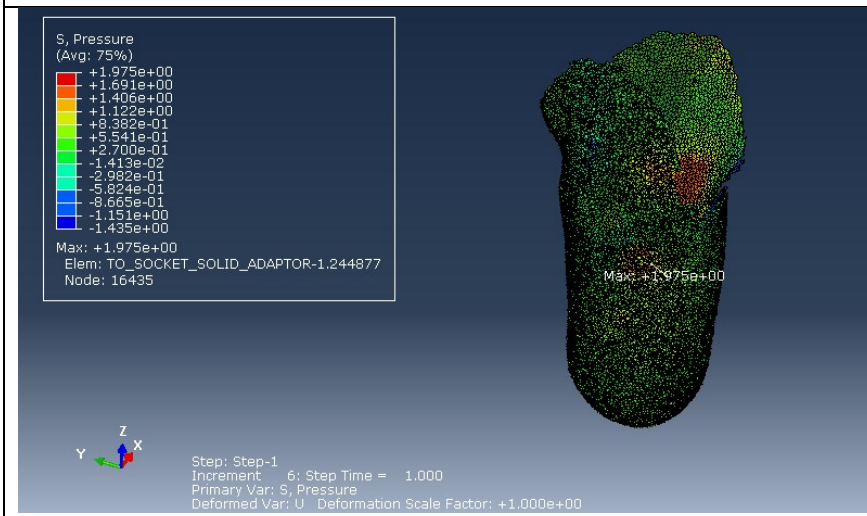
Moment (x, y, z): 23767.5;3584.63;
6075.9

If the PU disc diameter is 12 mm

$P = F/A$

Force = 1.79 MPa x (pi x (6 mm)²)=

Maximum Contact Force = 192.27 N



Jump

Force (x,y,z): -13.69;412.45;2883.65

Moment (x, y, z): -35517.9; -2968.68;
5037.4

If the PU disc diameter is 12 mm

$P = F/A$

Force = 1.975 MPa x (pi x (6mm)²)=

Maximum Contact Force = 223.37 N

Element Nodal values taken from the socket interior surface. CAE and ODB files provided by mentor Vahid Moosabeiki.

Appendix W.
Prototype cost estimation

Parts	Qty.	Description	Supplier	Cost per unit	Total price
Flexiforce A201 sensors	16	Force Sensitive Resistor	Mouser Electronics	15.87 €	253.92 €
PLA FDM printed socket	1	Printed in the workshop of the IDE faculty for free, real cost is not known. A price estimation is done consulting a website (Treatstock) that compares prices for 3D printing services	PMB Workshop	101.84 €	101.84 €
Adafruit Huzzah Feather ESP32	1	Microcontroller	Adafruit	18.14 €	18.14 €
HC4067 multiplexer	1		AliExpress	0.70 €	0.70 €
100 kΩ resistor	1		Applied Labs	0.10 €	0.10 €
100 nF capacitor	1		Applied Labs	0.20 €	0.20 €
Silicone stump	1	R PRO 10 - Silicone rubber 1:1 for silicone soft moulds	Reschimica	69.90 €	69.90 €
Aluminium fixture	1	Al6061-T6 cylinder block (ø60 x 120 mm)	PMB Workshop	17.50 €	17.50 €

Total cost = 462.30 €

The screenshot shows the Treatstock website interface for 3D printing services. At the top, there is a navigation bar with 'TREATSTOCK', 'Products', and 'Manufacturing services'. Below this is a search bar with a dropdown menu set to '3D Printing' and a search button. A 'Get instant quote' button is also visible.

The main content area is divided into several sections:

- Material Selection:** A section titled 'Select a file to change its material or color' shows a 3D model of a part. Below it, there are radio buttons for 'PLA' and a '3D Viewer' button.
- MATERIALS & COLORS:** A section with 'Need help?' and various material and color options. Materials include Resin, Nylons, Wood-filled Pla..., Polyesters/PETG, Flexible (TPU/T...), PLA (selected), Polycarbonates, ABS, Nylon Powders, and Durable Plastics. Colors include Black, Blue, White, Green, Red, Yellow, Gray, Orange, and a '+ More' option.
- IN FILL:** A dropdown menu set to '100'.
- Supplier List:** A list of suppliers with their details:
 - Uniswitch 3D:** Tilburg, Noord-Brabant. Response rate: less 2h. Completion rate: no info. Price: \$376.25. Delivery: \$7.50. Buy button.
 - 3DRene.com:** Weert, Limburg. Response rate: less 24h. Completion rate: average. Price: \$421.40. Free delivery. Buy button.
 - Schaefer engineering solutions:** The Hague, South Holland. Response rate: more 48h. Completion rate: no info. Price: \$2,355.33. Delivery: \$7.25. Buy button.
 - JVS 3D:** Hoogeveen, Drenthe. Response rate: more 48h. Completion rate: no info. Price: \$188.13. Delivery: \$10.00. Buy button.
 - AM-X Tech:** Landhorst, North Brabant. Response rate: more 48h. Completion rate: no info. Price: \$112.88. Free delivery. Buy button.
 - GAGAT:** Amersfoort, Utrecht. Response rate: more 48h. Completion rate: no info. Price: \$75.25. Delivery: \$10.00. Buy button.

At the bottom right, there are 'Back' and 'Next' navigation buttons.

Appendix X.
Graphical summary of the project

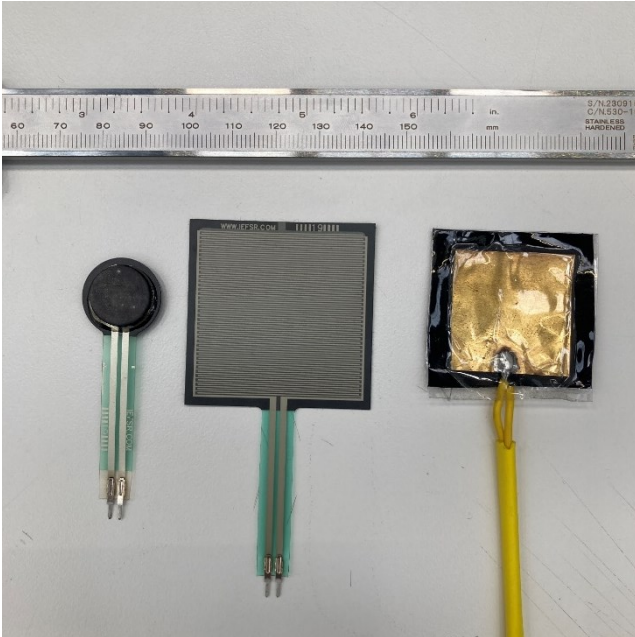


Figure 44. Round, square and self-made FSR (from left to right). All of these sensors peaked when under a weight of 5 kg.

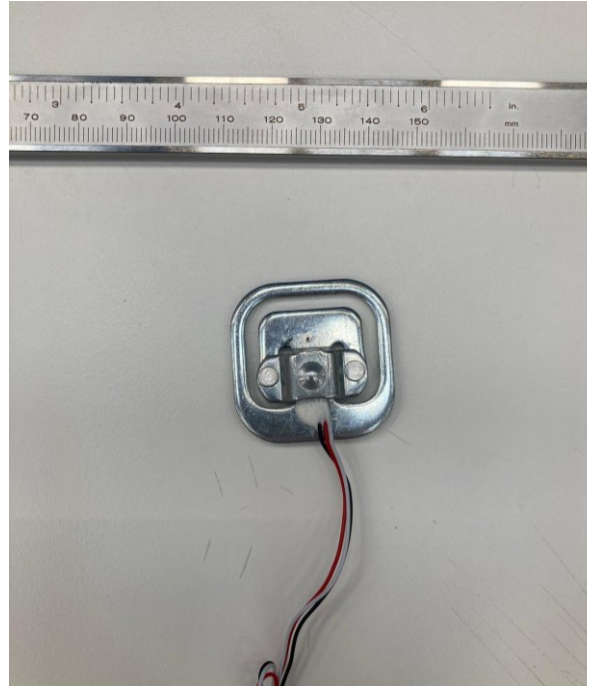


Figure 45. Load cell for scale. This type of sensor was briefly explored but discarded because of the size it would take up.

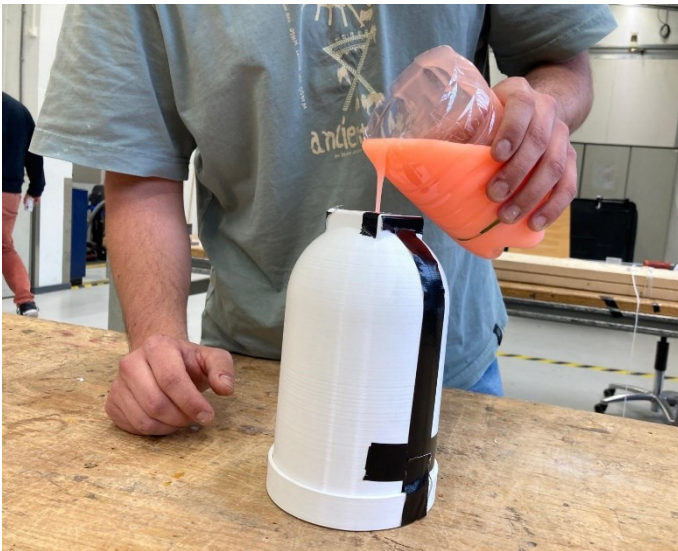


Figure 46. Pouring silicone into a mould to get the simplified stump

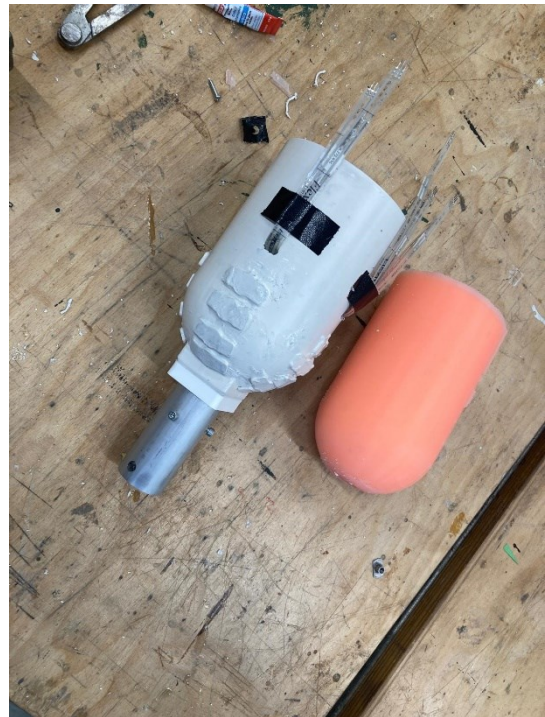


Figure 47. One of the first prototypes equipped with the FSRs next to the simplified stump



Figure 48. 3D printed prototype equipped and electronics circuit. Since this circuit uses a multiplexer, it just needs one resistor, so all those wires are not needed.

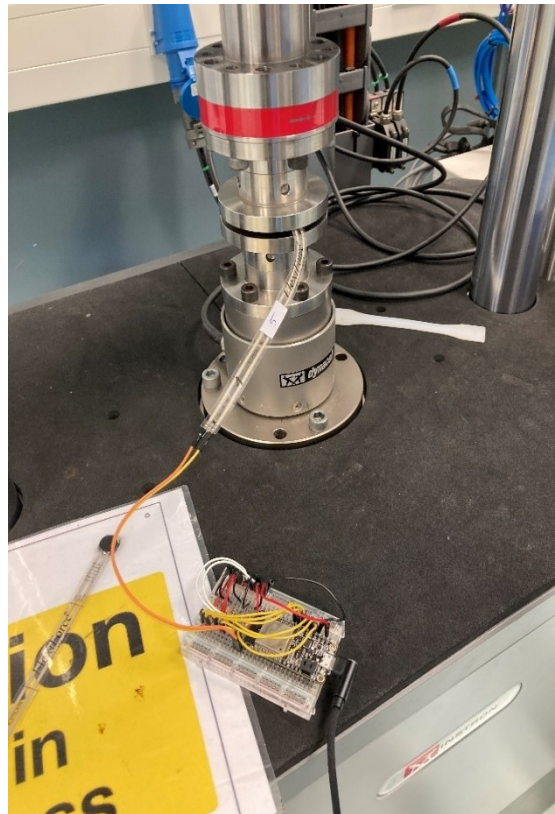


Figure 49. Flexiforce sensor tested in the cyclic loading machine.



Figure 50. Prototype with integrated socket test

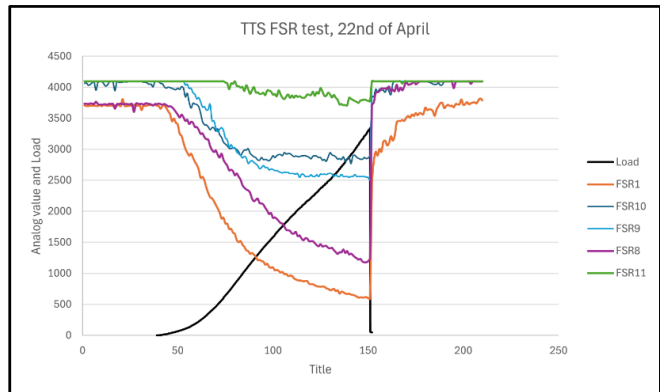


Figure 51. Testing results from Figure 45 test. The loading halted due to the top plastic part of the stump breaking



Figure 52. Here it is visible where the simplified stump part failed, on the left the aluminium fixture to connect the specimen to the cyclic loading machine is shown.



Figure 53. Realistic stump mould before demoulding.



Figure 54. Demoulded realistic socket.



Figure 55. 3D printed realistic socket with spaces to locate FSRs.

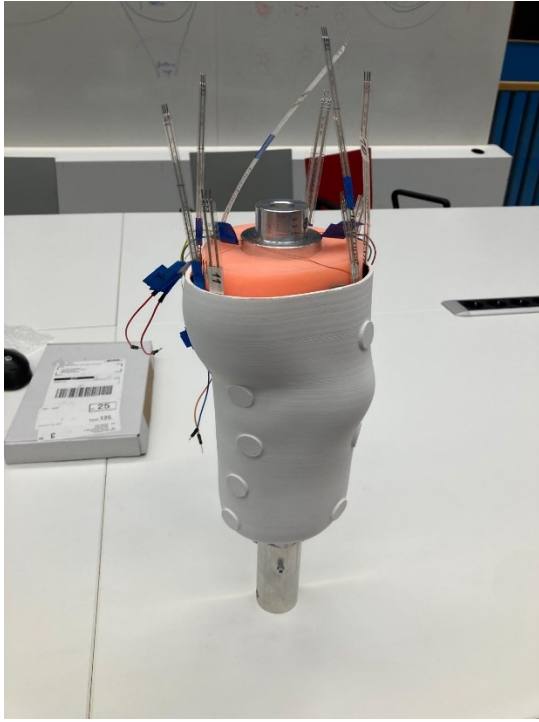


Figure 56. Realistic stump and matching prosthetic socket with FSR sensors.



Figure 57. FlexiForce A201 sensor and used PU discs to ensure a good contact on the sensing area.



Figure 58. Close up view of the circuit and connections while the socket is fixed in the cyclic loading machine ready to be tested.

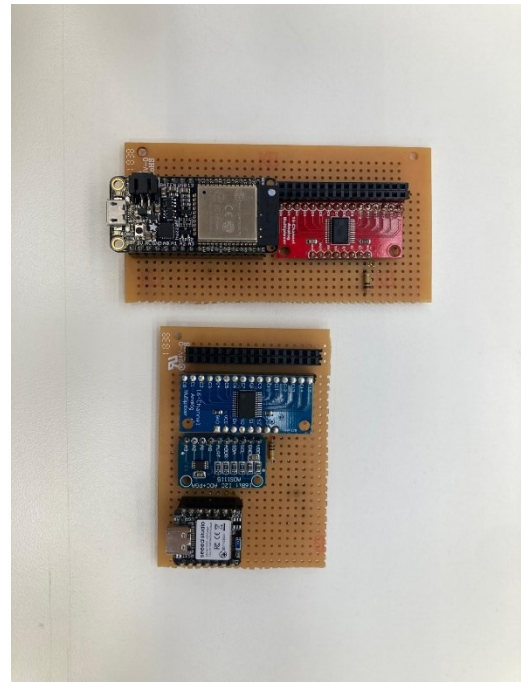


Figure 59. Last circuit iterations installed in perfboards. Circuit described in the main body of the report (top) and same circuit with a Seeeduino XIAO microcontroller and an ADS1115 16-bit ADC.

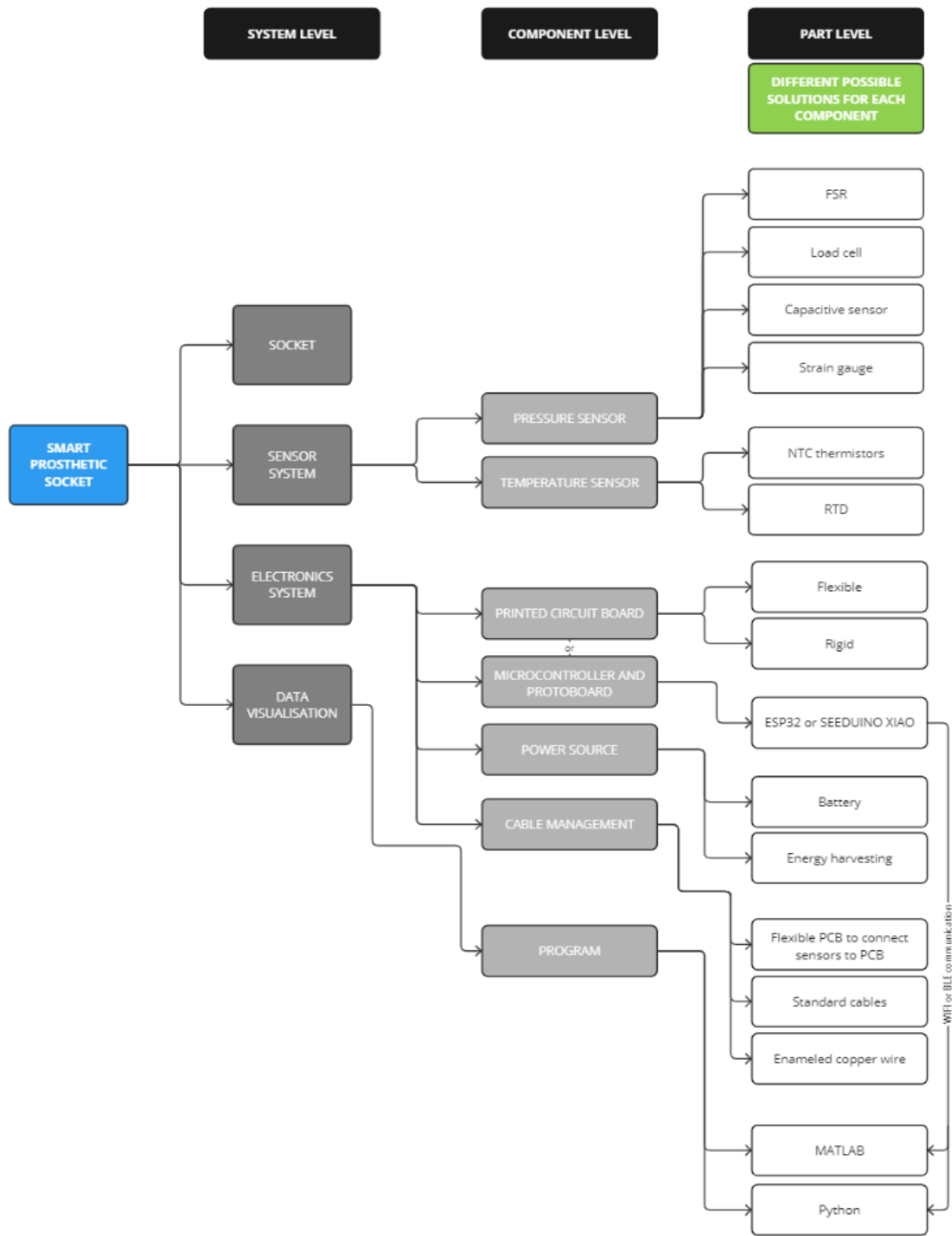


Figure 60. System and component tree for a smart prosthetic socket that monitors and visualizes stump pressure

Appendix Y.
Project brief



IDE Master Graduation Project

Project team, procedural checks and Personal Project Brief

In this document the agreements made between student and supervisory team about the student's IDE Master Graduation Project are set out. This document may also include involvement of an external client, however does not cover any legal matters student and client (might) agree upon. Next to that, this document facilitates the required procedural checks:

- Student defines the team, what the student is going to do/deliver and how that will come about
- Chair of the supervisory team signs, to formally approve the project's setup / Project brief
- SSC E&SA (Shared Service Centre, Education & Student Affairs) report on the student's registration and study progress
- IDE's Board of Examiners confirms the proposed supervisory team on their eligibility, and whether the student is allowed to start the Graduation Project

STUDENT DATA & MASTER PROGRAMME

Complete all fields and indicate which master(s) you are in

Family name	<input type="text" value="Andújar Arias"/>	IDE master(s) IPD	<input checked="" type="checkbox"/>	Dfi	<input type="checkbox"/>	SPD	<input type="checkbox"/>
Initials	<input type="text" value="S"/>	2 nd non-IDE master	<input type="text"/>				
Given name	<input type="text" value="Santiago"/>	Individual programme (date of approval)	<input type="text"/>				
Student number	<input type="text" value="5860105"/>	Medisign	<input type="checkbox"/>				
		HPM	<input type="checkbox"/>				

SUPERVISORY TEAM

Fill in the required information of supervisory team members. If applicable, company mentor is added as 2nd mentor

Chair	<input type="text" value="Wolf Song"/>	dept./section	<input type="text" value="MD SDE"/>	Ensure a heterogeneous team. In case you wish to include team members from the same section, explain why. Chair should request the IDE Board of Examiners for approval when a non-IDE mentor is proposed. Include CV and motivation letter. 2 nd mentor only applies when a client is involved.
mentor	<input type="text" value="Mohammad Mirzaali Mazandarani"/>	dept./section	<input type="text" value="ME Biomechanical Engineering"/>	
2 nd mentor	<input type="text" value="Vahid Moosabeiki Dehabadi"/>			
client:	<input type="text"/>			
city:	<input type="text"/>	country:	<input type="text"/>	
optional comments	<input type="text"/>			

APPROVAL OF CHAIR on PROJECT PROPOSAL / PROJECT BRIEF -> to be filled in by the Chair of the supervisory team

Sign for approval (Chair)

Name Date Signature

CHECK ON STUDY PROGRESS

To be filled in by SSC E&SA (Shared Service Centre, Education & Student Affairs), after approval of the project brief by the chair. The study progress will be checked for a 2nd time just before the green light meeting.

Master electives no. of EC accumulated in total _____ EC

Of which, taking conditional requirements into account, can be part of the exam programme _____ EC

X	YES	all 1 st year master courses passed
	NO	missing 1 st year courses

Comments: _____

Sign for approval (SSC E&SA)

Name Robin den Braber Date 28-03-2024 Signature RdB

APPROVAL OF BOARD OF EXAMINERS IDE on SUPERVISORY TEAM -> to be checked and filled in by IDE's Board of Examiners

Does the composition of the Supervisory Team comply with regulations?

YES	<input checked="" type="checkbox"/>	Supervisory Team approved
NO	<input type="checkbox"/>	Supervisory Team not approved

Comments: _____
- Wolf-Chair, Vahid-Mentor, Mohammad - "Client"

Based on study progress, students is ...

<input checked="" type="checkbox"/>	ALLOWED to start the graduation project
<input type="checkbox"/>	NOT allowed to start the graduation project

Comments: _____

Sign for approval (BoEx)

Name Monique von Morgen Date 24/4/2024 Signature [Signature]

Personal Project Brief – IDE Master Graduation Project

Name student Santiago Andújar Arias

Student number 5,860,105

PROJECT TITLE, INTRODUCTION, PROBLEM DEFINITION and ASSIGNMENT

Complete all fields, keep information clear, specific and concise

Project title Towards improved user comfort with knowledge-based design: integration of sensor system in a smart prosthetic socket

Please state the title of your graduation project (above). Keep the title compact and simple. Do not use abbreviations. The remainder of this document allows you to define and clarify your graduation project.

Introduction

Describe the context of your project here; What is the domain in which your project takes place? Who are the main stakeholders and what interests are at stake? Describe the opportunities (and limitations) in this domain to better serve the stakeholder interests. (max 250 words)

Lower limb amputees can experience issues such as poor in terms of breathability and heat dispersion especially. These factors can lead to amputees stopping to use their prosthesis due to discomfort and pain in the form of skin irritation, blistering, bacterial infections and overall, a reduced quality of life [1][2].

In this context, addressing the temperature, volume changes and shear stress within the residual limb and socket interface is key for comfort, functionality, and acceptance of the prosthesis in the long-term [4].

Conventional sockets have failed to overcome these issues, therefore there is a gap for developing smart systems that can collect, read and monitor data of the temperature, stresses and volume changes and automatically adjust actuators to improve the overall experience and comfort of the amputee in real time [5]. Besides improving comfort, this smart prosthesis can track patient progress over time to improve the evolution and , which nowadays is done through trial and error with the expertise of the prosthetist.

Stakeholders are amputees, healthcare professionals (vascular and trauma surgeons and prosthetists mainly), manufacturers and insurance companies. The goal of amputees is to have more comfort, good life quality and independence; insurance companies want to avoid high cost solutions; manufacturers want to provide a profitable and manufacturable good product.

→ space available for images / figures on next page

introduction (continued): space for images



image / figure 1

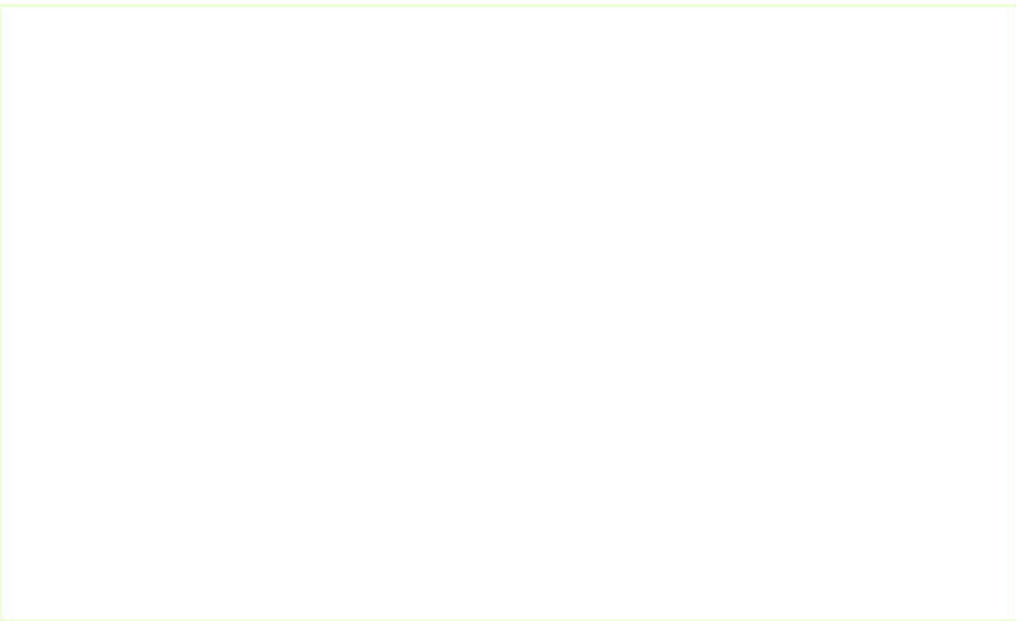


image / figure 2

Personal Project Brief – IDE Master Graduation Project

Problem Definition

What problem do you want to solve in the context described in the introduction, and within the available time frame of 100 working days? (= Master Graduation Project of 30 EC). What opportunities do you see to create added value for the described stakeholders? Substantiate your choice. (max 200 words)

During the Master Graduation Project, I want to improve the comfort for lower limb amputees, which is determined by the temperature inside the socket, as well as pressure, shear stress and volume changes. These parameters are patient specific and it is not known how they change.

Therefore, I will focus on integrating a sensor system that measures these parameters through the day to create a temperature and pressure map inside the socket. This is key to give a better understanding of how the stump changes through the day and improve the prosthesis design in the future based on data gathered by the sensor system.

Assignment

This is the most important part of the project brief because it will give a clear direction of what you are heading for. Formulate an assignment to yourself regarding what you expect to deliver as result at the end of your project. (1 sentence) As you graduate as an industrial design engineer, your assignment will start with a verb (Design/Investigate/Validate/Create), and you may use the green text format:

Design a functional prototype to evaluate the comfort parameters through a sensor and control system in smart prosthetic transibial socket for lower limb amputees.

Then explain your project approach to carrying out your graduation project and what research and design methods you plan to use to generate your design solution (max 150 words)

First step is the research of the different kinds of lower limb prosthetic sockets and investigate the user needs to create a list of requirements and a design vision. In this phase, user insights and company visit will be used to get more insights.

Design sprints of 2 weeks will be carried out to iteratively prototype on the system. The project will start with a technical verification of different pressure and temperature sensors. After that, a simulated temperature test will be conducted in the lab with sensors integrated in the socket. Similar tests will be carried out for a pressure test. These tests will increase in complexity and accuracy as the project goes, with the goal of achieving a sensor system that monitors comfort parameters from the prosthetic socket through the day. If possible, the final prototype will be tested with a user to gather insights and further recommendations.

Regarding methods, methods for creative ideation as well as for selecting and defining the embodiment design will be used. These could be brainstorming, lotus blossom, functional tree, decision matrix, morphological chart, rapid prototyping, design in a day, user testing, etc.

Project planning and key moments

To make visible how you plan to spend your time, you must make a planning for the full project. You are advised to use a Gantt chart format to show the different phases of your project, deliverables you have in mind, meetings and in-between deadlines. Keep in mind that all activities should fit within the given run time of 100 working days. Your planning should include a **kick-off meeting, mid-term evaluation meeting, green light meeting and graduation ceremony**. Please indicate periods of part-time activities and/or periods of not spending time on your graduation course project, if any (for instance because of holidays or parallel course activities).

Make sure to attach the full plan to this project brief.
The four key moment dates must be filled in below

Kick off meeting	28 Feb 2024
Mid-term evaluation	1 May 2024
Green light meeting	3 Jul 2024
Graduation ceremony	21 Aug 2024

In exceptional cases (part of) the Graduation Project may need to be scheduled part-time. Indicate here if such applies to your project

Part of project scheduled part-time	<input type="checkbox"/>
For how many project weeks	2
Number of project days per week	

Comments:
Holidays

Motivation and personal ambitions

Explain why you wish to start this project, what competencies you want to prove or develop (e.g. competencies acquired in your MSc programme, electives, extra-curricular activities or other).

Optionally, describe whether you have some personal learning ambitions which you explicitly want to address in this project, on top of the learning objectives of the Graduation Project itself. You might think of e.g. acquiring in depth knowledge on a specific subject, broadening your competencies or experimenting with a specific tool or methodology. Personal learning ambitions are limited to a maximum number of five.
(200 words max)

I want to tackle an engineering problem from a design point of view, as well as taking part in a project in the medical design field that requires a physical functional prototype. This kind of context of design engineering of medical devices is the field that I would like to be involved in professionally for the challenging aspect of it as well as for the positive impact it makes on the patients.

Besides that, I have these personal learning ambitions: electronics prototyping with Arduino or Raspberry Pi, PCB design, doing data analysis and visualization in Python, performing mechanical testing on prototypes, performing Finite Element Analysis Simulations and Topology optimisation.

References

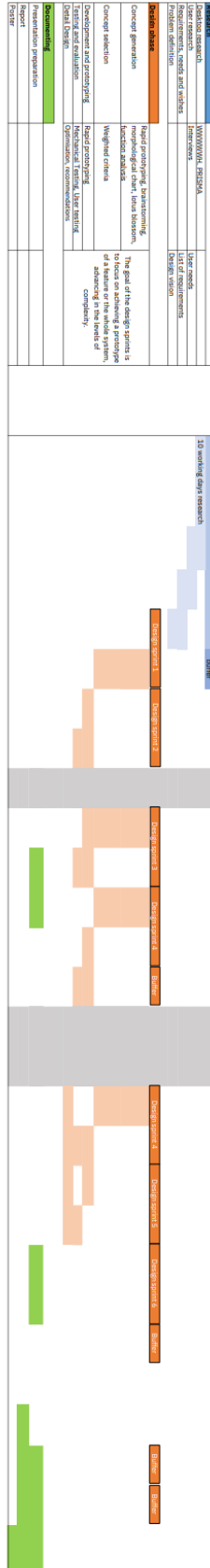
- [1] T. Dillingham, P. Le, M. Ej, and B. Ar, 'Use and satisfaction with prosthetic devices among persons with trauma-related amputations: a long-term outcome study', *Am. J. Phys. Med. Rehabil.*, vol. 80, no. 8, Aug. 2001, doi: 10.1097/00002060-200108000-00003.
- [2] S. Manz *et al.*, 'A review of user needs to drive the development of lower limb prostheses', *J. NeuroEngineering Rehabil.*, vol. 19, no. 1, p. 119, Nov. 2022, doi: 10.1186/s12984-022-01097-1.
- [3] L. Paterno, M. Ibrahim, E. Gruppioni, A. Menciassi, and L. Ricotti, 'Sockets for Limb Prostheses: A Review of Existing Technologies and Open Challenges', *IEEE Trans. Biomed. Eng.*, vol. 65, no. 9, pp. 1996–2010, Sep. 2018, doi: 10.1109/TBME.2017.2775100.
- [4] K. Ghoseiri and M. R. Safari, 'Prevalence of heat and perspiration discomfort inside prostheses: Literature review', *J. Rehabil. Res. Dev.*, vol. 51, no. 6, pp. 855–868, 2014, doi: 10.1682/JRRD.2013.06.0133.
- [5] S. Gupta, K. J. Loh, and A. Pedtke, 'Sensing and actuation technologies for smart socket prostheses', *Biomed Eng Lett*, vol. 10, no. 1, pp. 103–118, Nov. 2019, doi: [10.1007/s13534-019-00137-5](https://doi.org/10.1007/s13534-019-00137-5).

IDE Master Graduation Project

Santiago Andujar Alias

Project title: *Design of a smart prosthetic, removable socket for improved user comfort and accurate data measurement*

Project week	-2	-1	0	1	2	3	4	5	6	7	8	9	10	11	12	13	14	15	16	17	18	19	20	21	22	23	24	25	26
Calendar week	7	8	9	10	11	12	13	14	15	16	17	18	19	20	21	22	23	24	25	26	27	28	29	30	31	32	33	34	35
Working day week	1-5 Feb																												
Cumulative days at	5	10	15	20	25	30	35	40	45	50	55	60	65	70	75	80	85	90	95	100	105	110	115	120	125	130	135	140	145
Start of phase																													
End of phase																													



Project Phases

Phase	Methods	Final deliverables of the phase
Definition research	HW/WW/WH/PS/SM/A	User profiles
User research: needs and wishes	Interviews	User profiles
Problem definition		Design vision
Phase 1-10	Rapid prototyping, brainstorming, Concept generation, User selection, Weighted criteria	The goal of the design process is to focus on achieving a prototype that meets the user's needs and advancing in the levels of complexity.
Phase 11-20	Rapid prototyping, User selection, Weighted criteria	
Phase 21-30	Rapid prototyping, User selection, Weighted criteria	
Phase 31-40	Rapid prototyping, User selection, Weighted criteria	
Phase 41-50	Rapid prototyping, User selection, Weighted criteria	
Phase 51-60	Rapid prototyping, User selection, Weighted criteria	
Phase 61-70	Rapid prototyping, User selection, Weighted criteria	
Phase 71-80	Rapid prototyping, User selection, Weighted criteria	
Phase 81-90	Rapid prototyping, User selection, Weighted criteria	
Phase 91-100	Rapid prototyping, User selection, Weighted criteria	

Recommendations

Preparation preparation	
Report	

Other

--	--